

INVESTIGATIONS INTO THE FUNCTION OF ELP3 IN *TOXOPLASMA GONDII*

Leah R. Padgett

Submitted to the faculty of the University Graduate School  
in partial fulfillment of the requirements  
for the degree  
Doctor of Philosophy  
in the Department of Pharmacology and Toxicology  
Indiana University

August 2017

Accepted by the Graduate Faculty, Indiana University, in partial fulfillment of the requirements for the degree of Doctor of Philosophy.

---

Gustavo Arrizabalaga, Ph.D., Chair

---

Travis Jerde, Ph.D.

Doctoral Committee

---

Amber Mosley, Ph.D.

---

Richard M. Nass, Ph.D.

May 4, 2017

---

William J. Sullivan, Jr., Ph.D.

## ACKNOWLEDGEMENTS

I wish to thank first and foremost my mentor, Dr. Bill Sullivan, who provided me with exceptional training and mentorship. His optimism and passion for science is admirable and infectious. I appreciate him for being open to all of my crazy ideas and guiding me towards the most logical ones to test. I would also like to thank him for supporting my independent research while occasionally reminding me to focus.

My thesis committee has provided valuable suggestions regarding my research project and has supported me throughout this journey. I would like to thank each of my thesis committee members: Dr. Travis Jerde, Dr. Amber Mosely, Dr. Richard Nass and Dr. Gustavo Arrizabalaga. I especially would like to thank Dr. Gustavo Arrizabalaga for his enthusiasm for science and hallway pep-talks.

Next, I would like to thank my fellow IBMG graduate students, Joe Varberg and Kacie Lafavers. We have experienced the “ups” and the “downs” of this graduate school roller coaster ride together. Specifically, I would like to thank Joe for his brilliant mind and great scientific discussions, and Kacie for her statistical advice.

I would also like to thank all of the past and present members of the Sullivan and Arrizabalaga labs for their continuous support and advice throughout the years. I would like to thank Dr. Vicki Jeffers for her training in molecular parasitology techniques, support and friendship. I would also like to thank Dr. Mike Holmes for his insightful scientific conversations and help with the polyribosomal profiling experiments and Dr. Michael Harris for his advice regarding recombinant protein protocols.

This work would not be possible without the help of others. First, I would like to thank my collaborators Jenna Lentini and Dragony Fu at the Univeristy of Rochester for performing the *in vitro*  $\gamma$ -toxin cleavage assay. Next, I would like to thank Joe Varberg for being a great teammate and for his significant contribution to the work presented in Chapter 3 which was adapted from the published journal article “TgATAT-Mediated  $\alpha$ -Tubulin Acetylation Is Required for Division of the

Protozoan Parasite *Toxoplasma gondii*.” Additionally, I would like to thank Gustavo Arrizabalaga for performing the bioinformatics analyses presented in the published article “Targeting of tail-anchored membrane proteins to subcellular organelles in *Toxoplasma gondii*” which has been adapted for Chapter 4. I would also like to thank the American Heart Association for providing funding for my research, predoctoral fellowship grant 15PRE25550023.

Importantly, I would like to thank my family for their love and encouragement. My parents are my biggest cheerleaders and they have taught me that with hard work and perseverance, anything is possible. I would also like to thank Charles, my best friend and soulmate, for his support and to Cerrah, who reminds me that it is the little things in life that matter most.

Leah R. Padgett

## INVESTIGATIONS INTO THE FUNCTION OF ELP3 IN *TOXOPLASMA GONDII*

The parasite *Toxoplasma gondii* causes life-threatening infection in immunocompromised individuals. Our lab has determined that *Toxoplasma* Elongator protein-3 (TgElp3) is required for parasite viability. While catalytic domains are conserved, TgElp3 is the only component of the six-subunit Elongator complex present in *Toxoplasma*; moreover, TgElp3 localizes to the outer mitochondria membrane (OMM). These unusual features suggest that TgElp3 may have unique roles in parasite biology that could be useful in drug targeting. The goals of this thesis were to determine the function of TgElp3 and how the protein traffics to the OMM.

In other species, Elp3 mediates lysine acetylation of histones and alpha-tubulin, and its radical S-adenosyl methionine (rSAM) domain is important for the formation of tRNA modifications, which enhance translation efficiency and fidelity. Given its location, histones would not be an expected substrate, and we further determined that tubulin acetylation in *Toxoplasma* is mediated by a different enzyme, TgATAT. We found that overexpression of TgElp3 at the parasite's mitochondrion results in a significant replication defect, but overexpression of TgElp3 lacking the transmembrane domain (TMD) or with a mutant rSAM domain is tolerated. We identified one such modification, 5-methoxycarbonylmethyl-2-thiouridine (mcm<sup>5</sup>S<sup>2</sup>U) that is likely mediated by TgElp3. These findings signify the importance of TgElp3's rSAM domain for protein function, and confirms TgElp3 activity at the OMM is essential for *Toxoplasma* viability as previously reported.

To determine how TgElp3 traffics to the OMM, we performed a bioinformatics survey that discovered over 50 additional "tail-anchored" proteins present in *Toxoplasma*. Mutational analyses found that targeting of these TA proteins to specific parasite organelles was strongly influenced by the TMD sequence, including charge of the flanking C-terminal sequence.

Gustavo Arrizabalaga, Ph.D., Chair

## TABLE OF CONTENTS

<b>LIST OF TABLES</b> .....	x
<b>LIST OF FIGURES</b> .....	xi
<b>LIST OF ABBREVIATIONS</b> .....	xiii
<b>CHAPTER 1: Introduction</b> .....	1
1.1 <i>Toxoplasma gondii</i> , a protozoan parasite.....	1
1.2 Life cycle of <i>Toxoplasma</i> .....	4
1.3 <i>Toxoplasma</i> infection .....	7
1.4 Treatment of toxoplasmosis .....	8
1.5 Lysine acetylation as a drug target.....	9
1.6 History of Elp3 .....	10
1.7 Elp3 and human disease .....	13
1.8 Identification of an Elp3 homologue in <i>Toxoplasma</i> .....	13
1.9 Summary and hypotheses.....	15
<b>CHAPTER 2: Characterization of TgElp3</b> .....	17
2.1 Introduction.....	17
2.2 Materials and Methods .....	18
2.2.1 Plasmid DNA construction .....	18
2.2.1.1 BioID .....	18
2.2.1.2 Endogenous Replacement.....	18
2.2.1.3 Destabilization Domain .....	19
2.2.1.4 Ectopic Overexpression.....	19
2.2.1.5 Recombinant TgElp3 expression vectors.....	20
2.2.2 Parasite culture .....	21
2.2.3 Generation of transgenic parasites .....	21
2.2.4 Affinity purification of biotinylated proteins .....	23
2.2.5 Mass spectrometry analysis.....	24
2.2.6 Antibodies .....	24
2.2.7 Immunoblotting .....	25
2.2.8 Immunofluorescence assays.....	26
2.2.9 <i>Toxoplasma</i> growth assays.....	26

2.2.9.1	Plaque Assay .....	26
2.2.9.2	Doubling Assay .....	27
2.2.10	$\gamma$ -toxin modification assay tRNA .....	27
2.2.10.1	RNA isolation .....	27
2.2.10.2	Characterization of tRNAs treated with $\gamma$ -toxin in vitro .....	28
2.2.11	Recombinant protein expression and purification .....	28
2.2.12	Analysis of protein synthesis .....	30
2.2.12.1	Polyribosome profiling .....	30
2.2.12.2	Surface Sensing of Translation (SUnSET) .....	30
2.3	Results and Discussion .....	32
2.3.1	Attempt to identify TgElp3 interacting proteins using BioID .....	32
2.3.2	Endogenous replacement of TgElp3 .....	37
2.3.3	Expression of catalytically inactive TgElp3 using an inducible destabilization domain .....	38
2.3.4	Overexpression of wild-type and mutant TgElp3 .....	40
2.3.5	The mcm <sup>5</sup> s <sup>2</sup> U tRNA modification is present in <i>Toxoplasma</i> .....	46
2.3.6	Attempt to generate recombinant TgElp3 .....	51
2.3.7	Global translation is not altered by overexpression of TgElp3 .....	53
2.4	Concluding remarks .....	60
<b>CHAPTER 3: Tubulin acetylation, a critical PTM important for parasite</b>		
<b>viability, is mediated by TgATAT not TgElp3 .....</b>		
3.1	Introduction .....	62
3.2	Materials and Methods .....	64
3.2.1	Antibodies .....	64
3.2.2	Parasite culture and transfection .....	64
3.2.3	Generation of TgTUBA1 K40 mutant parasites .....	65
3.2.4	Endogenous tagging of TgATAT .....	65
3.2.5	Immunoblotting .....	66
3.2.6	IFAs .....	66
3.2.7	CRISPR-mediated disruption of <i>TgATAT</i> .....	67
3.3	Results .....	67

3.3.1 K40 acetylation is dispensable only if tubulin is stabilized through another mutation .....	67
3.3.2 Identification of an acetyltransferase that co-localizes with acetylated tubulin during tachyzoite division .....	70
3.3.3 Disruption of <i>TgATAT</i> leads to loss of $\alpha$ -tubulin K40 acetylation.....	75
3.3.4 Loss of K40 acetylation causes microtubule defects and impairs replication.....	77
3.4 Discussion.....	82
3.5 Concluding Remarks .....	86
<b>CHAPTER 4: Targeting of TgElp3 and other tail-anchored proteins to subcellular organelles in <i>Toxoplasma gondii</i></b> .....	<b>87</b>
4.1 Introduction.....	87
4.2 Materials and Methods .....	88
4.2.1 Parasite culture and transfection.....	88
4.2.2 Bioinformatics analyses .....	89
4.2.3 Plasmid DNA construction .....	89
4.2.3.1 HA-tagging vectors .....	89
4.2.3.2 YFP-fusion vectors .....	90
4.2.3.3 Domain-swap vectors .....	90
4.2.4 Immunofluorescence Assays .....	91
4.3 Results and Discussion .....	91
4.3.1 Identification of TA membrane proteins in <i>Toxoplasma</i> .....	91
4.3.2 Hydrophobicity of the TMDs in <i>Toxoplasma</i> .....	95
4.3.3 Localization of <i>Toxoplasma</i> TA proteins to various organelles .....	95
4.3.4 TMD and CTS are sufficient to target <i>Toxoplasma</i> TA proteins to the proper subcellular organelle.....	99
4.3.5 Targeting of TA proteins to the mitochondrion .....	99
4.3.6 Targeting of TA proteins to the ER and Golgi apparatus.....	104
4.4 Concluding Remarks .....	105
<b>CHAPTER 5: Conclusions</b> .....	<b>107</b>
5.1 Summary of Findings .....	107



5.2 Future Directions .....	109
5.2.1 Does Elp3 bind tRNA? .....	109
5.2.2 Does TgElp3 modify tRNA <i>in vitro</i> ? .....	109
5.2.3 Does overexpression of tRNA <sup>Lys</sup> and/or tRNA <sup>Glu</sup> rescue <sup>HA</sup> TgElp3 <sup>OE</sup> growth phenotype? .....	110
5.2.4 Does overexpression of TgElp3 affect protein synthesis?.....	110
5.2.5 Does TgElp3 overexpression alter parasite mitochondrial function?.	112
<b>APPENDICES</b> .....	113
Appendix A. Constructs and primers used in chapter 2. ....	113
Appendix B. Primers used in chapter 3. ....	116
Appendix C. Copyright permission for chapter 4. ....	117
Appendix D. Identification of 59 putative TA proteins in <i>Toxoplasma</i> . ....	118
Appendix E. Constructs used in chapter 4. ....	123
Appendix F. Primers used in chapter 4. ....	125
Appendix G. Comparison of <i>Toxoplasma</i> and <i>Arabidopsis</i> TA proteins.....	128
<b>REFERENCES</b> .....	134
<b>CURRICULUM VITAE</b>	

## LIST OF TABLES

Table 1. Proteins uniquely biotinylated in BL- <sup>HA</sup> TgEIp3 expressing parasites. ...	36
Table 2. The 9 putative TA proteins selected for experimental validation.....	94

## LIST OF FIGURES

Figure 1. A human foreskin fibroblast cell infected with <i>Toxoplasma gondii</i> .....	1
Figure 2. Illustration of <i>Toxoplasma gondii</i> cellular structure.....	3
Figure 3. Diagram of the <i>Toxoplasma</i> life cycle.....	5
Figure 4. Cartoon of the <i>Toxoplasma</i> lytic cycle.....	7
Figure 5. Elp3 is the only component of the Elongator complex found in <i>Toxoplasma</i> .....	14
Figure 6. Comparison of Elp3 protein structure. ....	15
Figure 7. BioID experimental workflow. ....	32
Figure 8. Identification of proximal TgElp3 proteins.....	34
Figure 9. Endogenous tagging of TgElp3. ....	38
Figure 10. <sup>ddHA</sup> TgElp3 protein regulation by Shield-1.....	39
Figure 11. Overexpression of <sup>HA</sup> TgElp3 <sup>OE</sup> in <i>Toxoplasma gondii</i> .....	41
Figure 12. Overexpression of TgElp3 causes a significant replication defect.....	43
Figure 13. Overexpression of TgElp3 in the ME49 parasite strain.....	45
Figure 14. Overexpression of TgElp3 causes hyper-modification of tRNA resulting in altered translation.....	46
Figure 15. Ctu1/Ctu2 and Elp3 are required for the mcm <sup>5</sup> s <sup>2</sup> wobble uridine modification. ....	48
Figure 16. Identification of the tRNA <sup>Glu</sup> mcm <sup>5</sup> s <sup>2</sup> modification in <i>Toxoplasma</i> . ....	50
Figure 17. Overexpression of Elp3 does not alter global translation.....	54
Figure 18. SUnSET analysis of active protein biosynthesis in <i>Toxoplasma</i> . ....	56
Figure 19. Protein biosynthesis varies between parasite vacuoles and is independent of Elp3 overexpression. ....	59
Figure 20. Ablation of K40 acetylation is not tolerated unless replaced by the K40Q acetyl-lysine mimic. ....	68
Figure 21. K40 acetylation is dispensible in the presence of the T239I oryzalin resistance mutation. ....	70
Figure 22. Comparison of ATAT/Mec-17 homologues.....	72
Figure 23. Expression of TgATAT and acetylated $\alpha$ -tubulin during the tachyzoite cell cycle.....	74

Figure 24. Selective targeting of GFP-Cas9 to the TgATAT locus eliminates K40 acetylation .....	76
Figure 25. Defects in nuclear division and segregation in parasites lacking $\alpha$ -tubulin K40 acetylation. ....	79
Figure 26. Centrosome duplication and apicoplast division in parasites lacking K40 acetylation.....	80
Figure 27. Daughter cytoskeleton completion is impaired upon loss of K40 acetylation. ....	82
Figure 28. Identification of putative tail-anchored (TA) proteins in <i>Toxoplasma</i> .....	93
Figure 29. Subcellular localization of tail-anchored (TA) proteins.....	99
Figure 30. Role of the C-terminal sequence (CTS) in subcellular localization of tail-anchored (TA) proteins. ....	101
Figure 31. C-terminal sequence swap of tail-anchored (TA) proteins alters subcellular localization.....	104

## LIST OF ABBREVIATIONS

ATAT	alpha tubulin acetyltransferase
aa	amino acid
AcH3	acetylated histone H3
AcTubulin	acetylated alpha-tubulin
ALS	amyotrophic lateral sclerosis
BioID	biotin identification
BL	biotin ligase
BLAST	basic local alignment search tool
bp	base pairs
BSA	bovine serum albumin
Cas9	Clustered regularly interspaced short palindromic repeat associated protein 9
cDNA	complementary deoxyribonucleic acid
Ce	<i>Caenorhabditis elegans</i>
coA	coenzyme A
CRISPR	clustered regularly interspaced short palindromic repeats
Ct	C-terminus
CHX	cycloheximide
CLIP	cross-linking immunoprecipitation
Cyt-b5	cytochrome b5
Ctu	cytosolic thiouridylase
DAPI	4',6-diamidino-2-phenylindole
DAS	distributed annotation systems
dd	destabilization domain
DEPC	diethyl pyrocarbonate
DHFR	dihydrofolate reductase
DHFR-TS	dihydrofolate reductase-thymidylate synthase
DMEM	Dulbecco's Modified Eagle Medium
dsDNA	double stranded deoxyribonucleic acid

DNA	deoxyribonucleic acid
dNTP	deoxyribonucleotide triphosphate
EDTA	ethylenediaminetetraacetic acid
EGTA	ethylene glycol-bis (2-aminoethylether)-N,N,N',N'-tetraacetic acid
Elp3	elongator protein 3
ER	endoplasmic reticulum
Fis1	mitochondrial fission 1 protein
FBS	fetal bovine serum
FD	familial dysautonomia
GAPDH	glyceraldehyde 3-phosphate dehydrogenase
GCN5	general control non-depressible 5
GET	guided entry of tail-anchored proteins
GFP	green fluorescent protein
GST	glutathione S-transferase
HA	hemagglutinin
HAT	histone acetyltransferase
HDAC	histone deacetylase
HeLa	Henrietta Lacks
HEPES	4-(2-hydroxyethyl)-1-piperazineethanesulfonic acid
HFF	human foreskin fibroblasts
HRP	horseradish peroxidase
hr	hour
Hs	<i>Homo sapiens</i>
Hs-tRNA <sup>Glu</sup>	<i>Homo sapiens</i> transfer ribonucleic acid glutamic acid
Hs-tRNA <sup>Ser</sup>	<i>Homo sapiens</i> transfer ribonucleic acid serine
HSC	heat shock cognate
HSP	heat shock protein
hx	hypoxanthine-xanthine-guanine phosphoribosyl transferase

HXGPRT	hypoxanthine-xanthine-guanine phosphoribosyl transferase
IFA	immunofluorescence assay
IMPDH	inosine-monophosphate dehydrogenase
IMC	inner membrane complex
IMC3	inner membrane complex 3
IP	immunoprecipitation
IPTG	isopropyl $\beta$ -D-1-thiogalactopyranoside
ISP1	inner membrane complex sub-compartment protein 1
KAT	lysine acetyltransferase
kb	kilobase
KD	Kyte and Doolittle
kDa	kiloDalton
KDAC	lysine deacetylase
mcm <sup>5</sup> U	5-methoxycarbonylmethyl-uridine
mcm <sup>5</sup> S <sup>2</sup> U	5-methoxycarbonylmethyl-2-thiouridine
MEC-17	mechanosensory abnormality protein 17
mins	minutes
<i>MinElp3</i>	<i>Methanocaldococcus infernus</i> elongator protein 3
MPA	mycophenolic acid
MTOC	microtubule-organizing center
mRNA	messenger ribonucleic acid
NCBI	National Center for Biotechnology Information
ncm <sup>5</sup> U	5-carbamoylmethyl-uridine
Nt	N-terminus
No.	number
NP	nonyl phenoxypolyethoxyethanol
OMM	outer mitochondrial membrane
PAM	photospacer adjacent motif sequence
PBS	phosphate buffered saline
Pf	<i>Plasmodium falciparum</i>

pLIC	plasmid ligation-independent cloning
PMSF	phenylmethylsulfonyl fluoride
PTM	posttranslational modification
RBD	ribonucleic acid-binding domain protein
RImN	radical S-adenosyl-L-methionine domain-containing protein
RIPA	radio immunoprecipitation assay buffer
RNA	ribonucleic acid
RNAPII	ribonucleic acid polymerase two
RS	radical S-adenosylmethionine
SAG1	surface antigen 1
rSAM	radical S-adenosylmethionine
SAM	S-adenosylmethionine
SDS	sodium dodecyl sulfate
SDS-PAGE	sodium dodecyl sulfate polyacrylamide gel electrophoresis
SERCA	sarcoplasmic-endoplasmic reticulum calcium adenosine 5'-triphosphatase
sg	single guide
sgRNA	single guide ribonucleic acid
SH	thiol
SNARE	soluble N-ethylmaleimide-sensitive factor attachment protein
SORTLR	sortilin-like receptor
<i>spp</i>	species
SRP	signal recognition particle
SUMO	small ubiquitin-like modifier
SUnSET	surface sensing of translation
TA	tail-anchored
TBST	tris-buffered saline tween
TM	trademark



TMD	transmembrane domain
TMHMM	transmembrane hidden markov model
tRNA	transfer ribonucleic acid
Tg	<i>Toxoplasma gondii</i>
Tg-tRNA <sup>Glu</sup>	<i>Toxoplasma gondii</i> transfer ribonucleic acid glutamic acid
Tg-tRNA <sup>Ser</sup>	<i>Toxoplasma gondii</i> transfer ribonucleic acid serine
Tt	<i>Tetrahymena thermophila</i>
TUBA1	tubulin alpha-1 chain
UBC	ubiquitin-conjugating enzyme
UPRT	uracil phosphoribosyltransferase
UTR	untranslated region
v	version
WB	Western blot
WT	wild-type
YFP	yellow fluorescent protein

## CHAPTER 1: Introduction

### 1.1 *Toxoplasma gondii*, a protozoan parasite

*Toxoplasma gondii* is an obligate intracellular protozoan parasite that was first identified in 1908 by two independent investigators (1, 2). The parasite's name originates from the Greek word toxon meaning bow-like and gundi, the African rodent from which *Toxoplasma* was first identified (2). As one of the most widely distributed parasites, *Toxoplasma* is capable of infecting virtually any nucleated cell in warm-blooded animals (3, 4). It is estimated that one-third of the world's population, including 60 million people in the United States, is seropositive for *Toxoplasma* infection (5). *Toxoplasma* must be within a host cell to replicate (Figure 1). The phylum Apicomplexa consists of *Toxoplasma* as well as other notorious threats to global health such as *Plasmodium spp.* and *Cryptosporidium spp.* Malaria which is caused by *Plasmodium* kills over half a million people a year (6) while *Cryptosporidium* infections are a major cause of waterborne illnesses throughout the world (7–9). Across the globe, these pathogens are responsible for significant morbidity and mortality in humans and livestock. *Toxoplasma* and its close relatives cause widespread disease throughout the world and thus warrant research to identify therapeutics to eradicate these pathogens.

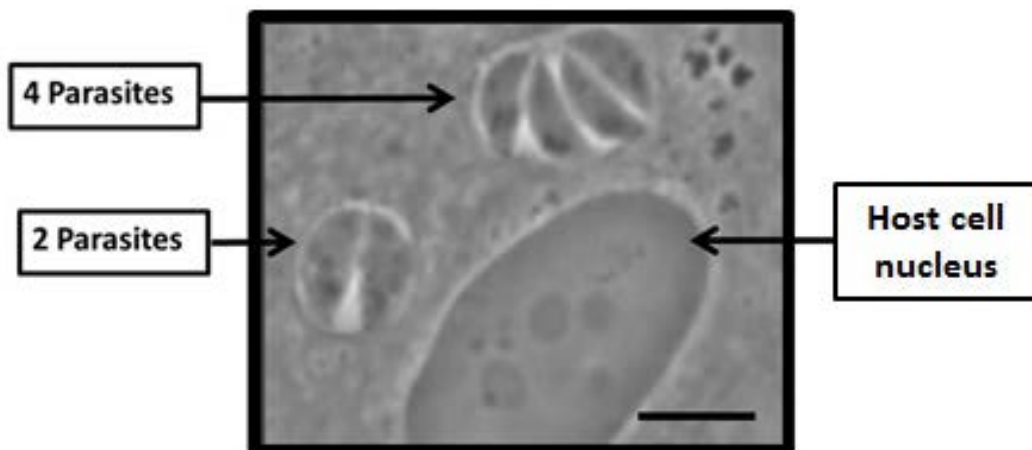


Figure 1. A human foreskin fibroblast cell infected with *Toxoplasma gondii*. An image of two parasite vacuoles within a human foreskin fibroblast cell in relation to the host cell nucleus. One parasite vacuole contains 2 parasites and the second vacuole contains 4 parasites. Scale bar= 5  $\mu$ m.

There are multiple *Toxoplasma* strains responsible for human infection. The three main clonal lineages are referred to as type I, II and III (10). While the type I strain is the most virulent, infections with type II and III strains are more common in people and animals (10). Outside of these three clonal lineages, there are other strains that appear to be more genetically diverse, particularly those identified in South America (11). These parasite strains are defined by several important differences including virulence, growth rate and cyst formation. In contrast to type I strains (e.g. RH and GT1), type II and III strains are less virulent, replicate slower, and readily form tissue cysts (12, 13). Since type II strains (e.g. ME49 and Pru) more readily form tissue cysts, they are used to study tachyzoite and bradyzoite differentiation (13). Interestingly, these three distinct clonal parasite lines genetically differ by only 1% (10).

*Toxoplasma* is an early-branching eukaryote it contains all of the traditional eukaryotic organelles including a nucleus, Golgi apparatus, endoplasmic reticulum and a single tubular mitochondrion (Figure 2). This single mitochondrion appears to have a reduced genome compared to higher eukaryotes. However, due to complications with purification techniques and nuclear pseudogenes, complete characterization of the *Toxoplasma* mitochondrial genome remains incomplete (14). To date, within the *Toxoplasma* mitochondrial genome there is evidence of fragmented rRNA genes along with three protein encoding genes: cytochrome c oxidase I (cox1), cytochrome c oxidase III (cox3), and cytochrome b (cob) (14–16). Of note, there is no evidence of mitochondrial encoded tRNA genes, indicating these tRNAs must be imported into the organelle for translation (17).

Parasite specific organelles in *Toxoplasma* include dense granules, rhoptries and micronemes which secrete proteins that coordinate invasion into the host cell and establishment of a parasitophorous vacuole (Figure 2). In addition to the nucleus and mitochondrion, the apicoplast also contains DNA. This apicoplast is derived from a secondary endosymbiotic event, a prokaryotic cyanobacterium was incorporated into a unicellular eukaryote which was subsequently engulfed by *Toxoplasma* (Figure 2) (18–20). The *Toxoplasma*

apicoplast is an essential organelle responsible for the biosynthesis of fatty acids and isoprenoids (19). The apicoplast is positioned in close proximity to the single mitochondrion and it is thought these organelles shuttle essential metabolic components to one another (18).

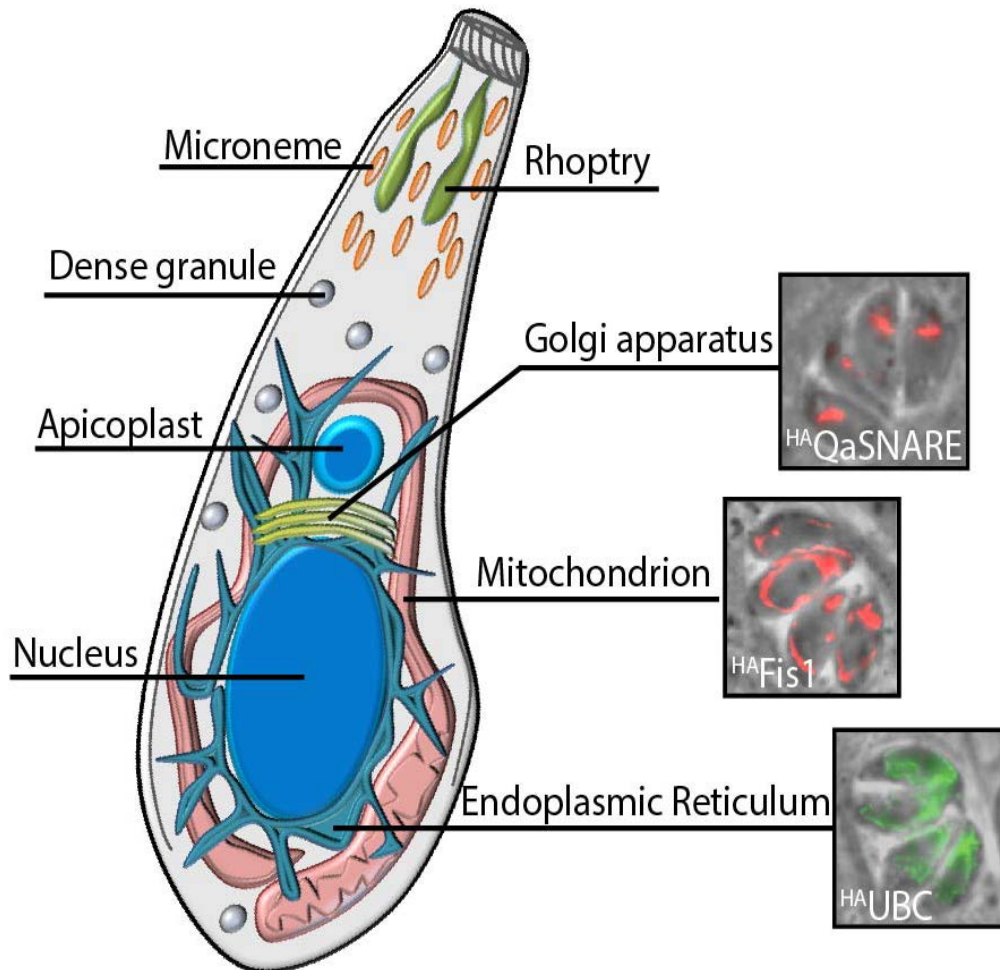


Figure 2. Illustration of *Toxoplasma gondii* cellular structure. Eukaryotic organelles present in *Toxoplasma* are the nucleus, endoplasmic reticulum, Golgi apparatus and a single mitochondrion. Parasite specific organelles include dense granules, rhoptries, micronemes and the apicoplast. Each immunofluorescence assay (IFA) image shows four intracellular parasites within a single vacuole stained with anti-HA to detect the designated tagged organellar protein.

## 1.2 Life cycle of *Toxoplasma*

As an intracellular pathogen, *Toxoplasma gondii* spends the majority of its life cycle within a host. *Toxoplasma* has a complex life cycle that can be subdivided into sexual and asexual phases, and throughout these phases the parasites can differentiate into three different infectious forms: sporozoite, bradyzoite and tachyzoite (21). Cats are the definitive host, meaning *Toxoplasma* can only sexually reproduce in the epithelium of the feline's small intestine (Figure 3). Parasites typically reach the cat intesting after the feline consumes oocysts (sporozoites) from the environment or tissue cysts (bradyzoites) from an infected animal. Once ingested by the cat, the parasites can differentiated into male and female gametocytes which leads to the formation of oocysts (21). These highly infectious sporozoite-containing oocysts are shed into the environment where they can be directly ingested or inhaled by intermediate hosts (22). Common sources of oocysts are contaminated water, fruits, or vegetables (23). Once within the intermediate host, which can be any warm-blooded vertebrate, the sporozoites are released from the oocysts and the parasites differentiate into tachyzoites, which have a doubling time of 6-8 hours (21).

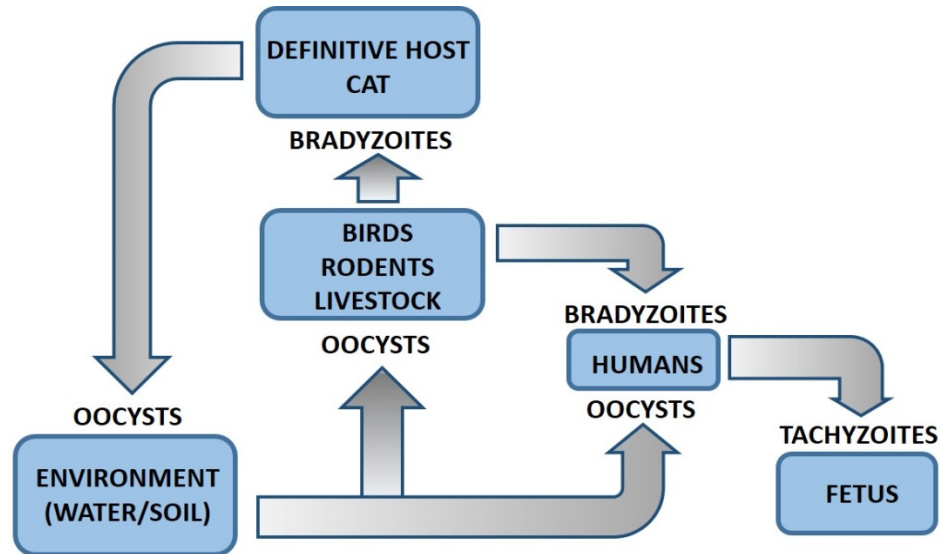


Figure 3. Diagram of the *Toxoplasma* life cycle.

Cats are the definitive host of *Toxoplasma* where the parasites can sexually reproduce. During infection cats shed oocysts into the environment, which are then ingested by animals including humans through contaminated water and food sources. Once inside the intermediate host, the sporozoite-containing oocysts differentiate into tachyzoites. Upon immune pressure, tachyzoites differentiate into the slower replicating or dormant bradyzoites. Bradyzoites within tissue cysts can be transmitted through predation. When the cat ingests oocysts from the environment or bradyzoites from infected prey, the life cycle is considered complete. Pregnant women who become infected for the first time can transmit tachyzoites to the fetus via the placenta.

As depicted in Figure 4, there are four main parts of the lytic cycle: attachment, invasion, replication and egress (24). Parasite attachment is mediated by recognition of host cell specific factors like surface glycoproteins (24–26). Following attachment, the parasite actively invades the host cell which causes invagination of the host cell membrane (27). This process continues until the parasite is fully internalized within a parasitophorous vacuole. Once inside the host cell, parasite replication can occur through a process termed endodyogeny (24). In endodyogeny, division begins with the parasite Golgi apparatus followed by the formation of two nascent daughters within the mother parasite. The first signs of the developing progeny are depicted as two dome-shaped structures which are made up of the inner membrane complex and subpellicular microtubules. As these daughter cells develop, the mother parasite

nucleus separates into the dome-shaped structures taking on a horseshoe like appearance. Expansion of the inner membrane complex and subpellicular microtubules of each daughter cell eventually surrounds one half of the mother nucleus, which eventually partitions into two separate nuclei. The progeny continue to grow until the mother parasite inner membrane complex disappears and the outer membrane becomes the plasma membrane for each daughter cell. Tachyzoites continue to divide by endodyogeny and after repeated rounds of replication the parasitophorous vacuole fills with parasites, overtaking the host cell. To continue to propagate, these tachyzoites must depart from their current host cell through a process called egress. Parasite egress can be initiated by several different factors including mechanical disruption of the host cell, the host immune response or through parasite specific mechanisms (28). Freshly egressed parasites then invade new host cells and continue to proliferate through repeating the lytic cycle.

The most serious consequences of *Toxoplasma* infection result from the lysis of host cells due to parasite egress. In healthy individuals, *Toxoplasma* is quickly controlled by the immune response (13). Upon exposure to interferon gamma and potentially other unidentified mechanisms, tachyzoites differentiate into the more slowly replicating bradyzoites (29, 30). These bradyzoites are encompassed within a cyst wall converted from the parasitophorous vacuole, and this cyst wall appears impervious to clearance by the immune system and current drug treatments (13, 31). Consequently, life-threatening opportunistic disease can arise due to reactivated infection during immune suppression (32).

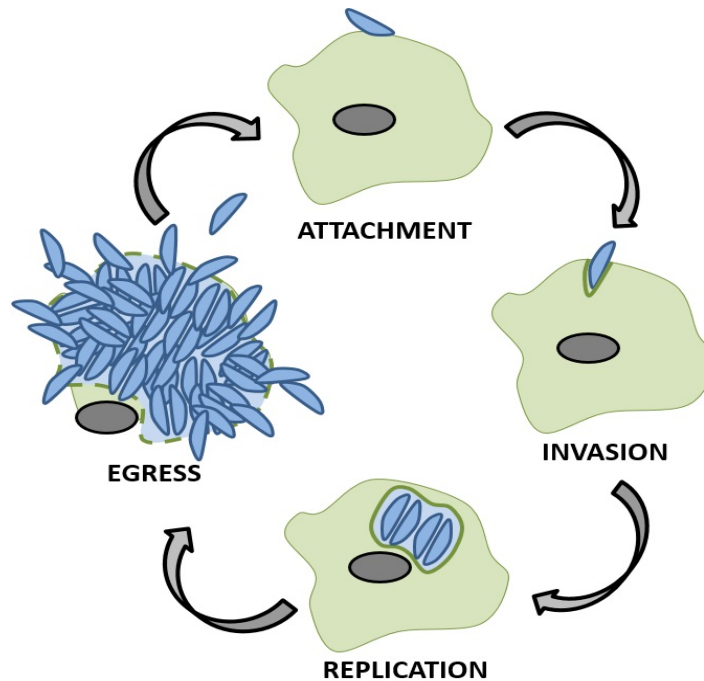


Figure 4. Cartoon of the *Toxoplasma* lytic cycle. Parasites (blue) first attach and then actively invade a host cell (light green) and form a parasitophorous vacuole (dark green). Once inside the host cell, the parasites replicate. Synchronous replication continues filling the host cell with parasites. Once full, a series of signals tell the parasites to actively egress which ruptures the host cell. These parasites attach to new host cells and the cycle continues. On average, the lytic cycle takes 30-40 hr for the RHΔ*hx* strain.

### 1.3 *Toxoplasma* infection

*Toxoplasma gondii* infection can be separated into acute and latent phases. Acute toxoplasmosis occurs during the initial or reactivated infection of the host. If the host is healthy, *Toxoplasma* infection may be asymptomatic or present with swollen lymph nodes and/or mild flu-like symptoms (32). These symptoms are typically a result of the host's immune response which readily clears the actively replicating tachyzoites (32). Some of these tachyzoites may escape the immune system by converting to the bradyzoite-containing cyst, where it will likely persist throughout the rest of the host's life (3, 32).

The latent stage of infection was originally thought to be benign. Although, recent studies have identified an association between latent *Toxoplasma* infection and some neurological diseases including depression, obsessive-



compulsive disorder, schizophrenia, Parkinson's disease and epilepsy (33–37). Interestingly, when rodents are infected with *Toxoplasma* they lose their aversion to cats and become attracted to cat urine, making them more susceptible to predation (38). Ingestion of a *Toxoplasma* infected rodent by a cat facilitates completion of the parasite life cycle (39). More studies are needed to determine if the latent infection causes adverse effects on the human host.

While the latent infection is controlled by the host immune system, serious problems can occur when the individual becomes immunocompromised. Particularly patients with AIDs, undergoing organ transplant or chemotherapy are at a high risk for reactivated acute infection (3, 32). This reactivated acute infection occurs when an infected individual's immune system becomes depressed (21). Loss of immune pressure triggers the latent bradyzoites to reconvert into the fast replicating tachyzoites (21). If not controlled, replicating tachyzoites can cause massive tissue destruction and even death. Consequences of acute toxoplasmosis include neurological symptoms, myocarditis, ocular lesions, and encephalitis (40–42).

Another serious disease caused by acute *Toxoplasma* infection is congenital toxoplasmosis which occurs when a pregnant woman becomes infected for the first-time and the tachyzoites are vertically transmitted to the fetus (43). Infection of the unborn fetus can cause spontaneous miscarriage or birth defects (43, 44). Congenitally infected infants may suffer from cognitive disorders, hydrocephalus, and vision or hearing impairments, and are prone to recurring bouts of reactivated infection throughout their lives (32).

#### **1.4 Treatment of toxoplasmosis**

Currently, there are no cures for toxoplasma infection, but there are drugs to treat acute toxoplasmosis. The primary drug regimen consists of a combination of sulfadiazine and pyrimethamine to target the folic acid synthesis pathway (45, 46). Sulfadiazine inhibits the dihydropteroate synthase (DHPS) to prevent formation of dihydrofolic acid and pyrimethamine inhibits dihydrofolate reductase (DHFR) to prevent the formation of tetrahydrofolic acid (45). The

combination therapy inhibits the synthesis of nucleic acid precursors resulting in death of the parasites (47).

Unfortunately, there are significant adverse side-effects associated with the anti-folate regimen. A number of individuals have sulfa allergies, in these cases clindamycin can be administered instead of sulfadiazine (48, 49). Clindamycin is an antibiotic that targets translation in the apicoplast organelle, but is not as effective at killing the parasite as sulfadiazine (50). A second problem lies with the toxicity of pyrimethamine. Despite having a higher affinity for the *Toxoplasma* DHFR enzyme, pyrimethamine can also target the human DHFR enzyme which can cause adverse side-effects including bone marrow suppression (51). To reduce these pyrimethamine induced side-effects, treatments are supplemented with folinic acid (52).

In the case of pregnant women who become infected for the first time, treatment with pyrimethamine is not advised in the first trimester. Since pyrimethamine can cross the placenta and is teratogenic, an alternative drug spiramycin is typically used (44). Spiramycin is unable to cross the placenta and is considered safe in pregnant women, fetus and newborn (53). This non-toxic macrolide will reduce transmission of *Toxoplasma* from the pregnant woman to the fetus; however, it will not affect the severity of disease in an already infected fetus (54). Depending on the severity of fetal infection, pyrimethamine is sometimes used.

Current therapies to treat toxoplasmosis are problematic since they cause many adverse side-effects and are unable to completely cure *Toxoplasma* infections. As the bradyzoite-containing cysts are impervious to current treatments, these cysts will remain embedded within host tissues and can reactivate to cause recurrent infection. A better understanding of *Toxoplasma* biology is needed to develop new drugs to combat this infectious pathogen.

### **1.5 Lysine acetylation as a drug target**

Lysine acetylation is an essential post-translational modification (PTM) in *Toxoplasma*. Lysine acetyltransferases transfer the acetyl group from acetyl

coenzyme A onto the epsilon-amino group of a lysine. Lysine deacetylases remove this PTM, making the modification reversible. Lysine acetylation is associated with many different biological processes including transcription, translation and metabolism. In *Toxoplasma*, over 400 acetylation sites are present on a variety of proteins in all subcellular compartments, including some parasite specific proteins (55).

Recent studies in protozoan parasites have established lysine acetylation as a valid drug target (56, 57). For example, inhibition of lysine deacetylases by inhibitors such as apicidin and FR235222 result in parasite death (58, 59). In conjunction, our laboratory identified garcinol as an inhibitor of the lysine acetyltransferase TgGCN5b, which may explain its potent activity against *Toxoplasma* and *Plasmodium* (60). Inhibition of TgGCN5b disrupts gene expression and stalls parasite replication (60). Interfering with lysine acetylation pathways in *Toxoplasma* reduces parasite viability (61). Therefore, examining these pathways in greater detail is a promising approach to identify novel therapeutics for toxoplasmosis.

### **1.6 History of Elp3**

In 1999, two independent studies in *Saccharomyces cerevisiae* established that Elongator protein 3 (Elp3) is the lysine acetyltransferase (KAT) component of the Elongator complex (62, 63). The Elongator complex was originally detected through purification of hyperphosphorylated RNA polymerase II (RNAPII) and implicated in chromatin remodeling during transcription elongation; hence, the Elongator complex was named (62). Further characterization of the Elongator complex identified a total of six individual subunits (Elp1-6) that form two sub complexes; these sub complexes are thought to dimerize and associate with RNAPII to mediate transcriptional elongation (64–66).

Given the high degree of sequence similarity between ScElp3 and members of the GCN5-related N-acetyltransferase (GNAT) superfamily, it was postulated that ScElp3 may possess KAT activity. An *in vitro* lysine

acetyltransferase assay revealed that recombinant Elp3 is capable of acetylating all four histones on their amino-terminal tails (63, 67). Since Elp3 associates with RNAPII and has KAT activity, it was theorized that Elp3 is the component of the Elongator complex responsible for acetylating histones to promote transcriptional elongation. In support of this model, Elp3 mutational studies identified two conserved tyrosine residues required for binding acetyl coenzyme A (acetyl coA), the cofactor required for Elp3 KAT activity (68).

In an independent forward genetics approach, yeast subjected to a toxic zymocin treatment developed resistant mutations in Elongator complex proteins, which were independently named as putative toxin target genes: TOT1, TOT2, and TOT3 (isoallelic with Elp1, Elp2 and Elp3) (69, 70). Zymocin is a heterotrimeric ( $\alpha\beta\gamma$ ) toxin produced by the *Kluyveromyces lactis* yeast strain that causes irreversible growth arrest of sensitive yeast strains, including *Saccharomyces cerevisiae* (69). The zymocin  $\alpha$  and  $\beta$  subunits act at the cell exterior to facilitate import of the  $\gamma$ -toxin (71). In agreement with previous findings, examination of yeast Elp3 mutants determined that zymocin resistance occurs through a RNAPII dependent mechanism (70, 72–75).

Characterization of the Elongator complex in humans was reported in 2002 (76). Consistent with studies in yeast, the human Elongator complex associates with RNAPII and recombinant human Elp3 acetylates histone H3 and histone H4 *in vitro* (76). In HeLa cells, under normal cell culture conditions Elp3 was found to predominantly localize to the cell nucleus, however some proteins were also detected in the cytoplasm (76). Not surprisingly, studies in *Arabidopsis thaliana* also identified homologues to all six components of the Elongator complex and interaction studies confirmed RNAPII association, suggesting Elongator is evolutionarily conserved in structure and function (77).

Preliminary work performed in multiple species has established Elp3 as the lysine acetyltransferase component of the Elongator complex. Nevertheless, the biological function of Elp3 is not well defined. Phenotypes associated with the loss of Elp3 range from regulation of neuronal migration and axon development in *Drosophila* to alterations in microtubule dynamics in humans and worms (78–

81). Disruption of Elp3 in mice causes impaired zygotic paternal genome demethylation (82). In *Arabidopsis thaliana*, an amino acid substitution (D to N) conserved in all Elp3 homologues causes reduced cell proliferation and malformed leaf structure (76). In *Saccharomyces cerevisiae*, Elp3 knockouts are viable but display a slow growth phenotype under stress conditions (63). Given the role of Elp3 in transcriptional elongation, disruption is likely to modify the expression of many genes, which might explain the pleiotropic phenotypes observed.

Recent evidence suggests that Elp3 may possess a second enzymatic activity as a tRNA modification enzyme. The formation of tRNA modifications is dependent on the radical S-adenosyl-L-methionine (rSAM) domain found in all Elp3 homologues (83). In *Toxoplasma* the rSAM domain contains a canonical CX<sub>3</sub>CX<sub>2</sub>C motif required for iron sulfur cluster formation while most other Elp3 homologues contain a non-canonical CX<sub>4</sub>CX<sub>9</sub>CX<sub>2</sub>C motif (83). Mutations in this cysteine motif result in loss of tRNA modifications *in vitro* (84). Interestingly, several studies demonstrated that overexpression of select tRNAs can suppress Elongator mutant phenotypes in yeast (63, 85). The Elongator complex is required for the synthesis of 5-methoxycarbonylmethyl (mcm<sup>5</sup>) and 5-carbamoylmethyl (ncm<sup>5</sup>) modifications present on uridines at the tRNA wobble position (86, 87). The effect of these wobble uridine tRNA modifications is thought to promote translation fidelity and efficiency, but the exact mechanisms are not well understood (88).

Future work is needed to determine if protein acetylation is the only biochemical activity of Elp3 or if it also functions as a tRNA modification enzyme. In either instance, the gene name Elongator protein 3 is relevant as it may be involved with transcriptional elongation through histone acetylation or translational elongation through tRNA modifications and disruption of either function would affect a broad range of cellular processes resulting in a multitude of different phenotypes.

## 1.7 Elp3 and human disease

Mutations in Elp3 are associated with several diseases in humans. Familial dysautonomia (FD) affects the sensory and autonomic nervous system causing defects in neuronal development. Mutations in Elp1 and Elp3 have been reported in FD patients (89, 90). Experimental studies using FD fibroblasts show a decrease in histone H3 acetylation and RNAPII density on select cell motility genes, indicating dysregulation of gene expression (91). Furthermore, alterations in tubulin acetylation and microtubule-based protein trafficking observed in Elongator mutants is suggested to be a contributing factor in FD disease (89). A second neurologic disease, amyotrophic lateral sclerosis (ALS), was found to be associated with Elp3 allelic variations in a genome-wide association study of almost 1500 individuals from three different populations (92). These neurological disease findings suggest Elp3 may have a critical role in neuron biology (93).

Elp3 is upregulated in human colon adenocarcinoma and breast cancer (94, 95). Studies identified that Wnt signaling induces Elp3 expression which in turn promotes translation of Sox9, a transcription factor implicated in tumorigenicity (94); through this mechanism Elp3 is crucial for maintaining a subpopulation of cells needed to trigger tumor initiation in the intestine. In an independent study, increased Elp3 expression was associated with an increased risk of breast cancer metastasis (95). Moreover, genetic ablation of Elp3 in a breast cancer mouse model strongly impaired invasion and metastasis formation (95). These findings suggest that Elp3 may play a role in cancer progression.

## 1.8 Identification of an Elp3 homologue in *Toxoplasma*

In 2013, our laboratory identified a homologue of Elp3 in *Toxoplasma* (83). Initial characterization of *Toxoplasma* Elp3 (TgElp3) unveiled several unusual features. In the phylum Apicomplexa, Elp3 is the only conserved component of the Elongator complex as no clear homologues of the other five Elongator subunits can be detected in genome sequences (Figure 5) (83).

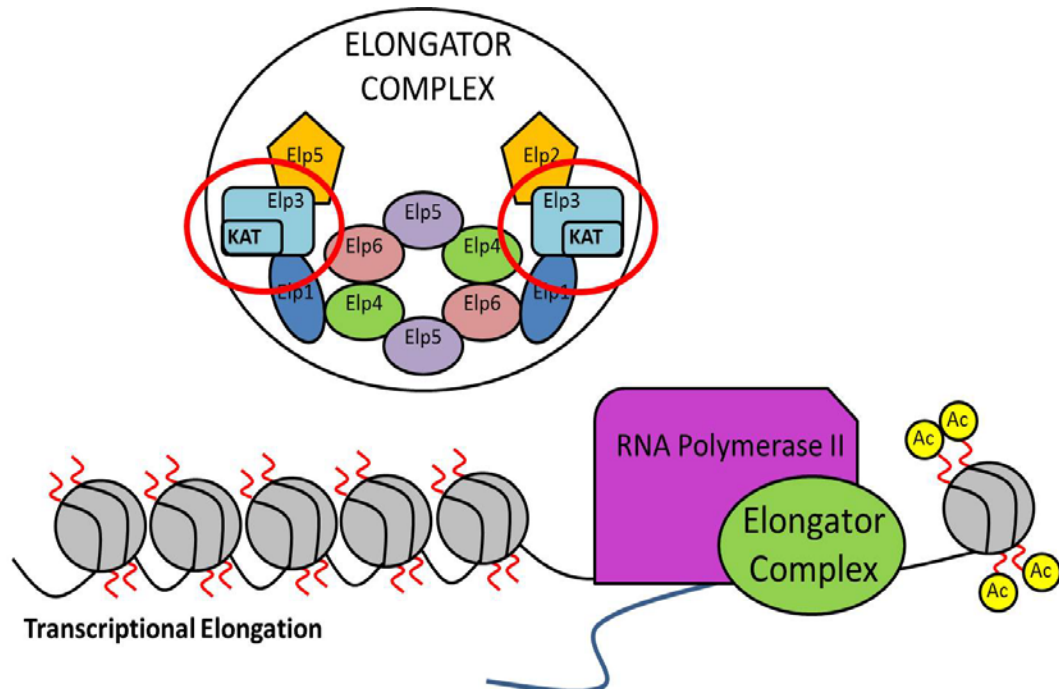


Figure 5. Elp3 is the only component of the Elongator complex found in *Toxoplasma*.

The Elongator complex consists of 6 core subunits (Elp1-Elp6) that dimerize and associated with RNAPII. Elp3 is the only subunit that contains known enzymatic domains and is responsible for acetylating histone tails to open up chromatin and facilitate transcriptional elongation. Ac=acetylated lysine.

Protein sequence alignments between *Toxoplasma* and other species determined that the catalytic KAT and rSAM domains are highly conserved and using an *in vitro* KAT assay, TgElp3 demonstrated acetyltransferase activity on histone H3 (83). Despite apparent enzymatic conservation, Elp3 homologues in *Toxoplasma* and other apicomplexans have some unique protein features. Specifically, there is an N-terminal protein extension and most strikingly, a C-terminal transmembrane domain (TMD) (83). Our laboratory found that the TMD is required for TgElp3 localization to the parasite's OMM (Figure 6) (83). Our laboratory also found that TgElp3 is a tail-anchored protein positioned with its catalytic domains protruding into the cytosol, representing the first tail-anchored lysine acetyltransferase reported in any species (83). Since localization of TgElp3 to the OMM is essential for *Toxoplasma* viability, examination of this protein and how it localizes to the parasite mitochondrion will provide insight into its evolutionary importance and may also identify novel therapeutic targets.

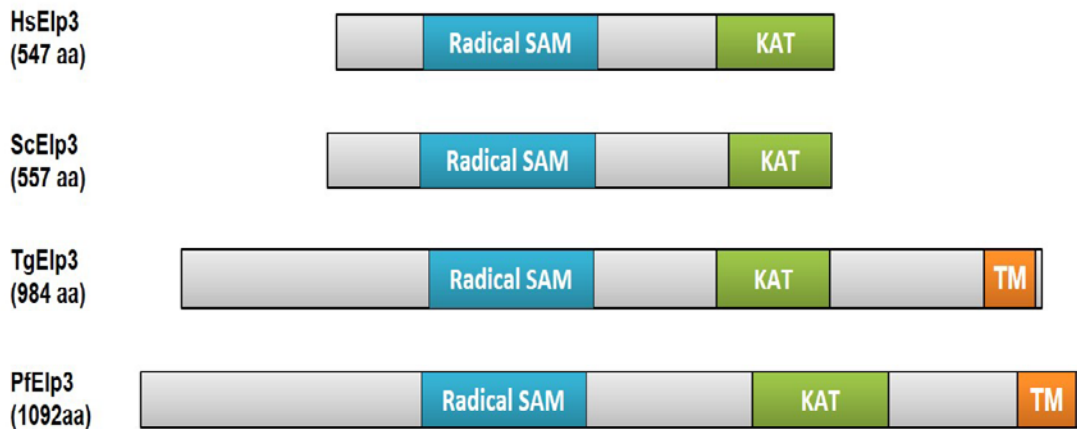


Figure 6. Comparison of Elp3 protein structure. Depiction of the conserved enzymatic domains from *Homo sapiens* (HsElp3), *Saccharomyces cerevisiae* (ScElp3), *Toxoplasma gondii* (TgElp3), and *Plasmodium falciparum* (PfElp3). The transmembrane domain is only present in the phylum Apicomplexa. Amino acids (aa); S-adenosylmethionine (SAM); lysine acetyltransferase (KAT); transmembrane (TM).

### 1.9 Summary and hypotheses

*Toxoplasma* is a prevalent pathogen that causes both acute and chronic infection. Current treatments only target the acute infection and are unable to completely clear the pathogen. Available drugs are problematic as they have serious side effects and/or cause allergic reactions. Identification of novel drug targets is needed to develop better therapies to treat *Toxoplasma* infection.

Disruption of protein acetylation in *Toxoplasma* is a viable approach to developing novel therapeutics. Our lab and others have shown that inhibition of lysine acetyltransferases and deacetylases is lethal to the parasite (61). However, the exact mechanisms of how these drugs work and/or what pathways they target is not fully understood. To increase our understanding of lysine acetylation in *Toxoplasma*, our lab has characterized several different lysine acetyltransferases including TgElp3. Examination of TgElp3 led to the identification of several unique features including the presence of a C-terminal transmembrane domain and localization to the OMM. Attempts to knockout the TgElp3 gene failed, suggesting that TgElp3 is essential for parasite viability.



Furthermore, using an *in vitro* lysine acetylation assay, our lab confirmed that TgElp3 has acetyltransferase activity on histone H3.

Given that TgElp3 possesses lysine acetyltransferase activity *in vitro*, localizes to the OMM and appears essential for *Toxoplasma* survival, **we hypothesize that TgElp3 lysine acetyltransferase activity at the outer mitochondrion is required for parasite viability.** Our hypothesis was examined by performing the following aims: 1) identify substrates of TgElp3, and 2) determine how TgElp3 is trafficked to the outer mitochondrial membrane. After performing several overexpression and mutational studies we identified that the rSAM domain is required for TgElp3 function. In other species, the rSAM domain is important for the formation of tRNA modifications. Therefore, **we subsequently hypothesized that overexpression of TgElp3 causes hypermodification of tRNA resulting in altered translation.** To test this hypothesis we explored the following aims: 1) determine if the Elp3 associated tRNA modification is present in *Toxoplasma*, and 2) assess protein synthesis in TgElp3 mutant parasite strains.

## CHAPTER 2: Characterization of TgElp3

### 2.1 Introduction

In other species, Elp3 has been implicated in a diverse array of enzymatic functions (96). Early studies in yeast and human cells identified Elp3 as a lysine acetyltransferase (62, 63, 67). *In vitro* studies determined histone H3 as a primary substrate of Elp3 and inactivation of the Elongator complex showed decreased acetylation *in vivo* (63, 67). With these studies, a working model emerged that Elp3 is the lysine acetyltransferase component of the Elongator complex, which promotes transcription through histone acetylation. Based on this model, Elp3 should primarily localize within the nucleus and associate with chromatin. In 2002, a pivotal study in yeast challenged this model as the Elongator complex was identified to mostly localize to the cytoplasm and could not be co-immunoprecipitated with chromatin (97). Furthermore, a subsequent study identified Elongator to associate with pre-mRNA and *in vitro* studies confirmed Elongator binds to RNA at a much higher affinity than DNA (98). In 2005, the first report of Elp3 as a tRNA modification enzyme showed that the Elongator complex is required for the synthesis of the 5-methoxycarbonylmethyl (mcm<sup>5</sup>) wobble uridine tRNA modification and that Elp3 co-immunoprecipitates with tRNA<sup>Glu</sup> in yeast (86). Given the diverse biological processes associated with Elp3, it is likely that Elp3 possesses multiple enzymatic functions, perhaps depending on the species, cell type, or subcellular localization.

We recently identified an unusual homologue of Elp3 in *Toxoplasma gondii* (TgElp3) that localizes to the outer mitochondrial membrane such that its catalytic domains face the cytosol (83). While the catalytic domains are conserved, TgElp3 is the only component of the six-subunit Elongator complex present (83). Using a lysine acetyltransferase assay, we have shown that TgElp3 can acetylate histone H3 *in vitro* (83). However, given the unique mitochondrial localization, histone H3 is an unlikely substrate for TgElp3 *in vivo*. Therefore, the biological role of TgElp3 remains unresolved; this chapter describes attempts to define the function of TgElp3.

## 2.2 Materials and Methods

### 2.2.1 Plasmid DNA construction

For all constructs, the In-Fusion HD cloning kit was used to insert DNA fragments into plasmid backbones (Clontech #011614). This directional cloning approach uses the In-Fusion Enzyme which efficiently fuses amplified DNA fragments containing 15 bp overlapping ends which match the destined backbone plasmid. Primers for each of the constructs are listed in Appendix A. The Phusion High Fidelity DNA Polymerase (Thermo Scientific #F530L) was used for all PCR amplification reactions. Details specific to each plasmid are below.

#### 2.2.1.1 BioID

*Toxoplasma* HA-tagged Elp3 cDNA was amplified using primers F1 and R1 from the previously published construct: TubHX-<sup>HA</sup>TgElp3 (83) and inserted into the HindIII restriction site of the pcDNA3.1mycBioID vector creating the mycBirA-<sup>HA</sup>TgElp3 fusion protein. Using primers F2 and R2 the fusion mycBirA-<sup>HA</sup>TgElp3 DNA sequence was amplified and inserted into the TubHX vector (99) digested with restriction enzymes EcorV and BglII. The construct design was confirmed through sequencing using primers F3 and R3.

#### 2.2.1.2 Endogenous Replacement

The upstream promoter region (~1500bp) of TgElp3 was amplified from RH $\Delta$ *hx* $\Delta$ *ku80* genomic DNA using primers F4/R4, and <sup>HA</sup>TgElp3 was amplified using primers F5/R5 from the previously published construct: TubHX-<sup>HA</sup>TgElp3 (83). These two PCR products were combined and used as template for a “stitching PCR” reaction using primers F4/R5. This reaction created the TgElp3prom+<sup>HA</sup>TgElp3cDNA PCR product. Next, the downstream region (~1500bp) of TgElp3 was amplified from RH $\Delta$ *hx* $\Delta$ *ku80* genomic DNA using primers F6 and R6. The TgElp3 downstream region amplicon was inserted into the HindIII restriction site of the pDHFR-TS plasmid (pDHFR-TS-dsElp3) (99, 100). This plasmid (pDHFR-TS-dsElp3) was then digested using DraIII and the

TgElp3prom+<sup>HA</sup>TgElp3cDNA PCR amplicon was inserted to create the <sup>HA</sup>TgElp3 endogenous replacement construct.

The QuickChange II XL Site-Directed Mutagenesis kit (Agilent Technologies. #200521) was used to generate the mutant constructs: <sup>HA</sup>TgElp3-rSAMmut(C284A) and <sup>HA</sup>TgElp3-KATmut(Y715/716A), using primers F7/R7 and F8/R8, respectively. Constructs were sequenced using primers F9 and R9. Prior to transfection, plasmids were linearized using the restriction enzyme SpeI. Parasites were screened for correct genomic integration using primers F10/R10 and F11/R11.

### 2.2.1.3 Destabilization Domain

The TubHX-DD-<sup>HA</sup>TgElp3 was previously created by Krista Stilger. To generate the mutant TubHX-DD-<sup>HA</sup>TgElp3 constructs, the QuickChange II XL Site-Directed Mutagenesis kit (Agilent Technologies. #200521) was used. Primers F7/R7 were used to create the TubHX-DD-<sup>HA</sup>TgElp3-rSAMmut(C284A) plasmid and primers F8/R8 were used to create the TubHX-DD-<sup>HA</sup>TgElp3-KATmut(Y715/716A) plasmid. Prior to transfection, plasmids were linearized using the NotI restriction digest enzyme.

### 2.2.1.4 Ectopic Overexpression

To generate the wild-type <sup>HA</sup>TgElp3<sup>OE</sup> construct, the open reading frame was amplified from RHΔ $hx$  cDNA and inserted at the BglIII restriction site within TubHX cloning vector (99). This vector uses the constitutively active *Toxoplasma* Tubulin promoter and contains an HXGPRT section marker. The QuickChange II XL Site-Directed Mutagenesis kit (Agilent Technologies. #200521) was used to generate the following mutant constructs: rSAM(C284A/C287A)<sup>OE</sup>, ΔTMD<sup>OE</sup>, KAT(Y715/716A)<sup>OE</sup>, KAT(Y716A)<sup>OE</sup>, KAT(Y715F/Y716F)<sup>OE</sup>, rSAM(C284A/C287A)/KAT(Y716A)<sup>OE</sup> and rSAM(C284A/C287A)/KAT(Y715F/Y716F)<sup>OE</sup>. Primers used for site-directed mutagenesis are listed in Appendix B. Site-Directed mutagenesis was performed multiple times using different primers to generate both cysteine mutations in the

rSAM domain and for the KAT+rSAM mutants. Prior to transfection each plasmid was linearized using the NotI restriction enzyme.

To overexpress TgElp3 in the type II ME49 parasite strain, wild-type TgElp3 was amplified from the <sup>HA</sup>TgElp3<sup>OE</sup> construct and inserted into the HindIII restriction site of the pDHFR plasmid using primers F12/R12.

#### **2.2.1.5 Recombinant TgElp3 expression vectors**

The TubHX<sup>HA</sup>TgElp3<sup>OE</sup> plasmid was used for all PCR reactions and full length TgElp3 without its TMD was amplified for all constructs unless otherwise stated. The F17/R17 primers were used to amplify TgElp3 which was inserted into the NdeI restriction site of the pET-19b plasmid (Novagen #69677) to generate the pET19b-10xHIS-EnzymaticElp3ΔTMD plasmid. The F18/R18 primers were used to amplify TgElp3 which was inserted into the NotI and NdeI restriction sites of the pET-30a (+) DNA plasmid (Novagen #69909) to generate the pET30a-EnzymaticElp3ΔTMD construct. Next, to generate the pGEX-4T-1-GST-EnzymaticElp3ΔTMD construct, the F19/R19 primers were used and the TgElp3 amplicon was inserted into the SmaI restriction site of the pGEX-4T-1 plasmid (GE Healthcare #28-9545-49).

Three 6xHIS-SUMO-Elp3 plasmids were generated with varying N-terminal extensions with full length 6HIS-SUMO-Elp3ΔTMD (primers F20/R20), partially truncated 6HIS-SUMO-Elp3ΔTMDshort1 (primers F20/R20.1), and removal of the N-terminus of TgElp3 just upstream of the rSAM domain, SUMO-Elp3ΔTMDshort2 (primers F20/R20.2). Each of these PCR amplicons was inserted into the SspI restriction site of the His6-Sumo-TEV (N terminal on backbone) vector (Addgene Plasmid #29659).

For the BacPAK<sup>TM</sup> (Clontech #631402) recombinant protein expression system, we used the BacPAK9 vector. We generated two constructs, a GST-tag and one with no tag. Primers F21 and R21 were used to amplify TgElp3 and this amplicon was inserted into the SmaI restriction site of the BacPAK9 plasmid. Primers F22 and R22 were used to amplify GST-Elp3 from the previously generated pGEX-4T-1-GSTconstruct; this amplicon was inserted into the SmaI

restriction site of BacPAK9. Construct designs were confirmed using sequencing primers F23/R23.

### **2.2.2 Parasite culture**

Since *Toxoplasma* is an intracellular pathogen, a host cell is required for parasite maintenance. For all experiments *Toxoplasma* was cultured in human foreskin fibroblasts (HFFs). HFFs were cultured with Dulbecco's Modified Eagle' Medium (DMEM) supplemented with 10% heat-inactivated fetal bovine serum (FBS) at 37°C and 5% CO<sub>2</sub>. The HFF medium was changed to DMEM supplemented with 1% FBS prior to parasite inoculation. Parasites were passed to a new confluent HFF flask once the host cell monolayer was completely lysed.

There are several common lab strains of *Toxoplasma* that were used throughout these studies. The RH $\Delta$ *hx* parasite strain is a hypervirulent type I strain that reproduces asexually by means of endodyogeny. This strain was originally isolated from a patient with the initials R.H. and has had the hypoxanthine-xanthine-guanine phosphoribosyl transferase (HXGPRT) gene knocked out ( $\Delta$ *hx*) for drug selection purposes (101). This RH $\Delta$ *hx* parasite strain was used for the BioID (section 2.3.1), inducible dominant-negative (section 2.3.3) and overexpression experiments (section 2.3.4). To facilitate double homologous recombination, the *ku80* gene was disrupted in the RH $\Delta$ *hx* parasite strain to generate RH $\Delta$ *hx* $\Delta$ *ku80* (102, 103). This parasite strain was used for the endogenous replacement studies (section 2.3.2). A third parasite strain used in section 2.3.4 is the type II ME49 strain. This parasite strain has a lower replication rate and exhibits a higher efficiency of tissue cyst formation *in vitro* and *in vivo* (104).

### **2.2.3 Generation of transgenic parasites**

To express various plasmids ectopically or to modify the endogenous locus, freshly egressed *Toxoplasma* tachyzoites were transfected. Prior to transfection, 25-75  $\mu$ g of DNA plasmid was linearized by restriction enzyme digest overnight to facilitate recombination (105). Following digestion,

Phenol:Chloroform:Isoamyl Alcohol was used to purify DNA. The precipitated DNA pellet was re-suspended in cytomix (120 mM KCl, 0.15 mM CaCl<sub>2</sub>, 10 mM K<sub>2</sub>HPO<sub>4</sub>/KH<sub>2</sub>PO<sub>4</sub> pH 7.6, 25 mM HEPES pH 7.6, 2 mM EDTA, 5 mM MgCl<sub>2</sub>, 1.2 mg/ml ATP, and 1.44 mg/ml glutathione), a buffer that mimics intracellular conditions and shown to increase parasite survival following electroporation (106).

For each transfection, approximately half of a freshly lysed T-25 cm<sup>2</sup> flask of parasites (~3 x 10<sup>7</sup> parasites) were washed and re-suspended in cytomix. Parasites were mixed with the re-suspended DNA and added to a 2 mm gap electroporation cuvette (Fisher #BTX620). For transfection, a BTX ECM 630 electroporator was used and the parasites were pulsed with 1.5 kV, 25 ohms and 25 µF (100, 107). Following transfection, parasites were split evenly between multiple flasks containing confluent HFF monolayers to isolate independent clones.

Drugs used for selection were added 24 hours post-transfection and parasites were maintained under selection for a minimum of three passages prior to isolation of individual clones. For plasmids containing the HXGPRT gene, 25 µg/mL of mycophenolic acid (MPA) and 50 µg/mL of xanthine (XAN) was used for selection (101). Parasites that do not possess a functional HXGPRT gene require inosine-monophosphate dehydrogenase (IMPDH) to synthesize guanine-based nucleotides (101). IMPDH is inhibited by MPA, resulting in death of parasites that have not integrated the exogenous plasmid containing the HXGPRT cassette. Parasites that have integrated the HXGPRT cassette with the addition of a guanine nucleotide precursor (XAN) can bypass the IMPDH pathway. A second selection cassette used in these studies contains the mutated dihydrofolate-thymidylate synthase (DHFR-TS) gene. DHFR-TS is required for *de novo* synthesis of purines and is inhibited by 1 µM pyrimethamine (100). Parasites that have integrated the mutated DHFR-TS gene are resistant to treatment with pyrimethamine.

Limiting dilution was used to isolate individual clones from populations of transfected parasites. Freshly egressed parasites were counted using a

hemocytometer and were diluted to 2.5 parasites/mL. Parasites were split into 96-well plates containing confluent HFFs and were left undisturbed for 5-7 days. The 96-well plates were screened for wells containing a single plaque, an indication of inoculation with a single parasite clone. Individual clones were transferred from the 96-well plate into two 24-well plates containing confluent HFFs. One plate was used for culturing until positive clones were identified and the second plate was used for screening. Endogenous replacement parasite clones were first screened by PCR and positive clones were confirmed by IFA and Western blot. Ectopic overexpressing parasite clones were first screened by IFA and positive clones were confirmed using Western blot. At least two positively identified clones from individual populations were further confirmed by sequencing.

Immediately following confirmation of correct transgene integration, positive clones were frozen down to create stocks for future use. A fifty percent lysed T-25 cm<sup>2</sup> flask of parasites was scraped and spun down. The resulting pellet was re-suspended in a 1:1 ratio of ice cold parasite medium to freezing mix (DMEM, 1% FBS and 25% DMSO) and then transferred into sterile cryogenic vials (Cole-Parmer #368632). The tubes were placed at -80°C in Styrofoam box for 24 hours before being moved to long term storage in liquid nitrogen.

#### **2.2.4 Affinity purification of biotinylated proteins**

Parasites were cultured in growth medium containing 50 µM biotin for 24 hours. Freshly egressed parasites were washed with phosphate buffered saline (PBS) and lysed with radio immunoprecipitation assay buffer (RIPA) buffer (20 mM Tris-HCL (pH 7.5), 150 mM NaCl, 1 mM Na<sub>2</sub>EDTA, 1 mM EGTA, 1% NP-40, 1% sodium deoxycholate, 2.5 mM sodium pyrophosphate, 1 mM β-glycerophosphate, 1 mM Na<sub>3</sub>VO<sub>4</sub>) supplemented with cOmplete™, Mini, EDTA-free protease inhibitor (Roche #11836170001) and sonicated twice for 30 seconds each time with a microtip sonicator. Lysate was incubated with magnetic Dynabeads MyOne™ Streptavidin C1 beads (Invitrogen # 65001) at 4°C for 12 hours on a rotator. Beads were washed twice with wash buffer 1 (2% SDS), once



with wash buffer 2 (0.1% deoxycholate, 1% Triton-X-100, 500 mM NaCl, 1 mM EDTA and 50 mM HEPES, pH 7.5), once with wash buffer 3 (250 mM LiCl, 0.5% NP-40, 0.5% deoxycholate, 1 mM EDTA and 10 mM Tris pH 8.1), twice with wash buffer 4 (50 mM Tris, pH 7.4 and 50 mM NaCl) and twice with PBS.

### **2.2.5 Mass spectrometry analysis**

A Thermo-Fisher Scientific LTQ Orbitrap Velos Pro mass spectrometer (Thermo-Fisher Scientific, Waltham, MA) interfaced with a Waters Acquity UPLC system (Waters, Milford, MA) was used for analysis. Samples were reduced with 10 mM DTT in 10 mM ammonium bicarbonate and then alkylated with 55 mM iodoacetamide. Alkylated samples (on bead) were digested by trypsin (Promega, Madison, WI) overnight at 37°C. Digested peptides were injected onto a C18 trapping column (NanoAcquity UPLC Trap column 180 µM x 20 mm, 5 µm, Symmetry C18) and subsequently onto an analytical column (NanoAcquity UPLC column 100 µm x 100 mm, 1.7 µm BEH130 C18). Peptides were eluted with a linear gradient from 3 to 40% acetonitrile in water with 0.1% formic acid developed over 90 minutes at room temperature at a flow rate of 500 nL/min, and the effluent was electro-sprayed into the LTQ Orbitrap mass spectrometer. Blanks were run prior to the sample to make sure there were no significant background signals from solvents or columns. SEQUEST(Thermo-Fisher Scientific) was used to search against ToxoDB (v10.0) to identify biotinylated proteins.

### **2.2.6 Antibodies**

The following primary antibodies were used at the dilutions indicated: rat anti-HA (1:2000, Roche #11867423001), rabbit anti-HA (1:2000, Cell Signaling Technology #3724), rabbit anti-TgE1p3 (1:2000), mouse anti-SAG1 (1:2000, Genway #MA1-83499), mouse anti-TgF<sub>1</sub>B-ATPase (1:4000) (108, 109), and mouse anti-puromycin clone 12D10 (1:2000, Sigma Aldrich #MABE343). Secondary HRP-linked antibodies for Western blot analysis included donkey anti-rabbit (1:2000, GE Healthcare #NA934), sheep anti-mouse (1:5000, GE

Healthcare #NA931) and goat-anti rat (1:2000, GE Healthcare #NA935). For IFA analyses, a 1:5000 dilution was used for secondary antibodies conjugated to a fluorophore (Alexa Fluor; Thermo Fisher #A11005, #A11006, #A11007 and #A11034).

### **2.2.7 Immunoblotting**

Infected HFFs containing intracellular parasites were scraped, syringe lysed with a 25-gauge needle and passed through a 3  $\mu$ m filter to remove host cell debris. Parasites were lysed in RIPA buffer supplemented with cOmplete™, Mini, EDTA-free protease inhibitor (Roche #11836170001) and sonicated three times on ice for 10 seconds with a microtip sonicator. Insoluble material was removed by centrifugation at 21,000 x g for 10 min at 4°C and cleared lysate was quantified using a detergent compatible (DC™) protein assay kit (Bio-Rad #5000111).

For each sample, equal amounts of protein were mixed with Laemmli sample buffer supplemented with 5% beta-mercaptoethanol and heated at 95°C for 10 min. Samples were centrifuged at 21,000 x g for 3 min and subjected to SDS-PAGE with precast 4 to 20% Mini-PROTEAN TGX gels (Bio-Rad #4568094). The Transblot SD semidry transfer system was used to transfer proteins to a nitrocellulose membrane (Bio-Rad #1703940). Blots were subjected to Ponceau S staining to ensure relatively equal protein loading and transfer. Membranes were then washed with Tris buffered saline-Tween 20 (TBST) and blocked with 5% milk-TBST for 30 min. Membranes were incubated with primary antibodies (see section 2.2.6) for 1.5 hr at room temperature or at 4°C overnight and then washed 3 x 10 min each time in TBST. Following the wash steps, membranes were incubated with secondary antibodies for 1 hr at room temperature and washed again for 3 x 10 min. Proteins were detected with SuperSignal™ West Femto Maximum Sensitivity Substrate (Thermofisher #34094) or Pierce™ ECL Plus Western Blotting Substrate (Thermofisher #32134) and imaged on a FluorChem R imager (Bio-Techne).

## **2.2.8 Immunofluorescence assays**

Freshly lysed parasites were inoculated onto confluent HFF monolayers grown on coverslips in a 24-well plate. Plates were fixed with 4% paraformaldehyde in PBS and blocked for 30 min in 3% BSA + PBS. Cells were permeabilized with 0.2% Triton X-100 in BSA-PBS for 10 min. Primary antibodies (see section 2.2.6) diluted in 3% BSA-PBS were applied overnight at 4°C. Coverslips were washed 3 x 10 min with PBS. Secondary antibodies diluted in 3% BSA-PBS were applied for 1 hr at room temperature and then washed for 3 x 10 min with PBS. The nucleic acid stain 4',6-diamidino-2-phenylindole dihydrochloride (DAPI, Life Technologies #D1306) diluted 1:1000 in PBS was applied for 10 min at room temperature and then washed 3 x 10 min at room temperature. Coverslips were mounted using Vectashield antifade mounting medium (Vector Labs #H-1000).

## **2.2.9 *Toxoplasma* growth assays**

### **2.2.9.1 Plaque Assay**

Plaque assays were used to assess parasite growth (110, 111). Intracellular parasites were harvested from the host cell monolayer by scraping, syringe lysing (25-gauge needle) and filtering through a 3.0 µm polycarbonate filter (Whatman). Parasites were counted using a hemocytometer and 500 parasites were inoculated into a single well of a 12-well plate containing confluent HFFs. For each assay, an individual parasite line was plated in triplicate. Four hours after inoculation, uninvaded parasites were removed and fresh medium was replaced. The cultures were incubated undisturbed for 6 days and then fixed with 100% ice-cold methanol. To visualize plaques, plates were stained with crystal violet. Pictures of individual plaques were taken at random using a Leica inverted DM16000B microscope (40x dry objective). The mean area of 30 plaques was measured using ImageJ for each of three independent experiments. For the RHΔ*hx* overexpression studies the plaque area was analyzed using two-way analysis of variance (ANOVA). For the ME49 overexpression studies, the plaque area was analyzed using the two-tailed student's t-test.

### **2.2.9.2 Doubling Assay**

Doubling assays were used to assess parasite replication (112, 113). Intracellular parasites were harvested as described above in section 2.2.9.1; 150,000 parasites were used to inoculate a HFF monolayer in a 6-well plate. The medium was changed after 4 hours to remove any uninvaded parasites. Plates were fixed at 18, 24, and 30 hours post inoculation using ice-cold methanol. To enhance visualization of the number of parasites within each vacuole, cells were stained using Diff Quick Stain Kit (Andwin Scientific). The number of parasites in 100 random vacuoles was counted for each parasite strain and the average number of parasites per vacuole was calculated; this assay was repeated three times. For the RH $\Delta$ hx overexpression studies, the average number of parasites per vacuole for each parasite line was analyzed using two-way ANOVA. For the ME49 overexpression studies, the average number of parasites per vacuole for each parasite line was analyzed using the two-tailed student's t-test.

### **2.2.10 $\gamma$ -toxin modification assay tRNA**

#### **2.2.10.1 RNA isolation**

Total RNA was extracted from both extracellular and intracellular parasites. For intracellular parasites two T-175 cm<sup>2</sup> flasks were scraped, syringe lysed using a 25-gauge needle and passed through a 3.0  $\mu$ m polycarbonate filter (Whatman) to remove host cell debris and washed three times in PBS. After the final wash, parasites were resuspended in 250  $\mu$ L of PBS and 750  $\mu$ L of TRIzol<sup>TM</sup> LS Reagent (Invitrogen) and RNA was isolated according to the manufacturer's protocol. For the extracellular parasite sample, two T-175 cm<sup>2</sup> flasks of freshly egressed parasites were filtered and further processed the same as the intracellular samples. The final RNA pellet was resuspended in 30  $\mu$ L of DEPC treated water and the RNA concentration was quantified using a Nanodrop. The absorbance of the RNA sample is measured at 260 and 280 nm. To check the quality of the total RNA and amount of host cell contamination, 3  $\mu$ g of RNA was run on a 0.8% agarose gel.

### 2.2.10.2 Characterization of tRNAs treated with $\gamma$ -toxin *in vitro*

For each sample, 5  $\mu$ g of total RNA was mixed with  $\gamma$ -toxin protein in 10 mM Tris-HCl, 10 mM MgCl<sub>2</sub>, 50 mM NaCl and 1mM dithiothreitol (pH 7.5) and incubated for 10 min at 30°C. The samples were separated on a 10% polyacrylamide, 8 M urea gel, and transferred to a Zeta-Probe membrane (Bio-Rad). Oligonucleotides used to detect tRNAs were 5'-GTATCCTAACCCACTAGACTACATGGGA-3' (Tg-tRNA<sup>Glu</sup>), 5'-TCTCCTTAACCACTCGGACACA-3' (Tg-tRNA<sup>Ser</sup>), 5'-CCAGGAATCCTAACCGCTAGACCATATGGGA-3' (Hs-tRNA<sup>Glu</sup>) and 5'-GCCTTAACCACTCGGCCATCACAGC-3' (Hs-tRNA<sup>Ser</sup>). Oligonucleotides were labeled by using adenosine [ $\gamma$ <sup>32</sup>P]-triphosphate (6000 Ci/mmol, Amersham Biosciences) and polynucleotide kinase (Roche Applied Science). Northern blots were visualized by autoradiography. These assays were performed in collaboration with Jenna Lentini and Dragony Fu at the University of Rochester.

### 2.2.11 Recombinant protein expression and purification

To produce recombinant TgEIp3 protein, bacteria (Rosetta<sup>TM</sup> 2(DE3) pLysS or ArticExpress<sup>TM</sup> competent cells) were grown to an OD600 of 0.6 in 500 ml of Luria broth containing ampicillin (or kanamycin) then induced with 0.5-1 mM isopropyl  $\beta$ -D-1-thiogalactopyranoside (IPTG) for 3-4 hrs at 37°C, or 1-3 hrs to overnight at 13°C. The Qiagen Ni-NTA Spin Kit (Qiagen # K950-01) under native conditions was used per the manufactures instructions. Briefly, the bacteria was pelleted at 3700 RPM for 30 min at 4°C. The pellet was re-suspended in lysis buffer (50 mM NaH<sub>2</sub>PO<sub>4</sub>, 300 mM NaCl, 10 mM imidazole, pH 8.0) supplemented with cComplete<sup>TM</sup>, Mini, EDTA-free protease inhibitor (Roche #11836170001), lysozyme (Roche #37059) and Benzonase Endonuclease (Novagen #706643). Lysates were incubated on ice for 30 mins and then centrifuged at 4°C for 20 mins and the insoluble pellet discarded. GST-tagged TgEIp3 antigen was purified over glutathione resin (Clontech cat# 635607) for at 3700 RPM 4 hrs at 4°C. The Ni-NTA column was equilibrated with lysis buffer and then loaded with cleared lysate containing His-Tagged-EIp3 and centrifuged at 1600 RPM for 10 mins at

4°C. The column was washed twice with wash buffer (50 mM NaH<sub>2</sub>PO<sub>4</sub>, 300 mM NaCl, 20 mM imidazole, pH 8.0). Elution buffer (50 mM NaH<sub>2</sub>PO<sub>4</sub>, 300 mM NaCl, 500 mM imidazole, pH 8.0) was added to the column to elute TgElp3 protein. Eluted protein was immediately stored in 20% glycerol. Protein was analyzed by Western blot, coomassie brilliant blue staining and/or silver staining.

For the GST-tagged proteins, a similar protocol was used except glutathione resin and different buffers were used. Briefly, the bacteria were pelleted and resuspended in GST buffer (125 mM Tris-HCl pH 8.0 and 150 mM NaCl) supplemented with cOmplete™, Mini, EDTA-free protease inhibitor (Roche #11836170001), lysozyme (Roche #37059), and Benzonase Endonuclease (Novagen #706643) and incubated on ice for 30 mins. Lysates were then centrifuged at 4°C for 20 mins and the insoluble pellet discarded. GST-tagged TgElp3 was purified over glutathione resin (Clontech cat# 635607) for 4 hrs at 4°C. GST-bound resin was washed 3 times with GST buffer followed by elution of GST-TgElp3 by incubating the resin in GST elution buffer (50 mM Tris-HCl pH 8.0 and 10 mM reduced Lglutathione) for 5 min at 4°C and collecting the supernatant.

The SF21 cell line derived from the fall army worm, *Spodoptera frugiperda* is used to propagate baculovirus. For these studies, we used Clontech's BacPAK™ expression according to the manufacturer's directions. Briefly, SF21 cells were maintained in Grace's Basic Medium (Clontech #631404) supplemented with yeastolate, lactalbumin hydrolysate, L-glutamine and 10% FBS at 27°C. Prior to transfection, plasmid DNA was purified using the Endotoxin-Free—NucleoBond Xtra Midi Plus EF kit (Clontech #740422.10). The BacPAK9-TgElp3 vector DNA was transfected using Bacfectin into the SF21 cells along with Bsu36I-digested BacPAK6 Viral DNA. *In vivo* homologous recombination between the plasmid and viral DNA rescues the viral DNA, and transfers the *TgElp3* gene to the viral genome. Five days after the addition of the Bacfectin-DNA mixture, the medium full of viruses was collected and stored at 4°C. The cells were collected and assessed for TgElp3 protein expression via Western blot, coomassie brilliant blue staining and/or silver staining. The collected virus

was propagated and used under various conditions as suggested in the manufacturer's protocol.

## **2.2.12 Analysis of protein synthesis**

### **2.2.12.1 Polyribosome profiling**

For polyribosome analysis, two T-175 cm<sup>2</sup> flasks of intracellular parasites were treated with 50 µg/mL of cycloheximide for 10 min (114, 115). Infected monolayers were scraped, syringe lysed using a 25-gauge needle and passed through a 3.0 µm polycarbonate filter (Whatman) to remove host cell debris and washed twice in ice-cold PBS containing 50 µg/mL of cycloheximide. Parasites were pelleted by centrifugation at 1000 x g for 10 min at 4°C and re-suspended in 500 µL of lysis buffer (20 mM Tris-HCL (pH 7.9), 150 mM NaCl, 10 mM MgCl<sub>2</sub>, 0.1% Triton, 50 µg/mL cycloheximide, and 0.04 U/µL RNaseOUT™ Recombinant Ribonuclease Inhibitor (ThermoFisher #10777019)). Parasites were passed through a 25-gauge needle several times to facilitate parasite lysis followed by a 10 min incubation on ice. Insoluble proteins were cleared by centrifugation at 21,000 x g for 10 min at 4°C and 400 µL of lysate was layered onto 10 to 50% sucrose gradients prepared in lysis buffer without Triton or RNaseOUT™ Recombinant Ribonuclease Inhibitor. Polyribosome complexes were resolved by centrifugation using a Beckman Coulter SW41Ti rotor at 40,000 rpm at 4°C for 2 hr. Gradients were fractionated by a BioComp Instruments gradient station and the absorbance was measured using an ISCO UA-6 absorbance monitor set at 254 nm.

### **2.2.12.2 Surface Sensing of Translation (SUnSET)**

To determine if the Surface of Sensing of Translation (SUnSET) technique could be used to assess protein synthesis in *Toxoplasma*, we assessed the incorporation of puromycin in freshly egressed RHΔ*hx* parasites. Approximately 2.5 x 10<sup>6</sup> parasites were incubated with 10 µg/mL puromycin (SIGMA #P8833) for 15 min before or after incubation with 100 µg/mL

cycloheximide for 10 min. Cells were pelleted and processed for Western blot analysis the same as referenced above in section 2.2.7.

To visually assess puromycin incorporation by IFA, confluent HFF monolayers grown on coverslips in a 24-well plate were inoculated with RH $\Delta$ *hx* parasites. To limit the amount of puromycin incorporation into the host cell and reduce host cell background, HFF cells were at least two weeks old before inoculation with parasites (116). Twelve hours post infection, 10  $\mu$ g/mL puromycin was added for 15 min before or after incubation with 50  $\mu$ g/mL cycloheximide (SIGMA #C7698) for 1 hr. Coverslips were fixed and processed for IFA analysis as referenced above in section 2.2.8.

To assess protein synthesis in parental RH $\Delta$ *hx* and <sup>HA</sup>TgElp3<sup>OE</sup> strains, the same procedure referenced above was followed except incubation times without or with 10  $\mu$ g/mL puromycin were for 10, 20 and 30 min. For intracellular parasites, 2 x T175 cm<sup>2</sup> flasks were each inoculated with 3.5 x 10<sup>6</sup> parasites. Puromycin was added (10  $\mu$ g/mL) 42 hr post infection. Following treatment, parasites were harvested at 10, 20 and 30 min. To remove host cell debris, flasks were scraped, syringe lysed (25-gauge needle) and passed through a 3.0  $\mu$ M polycarbonate filter. Samples were washed twice with ice-cold PBS and processed for Western blot analysis (section 2.2.7).

Since active translation is occurring in the HFF monolayer, the background signal can be high. High background can confound interpretation of puromycin signals. To circumvent this problem, we used a co-culture approach in which 3 x 10<sup>5</sup> parasites of each parasite line (RH $\Delta$ *hx* and <sup>HA</sup>TgElp3<sup>OE</sup>) were inoculated onto a single coverslip containing a confluent HFF monolayer. Medium was changed 4 hr post-infection to remove uninvaded parasites and puromycin (10  $\mu$ g/mL) was added 30 hr post-infection for 10, 20, and 30 mins. Coverslips were immediately fixed and processed for IFA analysis as referenced in section 2.2.8.



## 2.3 Results and Discussion

### 2.3.1 Attempt to identify TgEIp3 interacting proteins using BioID

To identify TgEIp3 substrates in *Toxoplasma* we performed the recently developed proximity dependent identification (BioID) assay (117, 118). BioID is an *in vivo* technique that allows for the identification of nearby proteins and potential interacting partners within a native biological environment (117). The BioID approach utilizes the fusion of a promiscuous biotin protein ligase from *Escherichia coli* to a target protein (e.g. TgEIp3); expression of this fusion protein in the presence of biotin results in proximity-dependent biotinylation of proteins within 10-20 nm to the fusion protein (117) (Figure 7).

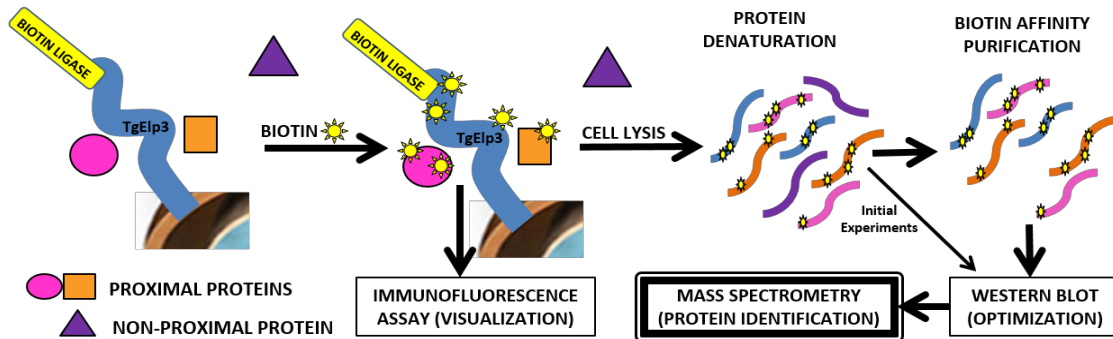


Figure 7. BioID experimental workflow.

Expression of a promiscuous biotin-ligase fused to TgEIp3 (BL-<sup>HA</sup>TgEIp3) in live parasites and incubation with biotin for 24 hrs leads to the selective biotinylation of proteins proximal to TgEIp3. Biotinylation of proteins is confirmed by IFA and Western blot analysis. For protein identification, cells are lysed and biotinylated proteins are affinity purified and subjected to mass spectrometry.

To identify TgEIp3 substrates we used the RH $\Delta$ *hx* parasite line to ectopically overexpress a BiotinLigase-<sup>HA</sup>TgEIp3 (BL-<sup>HA</sup>TgEIp3) fusion protein. Mitochondrial localization was confirmed by immunofluorescence assay (IFA) (Figure 8). To assess biotinylation, BL-<sup>HA</sup>TgEIp3 parasites were incubated with vehicle (negative control) or 50  $\mu$ M biotin for 24 hours and biotinylation was assessed by IFA and Western blot (Figure 8). As expected, we observed mitochondrial enrichment of biotinylated proteins with the biotin signal predominantly co-localizing with BL-<sup>HA</sup>TgEIp3; additionally, increased

biotinylation was observed in the biotin treated samples compared to vehicle by Western blot (Figure 8), indicating the biotin ligase fused to TgEIp3 is functional.

To identify TgEIp3 proximal proteins, BL-<sup>HA</sup>TgEIp3 and parental RHΔ*hx* parasites (negative control) were incubated with 50μM biotin for 24 hours. Parasites were lysed in RIPA buffer and brief sonication was performed to ensure complete lysis. Total lysate was subjected to affinity purification with streptavidin conjugated magnetic beads and captured biotinylated proteins were assessed by Western blot (Figure 8). Biotinylated proteins were observed in both the parental RHΔ*hx* and BL-<sup>HA</sup>TgEIp3 parasite strains, however, as expected there were significantly more biotinylated proteins detected in the BL-<sup>HA</sup>TgEIp3 parasite sample.

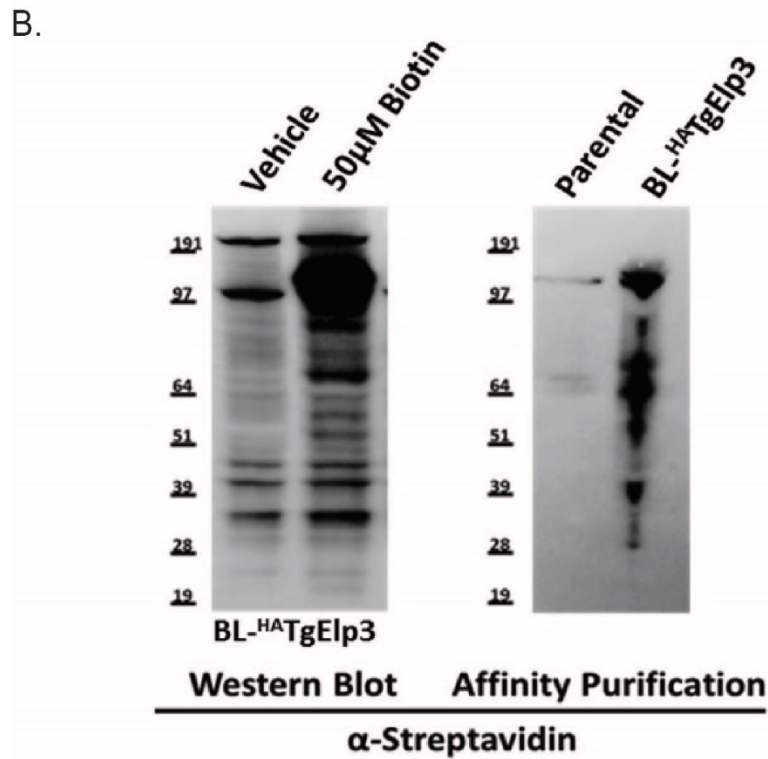
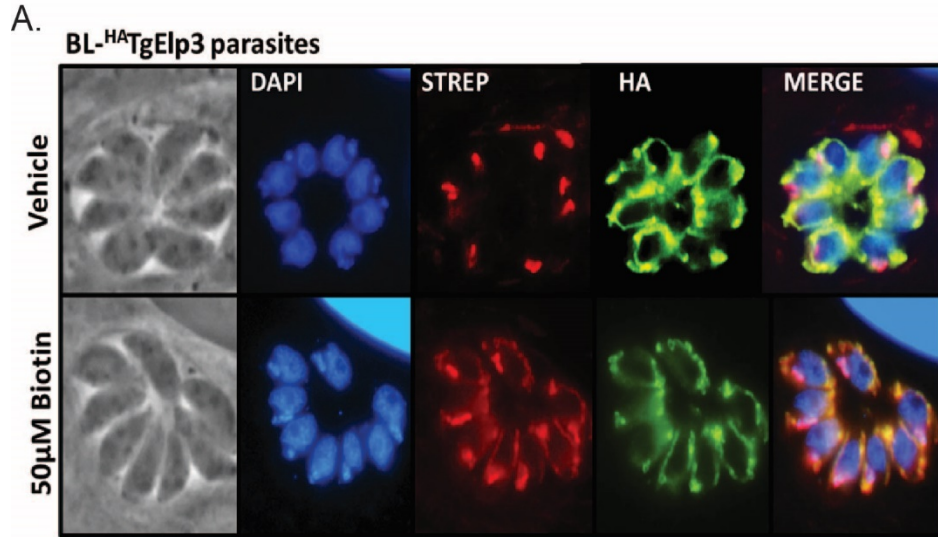


Figure 8. Identification of proximal TgElp3 proteins.  
 A. Immunofluorescence assay of BL<sup>HA</sup>.TgElp3 parasites at 24hrs treated with vehicle or 50  $\mu$ M biotin.  $\alpha$ -Streptavidin (red) detecting biotinylated proteins,  $\alpha$ -HA (green) detecting BirA<sub>HA</sub>TgElp3 merged with the DNA stain DAPI (blue). B. Total protein isolated from BL<sup>HA</sup>-TgElp3 expressing parasites treated with vehicle or 50  $\mu$ M biotin, probed with anti-Streptavidin; affinity purification of biotinylated proteins using  $\alpha$ -streptavidin beads from parental RH $\Delta$ hx and BL<sup>HA</sup>-TgElp3 treated with 50 $\mu$ M biotin for 24hrs. Protein eluted from beads and probed with anti-Streptavidin.

Since the amount of precipitated proteins was greater in the BL-<sup>HA</sup>TgElp3 sample, and many of the bands appeared unique, we hypothesized that these were likely potential substrates of TgElp3. Therefore we scaled up the affinity purification of biotinylated proteins and submitted the samples to the Indiana University School of Medicine mass spectrometry core facility for analysis. This analysis identified eight proteins unique to the BL-<sup>HA</sup>TgElp3 sample including TgElp3 (Table 1). To confirm specificity of these proteins, we repeated the affinity purification and mass spectrometry analysis for a total of three independent trials. Our second and third analyses identified eleven and fifteen proteins unique to the BL-<sup>HA</sup>TgElp3 sample (Table 1). TgElp3 was detected in all three BL-<sup>HA</sup>TgElp3 samples indicating the BioID assay worked. However, aside from TgElp3 no other proteins were consistently detected in all three trials. Therefore, we concluded that this approach was not reliably identifying potential TgElp3 substrates.

Table 1. Proteins uniquely biotinylated in BL-<sup>HA</sup>TgElp3 expressing parasites. Proteins identified in each experiment (Exp.) are listed with the number (No.) of peptides detected in order by accession number. Elp3 (bold) was the only protein detected in all three trials.

Exp.	Accession Number	Description	No. of Peptides
3	TGME49_002760	hypothetical protein	1
3	TGME49_005470	translation elongation factor 2 family protein, putative	2
3	TGME49_005580	hypothetical protein	1
1	TGME49_023940	hypothetical protein	3
3	TGME49_028630	hypothetical protein	1
2	TGME49_059630	hypothetical protein, conserved	1
3	TGME49_066640A	acetyl-coenzyme A synthetase, putative	2
2	TGME49_115610	hypothetical protein	1
2	TGME49_204020	60S ribosomal protein L8, putative	2
1	TGME49_216000	IMC3	2
2	TGME49_218260	histone H3.3 variant	2
2	TGME49_218520	microneme protein MIC6	1
3	TGME49_219140	EF-1 guanine nucleotide exchange domain-containing protein	1
3	TGME49_219630	flavodoxin domain-containing protein	1
3	TGME49_226410	EF-1 guanine nucleotide exchange domain-containing protein	2
1	TGME49_230940	hypothetical protein	3
3	TGME49_232940	heat shock protein HSP20	1
1	TGME49_235470	myosin-A	2
3	TGME49_267390	DNA-directed RNA polymerases I and III subunit RPAC1, putative	1
2	TGME49_282055	protein phosphatase PP2C-hn	1
1	TGME49_286420	elongation factor 1-alpha, putative	3
2	TGME49_288720	60S ribosomal protein L10, putative	1
1	TGME49_290660	RNA recognition motif-containing protein	2
3	TGME49_294670	translation initiation factor 3 subunit	2
2	TGME49_294800	putative elongation factor 1-alpha (EF-1-ALPHA)	1
2	TGME49_300200	histone H2AZ	1
3	TGME49_300200	histone H2AZ	1
<b>1</b>	<b>TGME49_305480</b>	<b>elongator complex protein ELP3</b>	<b>6</b>
<b>2</b>	<b>TGME49_305480</b>	<b>elongator complex protein ELP3</b>	<b>5</b>
<b>3</b>	<b>TGME49_305480</b>	<b>elongator complex protein ELP3</b>	<b>10</b>
3	TGME49_311230	hypothetical protein	2
2	TGME49_316400	alpha tubulin TUBA1, partial	2
3	TGME49_324600	heat shock protein	2
1	TGME49_411760	actin	2

### 2.3.2 Endogenous replacement of TgElp3

Considering that previous attempts to knockout TgElp3 have failed and localization at the mitochondrion is essential for parasite viability, we sought to characterize the molecular function of TgElp3 (83, 119). Since TgElp3 possesses two highly conserved enzymatic domains (radical S-adenosylmethionine (rSAM) and lysine acetyltransferase (KAT) domain) (83), we decided to take a targeted mutational approach to determine which domain(s) is required for TgElp3 function. As a control, we replaced the endogenous locus with hemagglutinin (HA)-tagged wild-type cDNA (<sup>HA</sup>TgElp3) in RHΔ*hxΔku80* parasites; recombination frequency was ~50%. Correct integration was confirmed by PCR and protein expression was assessed by Western blot and IFA analyses using the anti-TgElp3 and anti-HA antibodies (Figure 9). To determine if parasites could survive when either the radical SAM or KAT domains were mutated, we generated two more <sup>HA</sup>TgElp3 allelic replacement constructs: rSAM mutant (C284A) and KAT mutant (Y715A/Y716A); in other species, these rSAM and KAT mutations are critical for Elp3 function (68, 82, 84, 120). Despite several attempts, we were unable to generate rSAM or KAT mutants at the endogenous TgElp3 locus. Since the endogenous replacement of TgElp3 with wild-type recombinant <sup>HA</sup>TgElp3 was obtained, we conclude that both enzymatic domains are likely required for TgElp3 function.

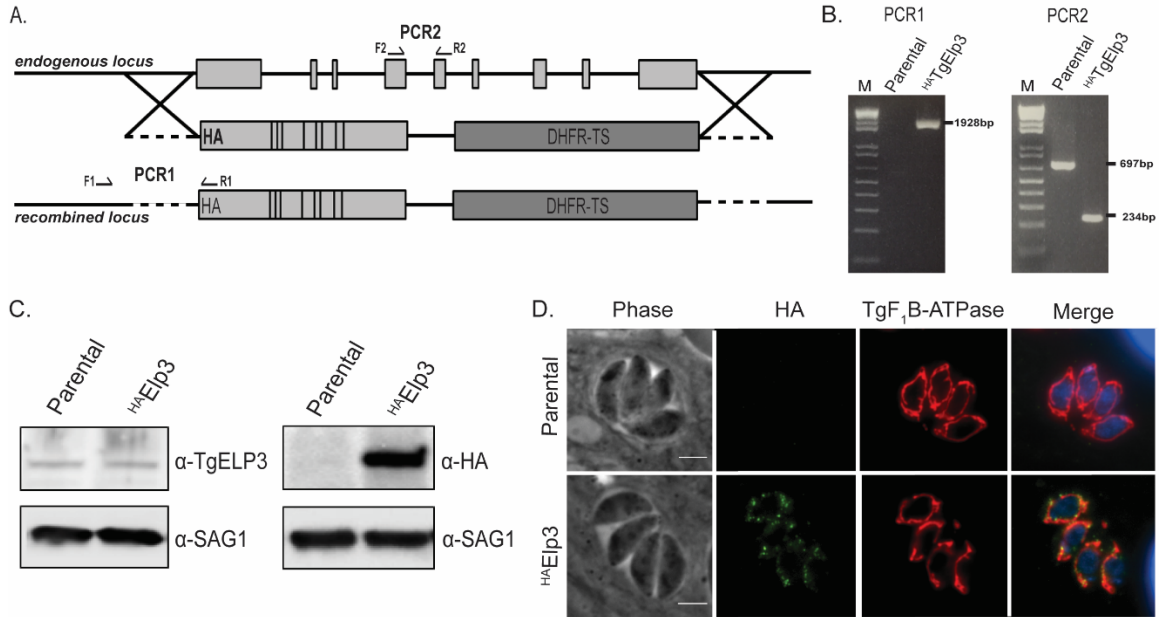


Figure 9. Endogenous tagging of TgElp3.

A. Diagram of the construct used to replace the endogenous TgElp3 locus by double homologous recombination. Arrows indicate location of PCR primers. For PCR1, the forward primer is located upstream of the recombination site and the reverse primer is located in the HA-tag. The PCR2 primers are intron spanning. B. Correct integration of <sup>HA</sup>TgElp3 at the endogenous locus is confirmed by PCR analysis. C. For each sample, 100 µg of protein was used for Western blot analysis of parental RHΔ*hxΔku80* and <sup>HA</sup>TgElp3 parasites. The blot was probed with anti-TgELP3, anti-HA and anti-SAG1 antibodies as a loading control. D. IFAs stained for anti-HA (green) and the mitochondrial maker anti-TgF<sub>1</sub>B-ATPase (red). Images merged with the DNA stain DAPI (blue). Scale bar, 3µm.

### 2.3.3 Expression of catalytically inactive TgElp3 using an inducible destabilization domain

As an alternative strategy to assess if both KAT and rSAM domains are required for TgElp3 function we used an inducible dominant-negative strategy. For this approach, we fused a destabilization domain (dd) onto TgElp3 which directs proteins to the proteasome for degradation; however, in the presence of the ligand Shield-1, the fusion protein is stabilized (121, 122). The constitutively active tubulin promoter was used to ectopically express dd fused to the N-terminus of <sup>HA</sup>TgElp3. Using the same wild-type and mutation sequences referenced above, we generated three clonal parasite strains in the RHΔ*hx* background: <sup>ddHA</sup>TgElp3, <sup>ddHA</sup>TgElp3-KATmut and <sup>ddHA</sup>TgElp3-rSAMmut. Initial

experiments to assess proteasomal rescue by Shield-1 were performed by IFA. With increased concentrations of Shield-1 (0-500nM), we observed an increase of  $^{ddHA}$ TgElp3 protein expression; however, removing Shield-1 for 24 hours did not result in the loss of  $^{ddHA}$ TgElp3 (Figure 10). Furthermore,  $^{ddHA}$ TgElp3 protein expression showed variability between parasite vacuoles (Figure 10). Since regulation of protein expression is dependent on degradation by the proteasome and TgElp3 traffics to the mitochondrion, we hypothesize that some  $^{ddHA}$ TgElp3 protein likely bypasses proteasome degradation by insertion into the mitochondrion via its TMD. Once anchored to the OMM,  $^{ddHA}$ TgElp3 protein is stabilized independent of Shield-1 concentrations. Considering elucidation of TgElp3 function requires tight regulation of protein expression and our preliminary experiments show inconsistent  $^{ddHA}$ TgElp3 protein control by Shield-1, we did not feel that this approach would be reliable for elucidating TgElp3 function.

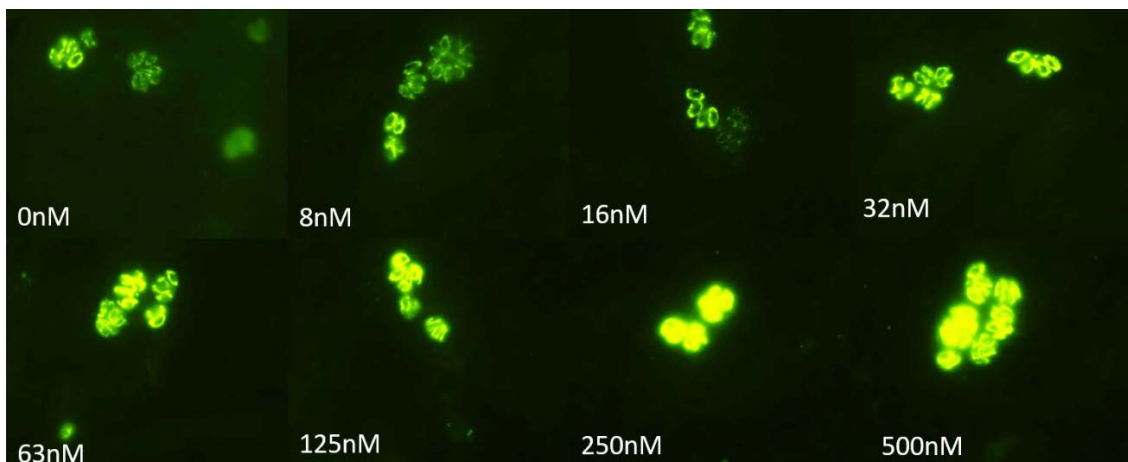


Figure 10.  $^{ddHA}$ TgElp3 protein regulation by Shield-1. Clonal  $^{ddHA}$ TgElp3 were maintained in 100nM shield. Freshly egressed parasites were inoculated onto coverslips containing a HFF monolayer. Medium was replaced with fresh medium with or without Shield-1 at various concentrations 2 hr post-infection. Plates were fixed at 24 hr and stained for anti-HA (green).  $^{ddHA}$ TgElp3 protein expression was still present without shield and variation of  $^{ddHA}$ TgElp3 expression was observed between vacuoles within the same treatment.



### **2.3.4 Overexpression of wild-type and mutant TgElp3**

Gene dosage is important for normal gene function and since we were unable to knockout, endogenously mutate or use an inducible dominant negative approach to study TgElp3, we sought to determine if overexpression of TgElp3 would be tolerated. We engineered a construct to ectopically overexpress <sup>HA</sup>TgElp3 driven by the constitutively active tubulin promoter. This construct was transfected into the RH $\Delta$ *hx* parasite strain and several independent clones were obtained. Overexpression of TgElp3 was confirmed by Western blot using the anti-TgElp3 and anti-HA antibodies (Figure 11). IFA analyses confirmed TgElp3 localization to the parasite mitochondrion using the established mitochondrial marker F<sub>1</sub>B ATPase (108, 109) (Figure 11).

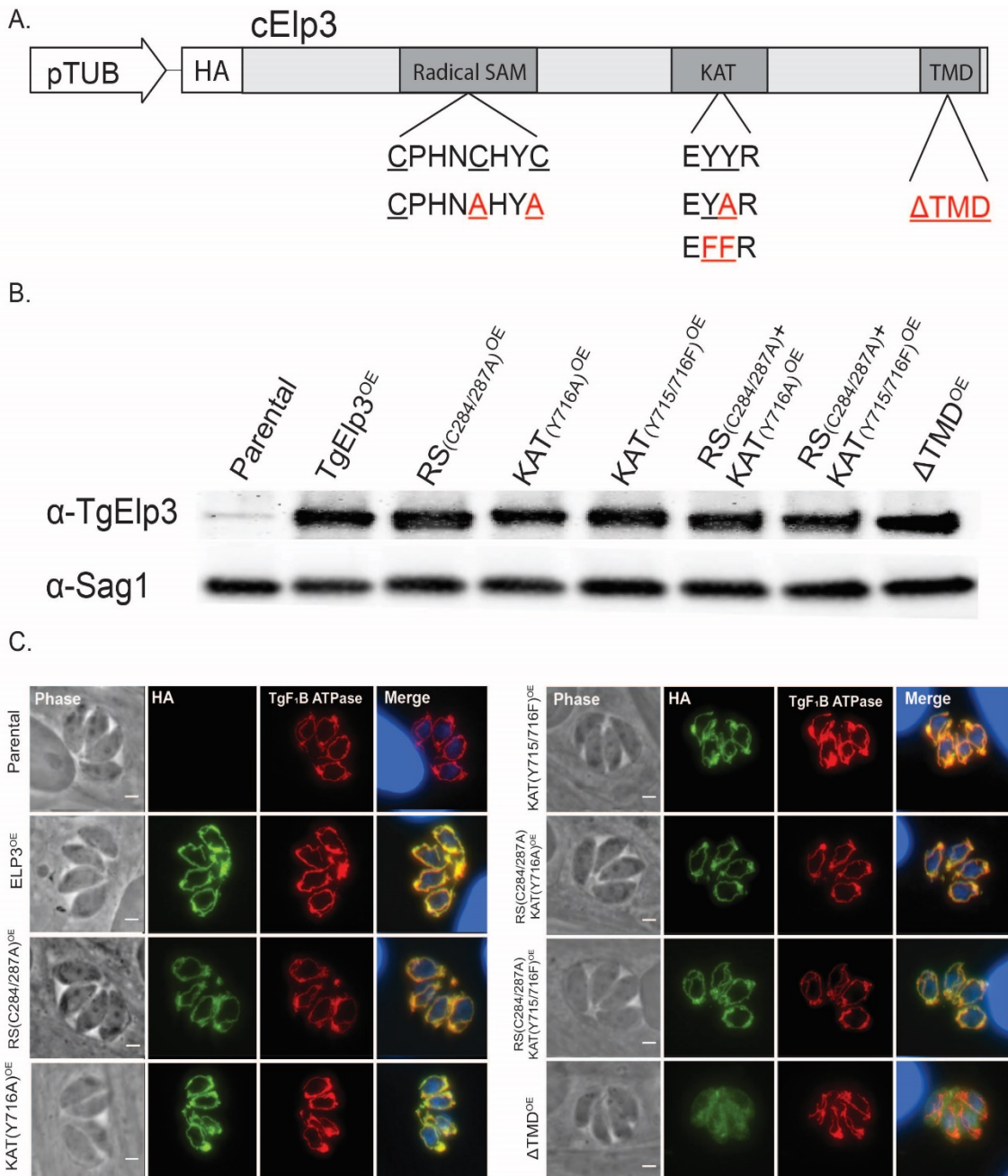
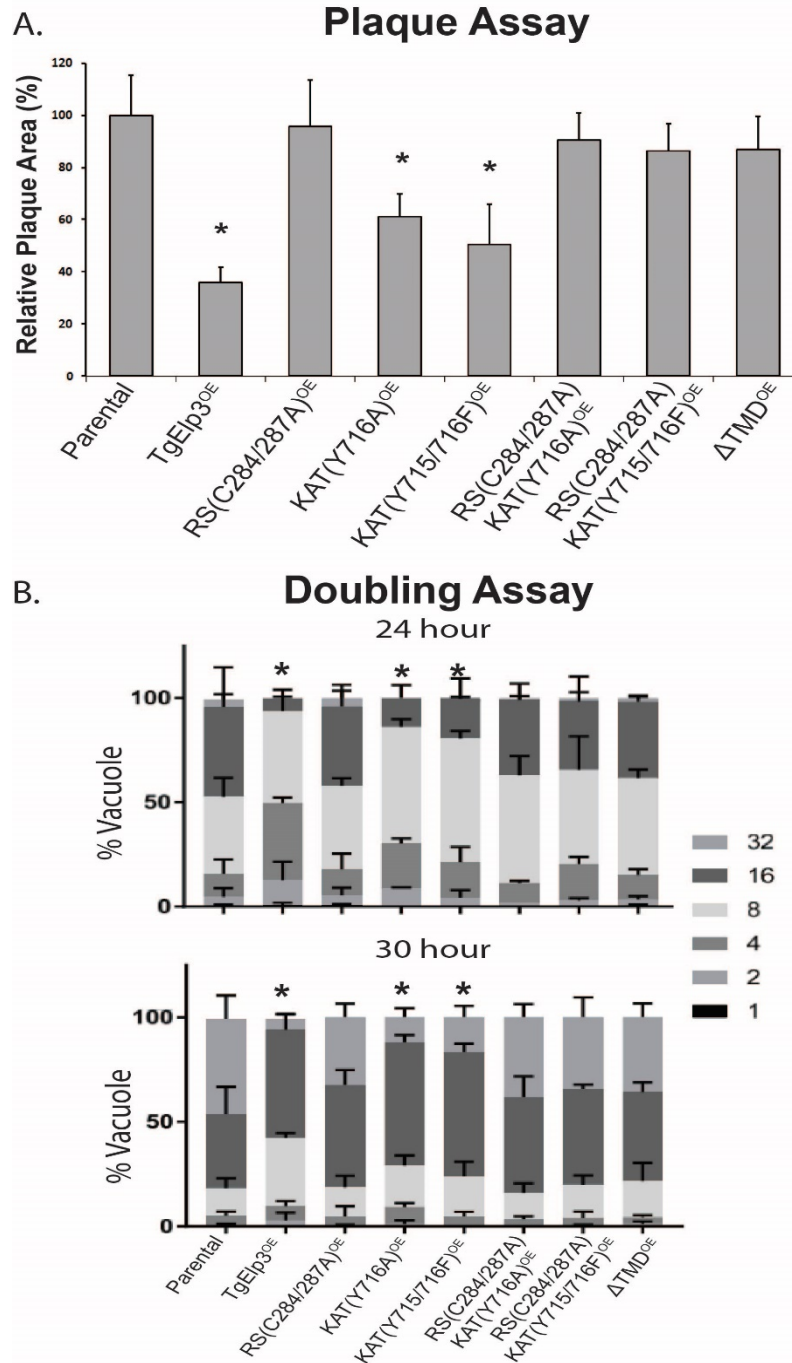


Figure 11. Overexpression of  $^{HA}TgElp3^{OE}$  in *Toxoplasma gondii*.  
 A. Schematic of the construct used to express  $^{HA}TgElp3^{OE}$  and various mutant forms. The constitutive tubulin promoter (pTub) was used to express full length HA-tagged TgElp3 cDNA (cElp3). Letters in red represent mutated amino acids.  
 B. Western blot analysis of protein (100  $\mu$ g) isolated from parental RH $\Delta$ hx,  $^{HA}TgElp3^{OE}$  and mutant  $^{HA}TgElp3^{OE}$  parasite strains using anti-TgElp3 and anti-SAG1 as a loading control.  
 C. IFA assay using anti-HA to detect TgElp3 (green), anti-TgF<sub>1</sub>B ATPase a known mitochondrial marker (red) merged with the DNA stain DAPI (blue), scale bar 3 $\mu$ m.

Upon initial observation, <sup>HA</sup>TgElp3 overexpressing parasites (<sup>HA</sup>TgElp3<sup>OE</sup>) appeared to grow slowly in culture. A plaque assay quantitatively confirmed a growth defect in the <sup>HA</sup>TgElp3<sup>OE</sup> parasites compared to the parental line (Figure 12). To further investigate this growth defect, we performed a doubling assay to assess parasite replication. <sup>HA</sup>TgElp3<sup>OE</sup> parasite replication rate was significantly slower at the 24 and 30 hour time points (Figure 12). This replication defect was observed in multiple independent clones and further confirmed in an independent type II <sup>HA</sup>TgElp3<sup>OE</sup> parasite strain (ME49) (Figure 13).

Interestingly, after passing the <sup>HA</sup>TgElp3<sup>OE</sup> parasites for several weeks (approximately 115 replications), some of the parasites would adapt and resume a normal replication rate; these adapted parasites were no longer expressing the <sup>HA</sup>TgElp3 ectopic copy as determined by IFA analysis. Loss of overexpression resulted in a mixed population of parasites and gradual restoration of growth. This occurred on multiple occasions and therefore the <sup>HA</sup>TgElp3<sup>OE</sup> parasites were routinely checked by IFA to ensure each assay was performed with a clonal parasite line. With the observed replication defect and frequent adaptation, we conclude that overexpression of TgElp3 is not well tolerated and there is strong selective pressure in *Toxoplasma* to silence its expression.



To investigate why TgElp3 overexpression is not well tolerated, we considered two possibilities: (1) independent of TgElp3 function, increased levels of protein at the OMM may generally induce mitochondrial dysfunction, and (2) the replication defect is specific to the enzymatic activity of TgElp3 at the mitochondrion. To address these possibilities we generated several mutant  $^{HA}TgElp3^{OE}$  constructs: rSAM(C284A/C287A) $^{OE}$ , KAT(Y715/716A) $^{OE}$  and a construct containing a premature stop codon to remove the transmembrane domain ( $\Delta TMD^{OE}$ ). Since we cannot control for the number of ectopic gene copies or where they integrate within the genome, at least two independent clonal parasite lines with equal TgElp3 protein expression were acquired for each of the mutant constructs (Figure 11).

Surprisingly, we were unable to obtain a KAT(Y715/716A) $^{OE}$  clone with TgElp3 protein expression comparable to the other overexpressing parasite strains. We hypothesized that the two tyrosine to alanine mutations may render the protein unstable. Therefore, we decided to generate two more versions of the KAT mutant overexpressing construct: (1) mutate a single tyrosine to alanine (Y761A), and (2) mutate both tyrosine residues to phenylalanine (Y715F/Y716F), a more physiologically relevant substitution. Using both of these KAT mutant constructs we easily obtained clonal parasites expressing TgElp3 protein comparable to the other overexpressing lines (Figure 11). In addition, we generated two double mutant parasite lines, each containing a rSAM and KAT mutation: (1) rSAM(C284A/C287A)/KAT(Y716A) $^{OE}$ , and (2) rSAM(C284A/C287A)/KAT(Y715F/Y716F) $^{OE}$  (Figure 11). For all parasite strains, protein expression was assessed by Western blot and localization at the mitochondrion (except for  $\Delta TMD^{OE}$ ) was confirmed by IFA using the anti-HA antibody (Figure 11).

Using the transgenic  $^{HA}TgElp3^{OE}$  parasite lines, we performed a plaque assay to assess parasite growth. Interestingly, compared to parental parasites, the KAT(Y761A) $^{OE}$  and KAT(Y715F/Y716F) $^{OE}$  parasites as well as the previously characterized wild-type  $^{HA}TgElp3^{OE}$  parasites all grew significantly slower (Figure 12). In contrast, parasites expressing a rSAM mutation or mislocalized TgElp3

( $\Delta$ TMD<sup>OE</sup>) grew at the same rate as parental parasites (Figure 12). Doubling assays were performed to assess parasite replication. Consistent with the plaque assay growth defect results, a significant replication defect was detected in the wild-type <sup>HA</sup>TgEIp3<sup>OE</sup>, KAT(Y761A)<sup>OE</sup> and KAT(Y715F/Y716F)<sup>OE</sup> parasite lines at 24 and 30 hour time points (Figure 12). Assuming these mutations ablate KAT activity, these data suggest that KAT activity is not associated with the slowed growth phenotype.

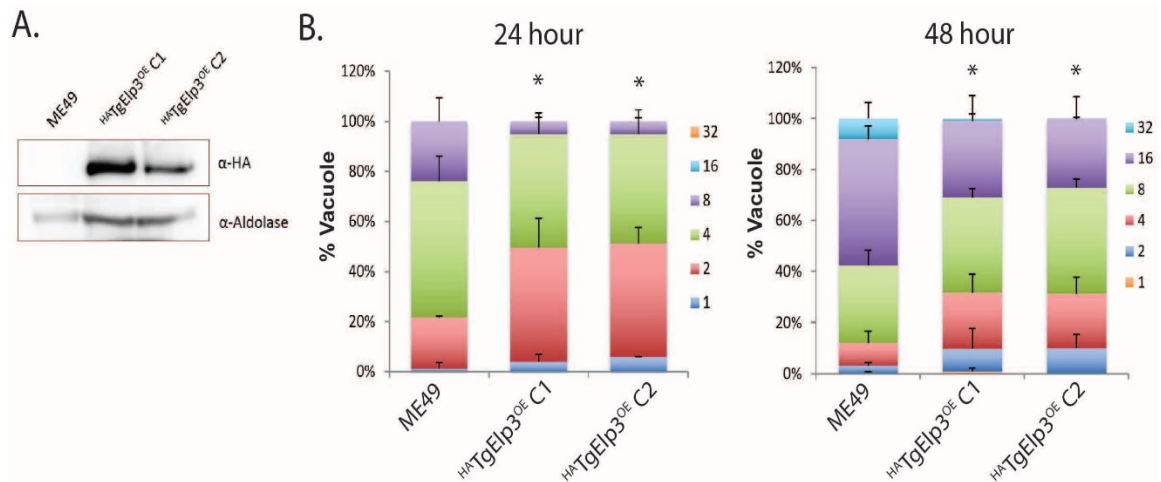


Figure 13. Overexpression of TgEIp3 in the ME49 parasite strain. A. Western blot analysis of parental ME49 and two independent <sup>HA</sup>TgEIp3<sup>OE</sup> clonal isolates (designated C1 and C2) using anti-HA and anti-aldolase as a loading control. B. Doubling assays were performed to assess parasite growth. The infected cultures were examined at 24 hr and 48 hr time points. Parasite replication was monitored by quantifying the number of parasites in 100 random vacuoles. The number of parasites per vacuole is shown \**P*<0.05 (two-tailed student's t-test).

Also consistent with the plaque assays, overexpression of TgEIp3 harboring a rSAM mutation or mislocalized <sup>HA</sup>TgEIp3<sup>OE</sup> ( $\Delta$ TMD<sup>OE</sup>) did not alter parasite replication. Considering that all of the TgEIp3 rSAM mutant overexpressing parasites grew the same as parental, we conclude that increased TgEIp3 at the OMM does not physically interfere with mitochondrial function and that the rSAM domain is essential for TgEIp3 function. Moreover, mislocalization of wild-type <sup>HA</sup>TgEIp3<sup>OE</sup> was also tolerated, suggesting the replication defect is specific to the enzymatic activity of TgEIp3 at the mitochondrion. Since

overexpression of KAT mutants of TgElp3 still grew slowly, the rSAM domain appears to be more important than the KAT domain in producing the slowed growth phenotype. In summary, these results signify the importance of TgElp3's rSAM domain for protein function, and confirm TgElp3 activity is dependent on localization to the OMM.

### 2.3.5 The $mcm^5s^2U$ tRNA modification is present in *Toxoplasma*

Our mutational approaches identified the rSAM domain as essential for TgElp3 function. In other species, rSAM domain of Elp3 is important for the formation of tRNA modifications, which enhance translation efficiency and fidelity (123–125). Specifically, Elp3 is required for the synthesis of 5-methoxycarbonylmethyl ( $mcm^5$ ) and 5-carbamoylmethyl ( $ncm^5$ ) groups present on uridines at the wobble position in tRNA (86). Given the significant replication defect observed in the  $^{HA}TgElp3^{OE}$  parasite strain, we hypothesized that overexpression of TgElp3 causes hyper-modification of tRNA resulting in altered translation (Figure 14).

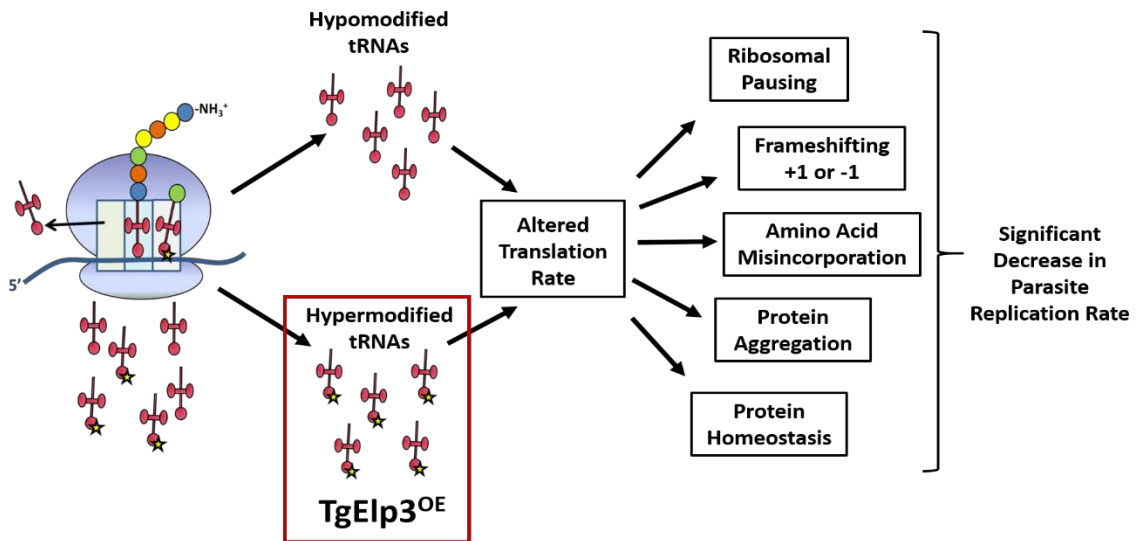


Figure 14. Overexpression of TgElp3 may cause hyper-modification of tRNAs resulting in altered translation rate and slowed parasite growth. A biological model of how dysregulation of tRNA modifications may alter translation rate and affect parasite growth. Red cloverleaf structures=tRNA, yellow stars=modified nucleosides.

In *Saccharomyces cerevisiae*, loss of EIp3 correlates with the loss of the  $mcm^5$  side-chain generating resistance to the *Kluyveromyces lactis* killer toxin ( $\gamma$ -toxin) (69, 86, 126). The  $\gamma$ -toxin is a tRNA endonuclease that cleaves tRNA 3' of the wobble nucleoside 5-methoxycarbonylmethyl-2-thiouridine ( $mcm^5s^2U$ ) (127) (Figure 15). The  $mcm^5s^2U$  tRNA modification identified in *S. cerevisiae* is only present in lysine, glutamic acid and glutamine tRNAs, and its formation requires two enzymes: (1) EIp3 for the formation of  $mcm^5$ , and (2) cytosolic thiouridylase (Ctu1/Ctu2) for the formation of the 2-thio ( $s^2$ ) group (95, 125, 128–130). Blast analyses of the *Toxoplasma* proteome using *S. cerevisiae* Ctu1/Ctu2 sequences identified two putative cytosolic thiouridylase proteins, TGME49\_309020 and TGME49\_294380, suggesting that the  $mcm^5s^2U$  tRNA modification likely exists in *Toxoplasma*.



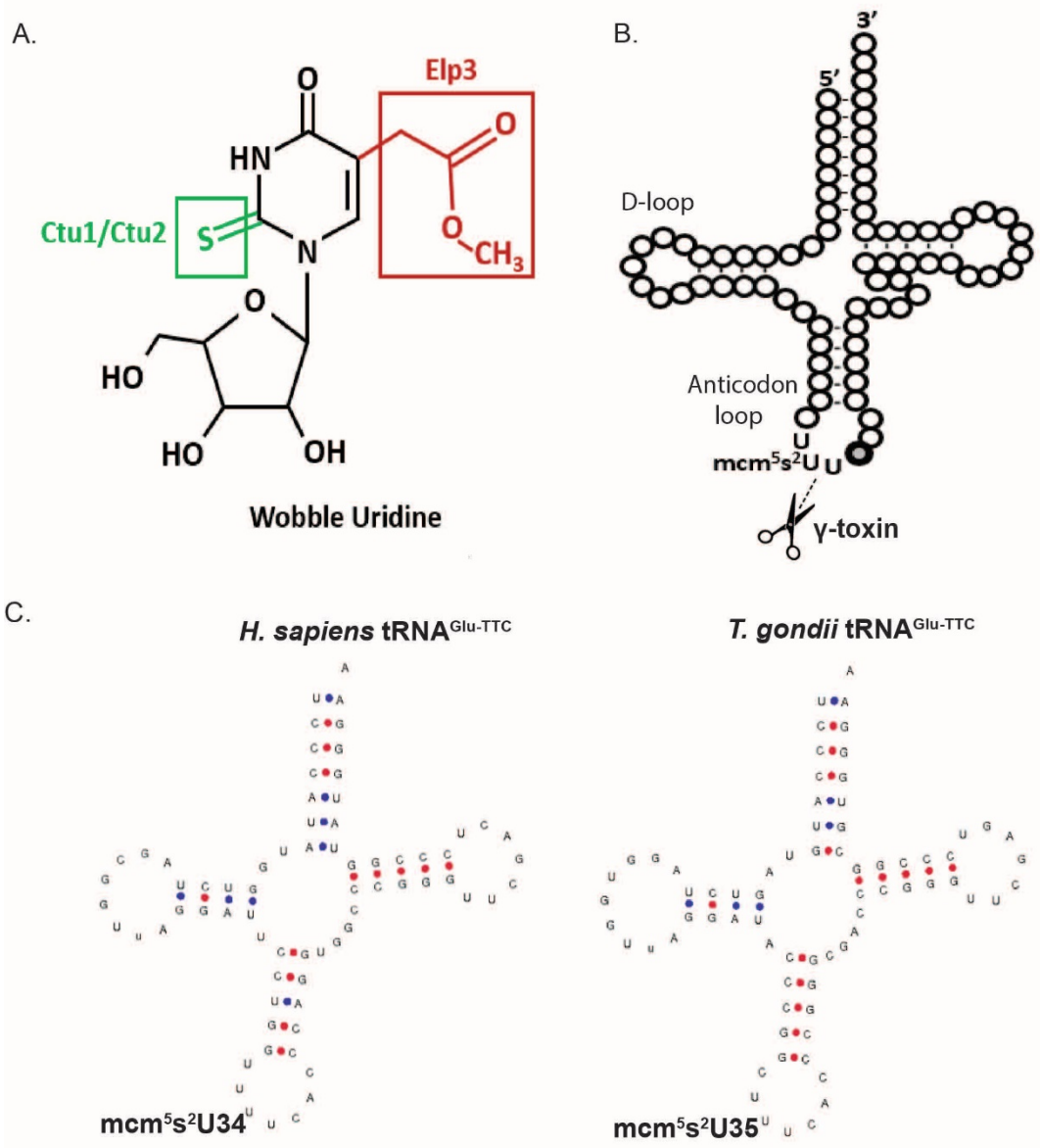


Figure 15. Ctu1/Ctu2 and Elp3 are required for the  $mcm^5s^2$  wobble uridine modification.

A. Elp3 and Ctu1/Ctu2 pathways are required for the  $mcm^5$  and  $s^2$  modifications, respectively, at the wobble uridine position. B. Depiction of where the  $\gamma$ -toxin endonuclease cleaves the  $mcm^5s^2U$  tRNA modification. C. Structure of human (Hs-tRNA<sup>Glu</sup>) and *Toxoplasma* glutamic acid tRNA (Tg-tRNA<sup>Glu</sup>).

To determine if the  $mcm^5s^2U$  tRNA modification exists in *Toxoplasma*, we performed an *in vitro* enzymatic assay using recombinant  $\gamma$ -toxin in collaboration with Dragony Fu's lab at the University of Rochester. Total RNA samples from parental RH $\Delta$ hx,  $^{HA}TgEIp3^{OE}$  and rSAM(C284A/C287A) $^{OE}$  parasite lines along with an HFF control sample were incubated with recombinant  $\gamma$ -toxin or an empty vector control. To assess cleavage, we designed Northern blot probes specific to *Toxoplasma* glutamic acid tRNA (Tg-tRNA<sup>Glu</sup>) as well as a control probe for serine tRNA (Tg-tRNA<sup>Ser</sup>); since tRNA<sup>Ser</sup> is not known to possess the  $mcm^5s^2U$  tRNA modification, we do not expect to see cleavage. Considering *Toxoplasma* is an intracellular pathogen, host cell contamination is likely. To address this concern we used RNA extracted from both intracellular and extracellular parasites, and included Northern blot probes specific to human glutamic acid (Hs-tRNA<sup>Glu</sup>) and serine tRNAs (Hs-tRNA<sup>Ser</sup>). Interestingly, Tg-tRNA<sup>Glu</sup> contains an extra nucleotide in the D-loop making it 73 bp long compared to the Hs-tRNA<sup>Glu</sup> composed of 72 bp. This extra base pair makes the *Toxoplasma* wobble uridine base pair 35, not 34 which is typically found (Figure 15).

Upon treatment with  $\gamma$ -toxin the amount of full length Tg-tRNA<sup>Glu</sup> decreased, indicating the presence of the  $mcm^5s^2U$  tRNA modification in *Toxoplasma* (Figure 16). A similar pattern was observed in the HFF control sample when probed with anti-Hs-tRNA<sup>Glu</sup> (Figure 16). As expected, there was no decrease in full length Tg-tRNA<sup>Ser</sup> or Hs-tRNA<sup>Ser</sup> with treatment of  $\gamma$ -toxin, indicating an absence of the  $mcm^5s^2U$  tRNA modification. Of note, the Hs-tRNA<sup>Ser</sup> probe appears to detect tRNA in the parasite sample; however, the Tg-tRNA<sup>Ser</sup> seems specific to *Toxoplasma*.

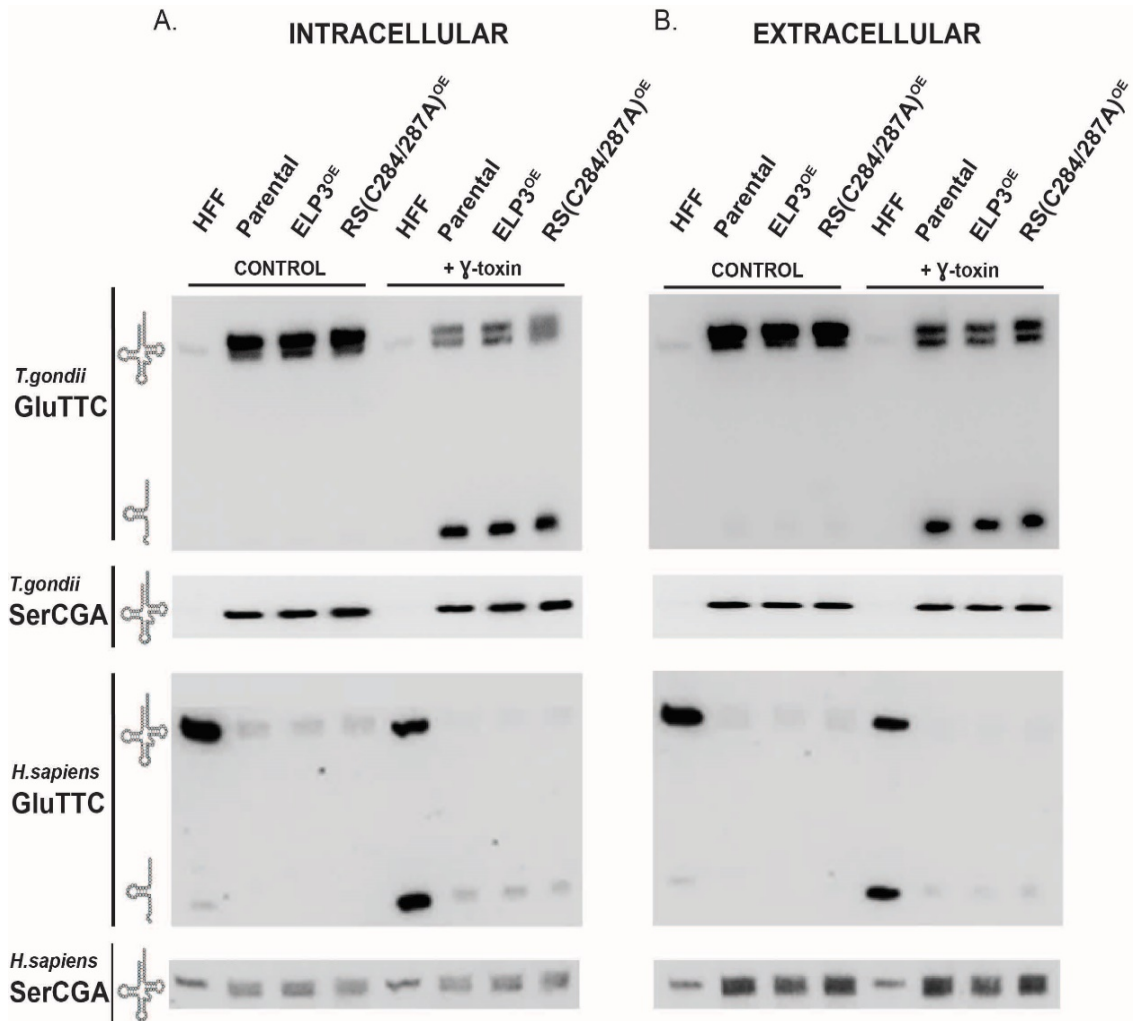


Figure 16. Identification of the tRNA<sup>Glu</sup> mcm<sup>5</sup>s<sup>2</sup> modification in *Toxoplasma*. Northern blot of 5 μg total RNA isolated from intracellular (A) and extracellular (B) RHΔ*hx*, <sup>HA</sup>TgEIp3<sup>OE</sup> and rSAM(C284A/C287A)<sup>OE</sup> parasites and uninfected host cells (HFF) sample incubated without or with the γ-toxin endonuclease for 10 min at 30°C. GluTTC and SerCGA probes specific to *T. gondii* and *H. sapiens* were used. The probe used for each blot is listed on the left.

Unexpectedly, a doublet was observed in the *Toxoplasma* samples when using the Tg-tRNA<sup>Glu</sup> probe. Initially, we thought this may be due to host cell contamination, however, when using the Hs-tRNA<sup>Glu</sup> probe against the *Toxoplasma* samples, we did not detect Hs-tRNA<sup>Glu</sup> (Figure 16). Non-specific binding of the Tg-tRNA<sup>Glu</sup> probe to another *Toxoplasma* tRNA could explain the doublet. The *Toxoplasma* aspartic acid tRNA (Tg-tRNA<sup>Asp</sup>) shares the closest sequence homology, matching 17 of the 28 nucleotides in the Tg-tRNA<sup>Glu</sup> probe.

Despite some sequence similarity between the Tg-tRNA<sup>Glu</sup> and Tg-tRNA<sup>Asp</sup> sequences, there is only a one-third mismatch between Tg-tRNA<sup>Glu</sup> probe and the Tg-tRNA<sup>Asp</sup> sequence making it unlikely to be the cause of the doublet. Another possibility is that there may be a portion of Tg-tRNA<sup>Glu</sup> that has some unresolved secondary structure causing a band shift in the gel. Curiously, a doublet has also been observed in *S. cerevisiae* when probed for the glutamic acid tRNA (87), but an explanation remains unknown.

There was no difference in levels of intact or cleaved Tg-tRNA<sup>Glu</sup> levels between the parental, TgElp3<sup>OE</sup> and rSAM(C284A/C287A)<sup>OE</sup> samples, indicating the TgElp3<sup>OE</sup> replication defect is not a result of hyper-mcm<sup>5</sup>s<sup>2</sup>U tRNA<sup>Glu</sup> modifications. Seeing that this assay does not directly test for all Elp3 tRNA modifications and a second enzyme is required for the mcm<sup>5</sup>s<sup>2</sup>U modification, this could explain why we observed no difference. In other species, Elp3 is known to modify 11 different tRNAs and this assay examines only tRNA<sup>Glu</sup> (86, 87). In conclusion, we were able to identify the first tRNA modification (mcm<sup>5</sup>s<sup>2</sup>U) in *Toxoplasma*. However, we still do not know the cause of the TgElp3<sup>OE</sup> replication defect.

### 2.3.6 Attempt to generate recombinant TgElp3

Recently, an *in vitro* tRNA modification assay was developed by Raven Huang (84). This assay used recombinant Elp3 from archaeal *Methanocaldococcus infernus* (*MinElp3*), a synthetic tRNA<sup>Arg</sup> and [<sup>14</sup>C] acetyl-CoA. In the presence of *MinElp3*, a covalent attachment of the [<sup>14</sup>C] acetyl group to the tRNA occurs, demonstrating catalysis by *MinElp3*; catalysis does not occur when *MinElp3*'s rSAM or KAT domains are mutated, suggesting that both domains are required to modify tRNA (84). To test TgElp3 in this assay, a minimum of 1mg of purified protein is required. Using 5 x T-150s of freshly egressed parasites, we were able to purify only ~1µg of <sup>HA</sup>TgElp3 protein. To generate enough TgElp3 protein to perform the *in vitro* tRNA modification assay, it was necessary to employ a heterologous recombinant protein expression system.

In attempts to generate sufficient recombinant TgElp3 protein, we engineered several TgElp3 expression constructs, each with the TMD removed (TgElp3 $\Delta$ TMD). For expression, we used the Rosetta (DE3) pLysS competent cells which are designed to enhance the expression of eukaryotic proteins that contain codons rarely used in *Escherichia coli*. Despite trying several different N-terminal epitope tags (10 x Histidine, GST, SUMO and no tag), we were unable to purify soluble TgElp3. Next, we tried expressing TgElp3 in a second *E. coli* competent cell line specifically engineered to overcome the hurdle of protein insolubility, Artic Express Competent Cells. This cell line expresses several protein chaperones which aid in protein folding to increase protein solubility. Nevertheless, we were unable to purify soluble protein.

We also attempted to use a heterologous eukaryotic system to express TgElp3. We chose the baculovirus gene expression system in *Spodoptera frugiperda* (SF21) cells to express TgElp3. We generated two TgElp3 $\Delta$ TMD constructs (with or without a GST-tag) for use in Clontech's BacPAK<sup>TM</sup> Baculovirus Expression System. Using the SF21 cells, we were able to express high amounts of TgElp3 protein but the majority was insoluble.

The reason for TgElp3's insolubility is likely due to its rSAM domain. The rSAM domain contains a canonical cysteine motif (CX<sub>3</sub>CX<sub>2</sub>C) that forms an iron-sulfur cluster [4Fe-4S]. This iron-sulfur cluster is thought to reductively cleave S-adenosyl-L-methionine (SAM) to generate a radical required for a methylation reaction (131). The iron-sulfur cluster relies on three iron atoms ligated to each of the three cysteines, while the fourth iron atom presumably binds the co-factor SAM (132, 133). As this cluster is only bound by three protein derived cysteine ligands rather than four, the [4Fe-4S] cluster tends to be extremely labile in the presence of oxygen, frequently degrading to other iron-sulfur cluster forms (134–136). This has been observed with other rSAM domain containing proteins and consequently in the presence of oxygen, precipitation of protein occurs (137–139). In summary, under the conditions we tried, we were unable to produce enough soluble TgElp3 protein to perform the *in vitro* tRNA modification assay.

### 2.3.7 Global translation is not altered by overexpression of TgElp3

The rate of protein synthesis is not uniform along mRNAs; one influential factor is the rate of codon-anticodon base pairing, in which the first two codon positions interact in a Watson-Crick base pair manner while the third codon position can form a non-canonical (wobble) pair. This wobble base pairing is heavily influenced by tRNA modifications that can alter translation fidelity and efficiency (138, 140). Altered translation rates can globally affect protein levels as this was recently observed in *S. cerevisiae* lacking Elp3/Uba4; the loss Elp3/Uba4 resulted in the loss of wobble uridine mcm<sup>5</sup> and mcm<sup>5</sup>s<sup>2</sup> tRNA modifications and decreased protein levels (141). Several other studies, including one in mammalian cells, have identified Elp3 as an important regulator of translation (95, 125, 142, 143).

The growth defect we observed in <sup>HA</sup>TgElp3<sup>OE</sup> parasites could be due to excessive TgElp3 mediated tRNA modification, which would lead to altered translation. Since we have been unable to confirm TgElp3 as a tRNA modification enzyme, we decided to assess protein synthesis in the parental RHΔ*hx* and <sup>HA</sup>TgElp3<sup>OE</sup> parasite strains using two independent methods, polyribosome profiling and Surface Sensing of Translation (SUnSET) analyses.

To evaluate the effect of TgElp3 overexpression on global translation we performed polyribosome profiling. This technique uses a sucrose gradient to separate mRNA associated ribosome complexes. Separation of these complexes is based on the number of associated ribosomes: free ribosome (small or large ribosome subunit), monosome (one ribosome residing on an mRNA) and polysome (multiple ribosomes residing on an mRNA). We treated freshly lysed parasites with cycloheximide to block the translocation step in protein synthesis essentially “freezing” the ribosomal mRNA complexes. Parasite lysate was then subjected to polyribosome fractionation and analyzed by UV spectrometry. No overt differences were observed between parental RHΔ*hx* and <sup>HA</sup>TgElp3<sup>OE</sup> parasite strains (Figure 17).

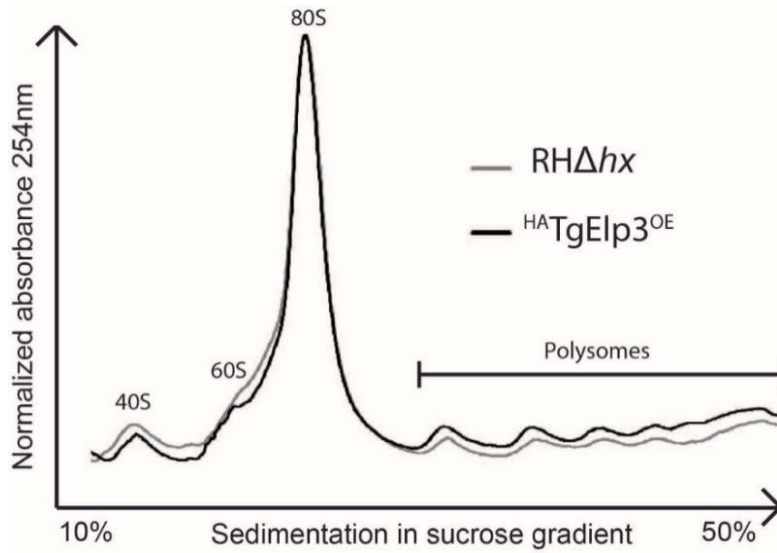


Figure 17. Overexpression of Elp3 does not alter global translation. Equal amounts of lysate from parental RH $\Delta$ hx and <sup>HA</sup>TgElp3<sup>OE</sup> parasite strains were separated on a 10 to 50% sucrose gradient and polyribosome profiles were generated.

In addition to polyribosome profiling which provides a snapshot of translation at the mRNA level, we performed a second method to assess translation at the protein level, SUnSET. This method uses puromycin, a tyrosyl-tRNA analog that is incorporated into nascent polypeptide chains. Puromycin incorporation inhibits further protein synthesis and results in C-terminally labeled proteins (144, 145).

To determine if SUnSET could be used to assess protein synthesis in *Toxoplasma*, we treated RH $\Delta$ hx parasites with puromycin before or after treatment with the protein synthesis inhibitor cycloheximide. Puromycin incorporation into *Toxoplasma* proteins was assessed by Western blot and IFA; minimal detection of puromycin was observed in the untreated parasites (control), cycloheximide only treatment (CHX) and treatment with cycloheximide followed by puromycin (CHX + Puro). In contrast, strong puromycin incorporation was detected in parasites treated with only puromycin (Figure 18). These results verify that the SUnSET method works in *Toxoplasma* and that puromycin incorporation is specific to protein synthesis.

We applied the SUnSET method to determine if protein synthesis is altered in our TgEIp3 overexpression parasite strain. Freshly egressed extracellular parasites (parental RH $\Delta$ hx and <sup>HA</sup>TgEIp3<sup>OE</sup>) were incubated with puromycin for 10, 20 and 30 minutes. At each time point, parasites were spun down and immediately lysed to halt puromycin incorporation. Puromycin incorporation was assessed by Western blot analysis; no overt differences were detected between the parental RH $\Delta$ hx and <sup>HA</sup>TgEIp3<sup>OE</sup> parasite strains (Figure 18). Since we used intracellular parasites, there is a risk of host cell contamination. Therefore, we repeated the experiment using freshly egressed parasites which also showed no difference (Figure 18).



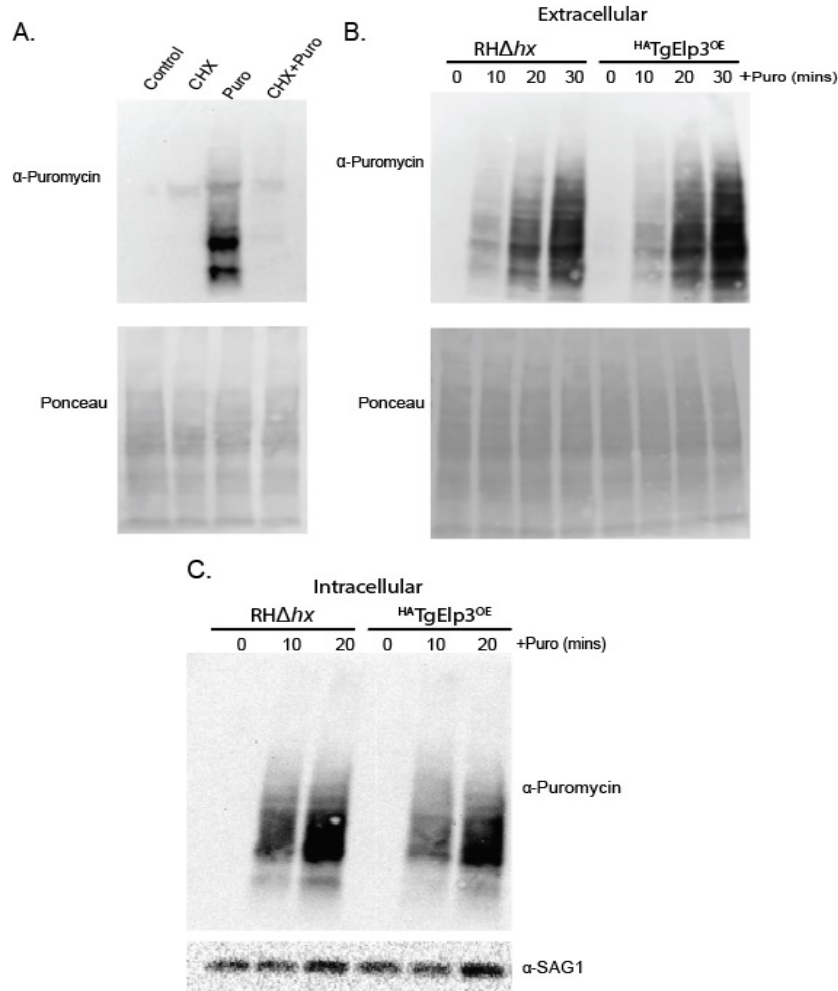


Figure 18. SUnSET analysis of active protein biosynthesis in *Toxoplasma*. A. Freshly egressed *RHΔhx* parasites incubated in normal growth medium with 100 μg/mL cycloheximide (CHX), 10 μg/mL puromycin (Puro) or both (CHX+Puro). Western blot analysis of each sample (100 μg) probed with anti-puromycin. Ponceau staining shows relatively equal loading and transfer. Puromycin is incorporated into *Toxoplasma* proteins (Puro) while cycloheximide treatment blocked puromycin incorporation (CHX+Puro); this data confirms that SUnSET analysis works in *Toxoplasma*. B. Freshly egressed *RHΔhx* and *HA<sup>TgEIp3</sup>OE* parasites incubated with 10 μg/mL puromycin (Puro) for 10, 20 and 30 minutes. At each time point cells were immediately lysed and subjected to SDS-PAGE and Western blotting using anti-puromycin antibody. Ponceau staining shows relatively equal loading and transfer. A time dependent increase of puromycin incorporation is observed in both parasite strains. C. Intracellular *RHΔhx* and *HA<sup>TgEIp3</sup>OE* parasites incubated with 10 μg/mL puromycin for 10 and 20mins. Parasites were physically removed from host cells and filtered to remove host cell debris. Lysates were immediately prepared and Western blot analysis of each sample (100 μg) was probed with anti-puromycin and anti-SAG1 for a loading control.

In addition to Western blot analysis, we also assessed puromycin incorporation by IFA analysis. Since the HFF host cells are also actively synthesizing proteins, they will also incorporate puromycin and create high background levels. Therefore, to more accurately assess puromycin incorporation, we performed co-culture experiments where both parental RH $\Delta$ hx and <sup>HA</sup>TgElp3<sup>OE</sup> parasites were inoculated onto the same coverslip containing confluent HFF cells. After 30 hours, puromycin was added and coverslips were fixed at 10 and 20 minutes. Puromycin incorporation was similar between parental RH $\Delta$ hx and <sup>HA</sup>TgElp3<sup>OE</sup> parasites (Figure 19). However, the amount of protein biosynthesis as indicated by puromycin incorporation across individual parasite vacuoles varied and was independent of parasite strain (Figure 19). This variation could be associated with parasite cell cycle, but further studies are needed. In summary, using polyribosome profiling and the SUnSET method to assess protein synthesis unveiled no differences between the parental RH $\Delta$ hx and <sup>HA</sup>TgElp3<sup>OE</sup> parasite strains.

In a *S. cerevisiae* *Elp3/Uba4* knockout strain, the loss of the mcm<sup>5</sup>s<sup>2</sup> tRNA modification is associated with drastically decreased protein levels as determined by Coomassie blue staining, but protein levels were partially restored with overexpression of tRNA<sup>Lys</sup> (141). In a subsequent study, ribosome footprint profiling identified an accumulation of ribosomes at the GAA and CAA codons in a knockout *Elp3* yeast strain, suggesting that these codons were translated less efficiently by hypomodified tRNAs; however, polyribosome gradient profiles of the mcm<sup>5</sup>s<sup>2</sup> deficient strains were indistinguishable from wild-type, suggesting that this technique may not be sensitive enough to identify small alterations in global protein synthesis (138). Since the initiation step is typically the rate-limiting step of eukaryotic translation and tRNA modifications predominantly affect translation elongation, these may be missed by global protein synthesis assays (146, 147). In addition, the mcm<sup>5</sup>s<sup>2</sup> tRNA modifications may alter protein synthesis of only a subset of mRNA transcripts which further limits the ability to detect changes at a global level. Future studies are needed to determine if small changes in protein

synthesis may be the cause of the significant growth defect identified in the  $^{HA}TgEIp3^{OE}$  parasite strains.

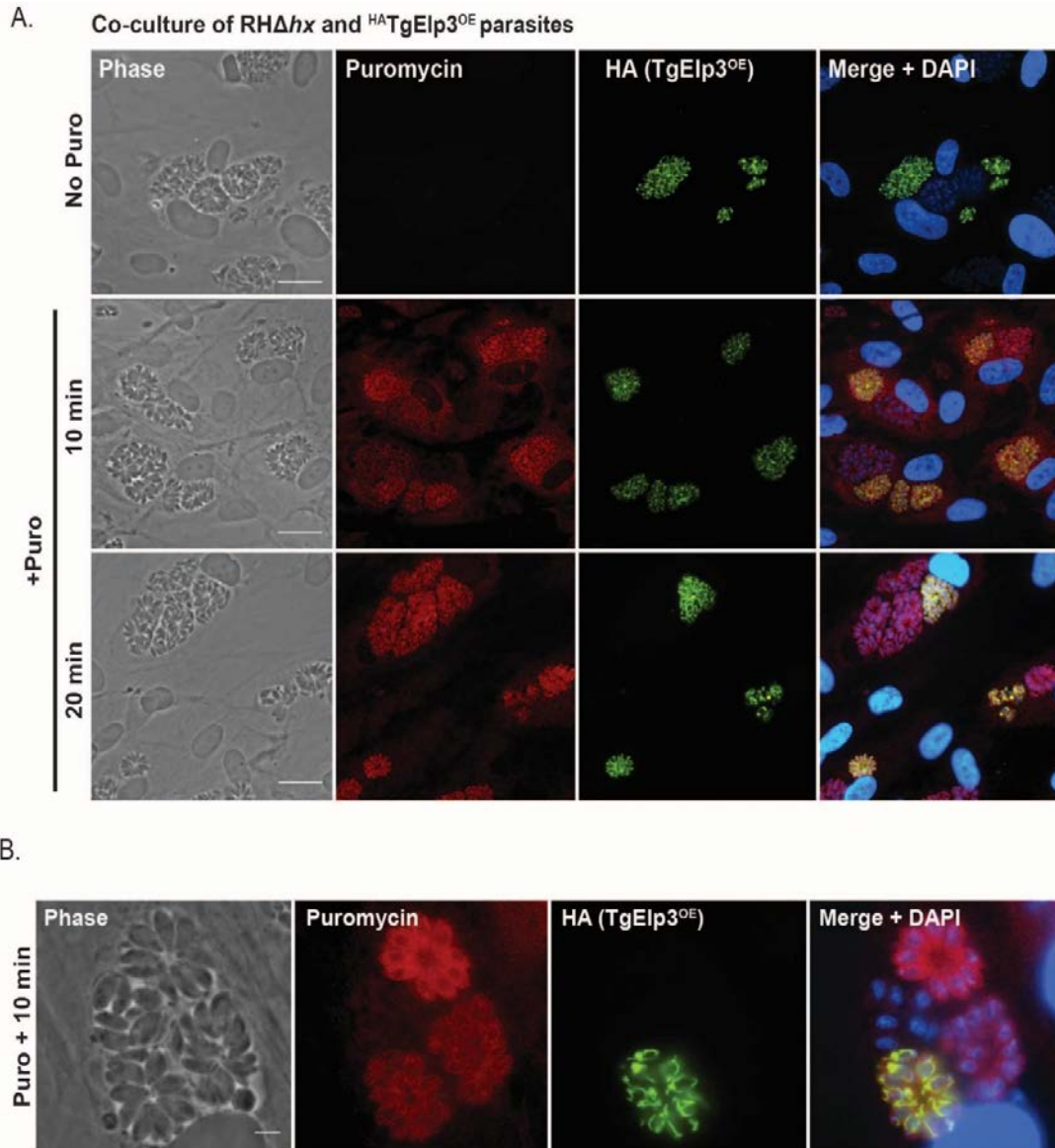


Figure 19. Protein biosynthesis varies between parasite vacuoles and is independent of Elp3 overexpression.  
 A. Co-culture of equal numbers of  $RH\Delta hx$  and  $^{HA}TgElp3^{OE}$  parasites incubated with puromycin for 10 and 20 mins at 30 hr post-infection. Coverslips were fixed and stained for anti-puromycin (red) to detect protein biosynthesis, anti-HA to differentiate the  $^{HA}TgElp3^{OE}$  parasites from the  $RH\Delta hx$  parasites and merged with the DNA stain DAPI (blue), scale bar 25  $\mu m$ . Variation in puromycin staining is observed across parasite vacuoles and is independent of parasite strain. B. Another example of variation of parasite protein biosynthesis as detected by anti-puromycin (red), scale bar 2  $\mu m$ .

## 2.4 Concluding remarks

In these studies, we determined that overexpression of TgElp3 at the parasite's mitochondrion results in a significant replication defect, but overexpression of TgElp3 lacking the TMD domain or with a mutant rSAM domain is tolerated. These findings signify the importance of TgElp3's localization to the mitochondrion and the functional activity of the rSAM domain. In other species, the rSAM domain of Elp3 is responsible for post-transcriptional tRNA modifications, specifically the  $mcm^5$  and  $ncm^5$  wobble uridine modifications. These tRNA modifications are thought to alter protein synthesis in a context dependent manner, but the exact mechanisms are not well understood (138, 141). Although we cannot rule out TgElp3 KAT activity, these findings broadened our focus from only exploring TgElp3 as a KAT to investigating its potential role as a tRNA modification enzyme. Currently, there are no reports on tRNA modifications in *Toxoplasma*.

Using the *in vitro*  $\gamma$ -toxin assay in collaboration with Dragony Fu's lab at the University of Rochester we identified the first tRNA modification in *Toxoplasma*, tRNA<sup>Glu</sup>  $mcm^5s^2U35$ . This wobble uridine modification is predicted to change the physical interaction between the anticodon and codon with the  $mcm^5$  modification preferentially translating –G ending codons while the  $mcm^5s^2$  favors –A ending codons (148, 149). In these studies, we were unable to attribute the TgElp3<sup>OE</sup> replication defect to changes in the tRNA<sup>Glu</sup>  $mcm^5s^2U35$  modification. Knowing that the tRNA<sup>Glu</sup>  $mcm^5s^2U35$  modification requires a second enzyme, Ctu1/Ctu2, and that we do not have a way to directly measure the Elp3 specific  $mcm^5$  modification, we diverted our efforts to assess protein synthesis. Using two independent methods, polyribosome profiling and SUnSET, we did not detect differences in TgElp3<sup>OE</sup> global protein synthesis compared to the parental RH $\Delta$ hx. However, these methods may not be sensitive enough to identify small changes in protein synthesis and codon specific translation defects may only affect a few genes required for a particular cellular process. More studies are needed to confirm that overexpression of TgElp3 does not alter translation of a subset of mRNA transcripts.

Previous reports on Elp3 are associated with many different biological processes specifically its function as either a tRNA modification enzyme and/or a lysine acetyltransferase. In *Toxoplasma*, TgElp3 is anchored to the outer mitochondrial membrane with its catalytic domains protruding into the cytosol. With this unique location, TgElp3 may possess one or the other, or both enzymatic activities. Due to the complete lack of tRNA genes in the mitochondrial genome, *Toxoplasma* must import all tRNAs required for mitochondrial translation (17). Several reports suggest that tRNA modifications could regulate which tRNAs are imported into the mitochondria and which remain in the cytosol (150, 151). For example, in *Leishmania tarentolae* nuclear encoded tRNAs containing the mcm<sup>5</sup> modification are found mostly in the mitochondria; in contrast, cytosolic tRNAs contain both the mcm<sup>5</sup> and s<sup>2</sup> modifications (mcm<sup>5</sup>s<sup>2</sup>), indicating that the cytosol specific 2-thioloaion could play an inhibitory role in mitochondrial tRNA import (150). A similar mechanism may be present in *Toxoplasma*, but further studies are needed.

Since we have shown that TgElp3 can acetylate histone H3 *in vitro*, it is reasonable to consider that TgElp3 is a bona fide lysine acetyltransferase *in vivo* (83). To date, TgElp3 is the only putative lysine acetyltransferase localized to the *Toxoplasma* mitochondrion and with the identification of twenty acetylated mitochondrial proteins, it is reasonable to think that these proteins may be acetylated by TgElp3 prior to import (83, 125). Given TgElp3's KAT domain juts out into the cytosol, acetylation of cytosolic proteins is also likely. The cytosolic protein alpha-tubulin has been identified as a substrate of Elp3 in humans and yeast, making it a logical choice to explore as a potential substrate of TgElp3. The next chapter investigates TgElp3 as an alpha-tubulin acetyltransferase in *Toxoplasma*.

## **CHAPTER 3: Tubulin acetylation, a critical PTM important for parasite viability, is mediated by TgATAT not TgEIp3.**

### **3.1 Introduction**

Constructed from tubulin monomers, microtubules are a component of the cytoskeleton and are required for a variety of steps in *Toxoplasma* biology including parasite replication (152). Upon invasion, tachyzoites undergo a form of asexual division termed endodyogeny in which two daughter parasites assemble within the mother parasite (153, 154). This complex process is dependent upon the function of two distinct microtubule populations (155, 156). The spindle microtubules originate from a microtubule organizing center (MTOC) termed the centrosome, and ensure proper chromosome segregation and karyokinesis as the parasite completes each round of closed (intranuclear) mitosis (155, 156). Progression through mitosis is partnered with expansion of the daughter parasite cytoskeleton driven by elongation of the 22-subpellicular microtubules from a second MTOC, the apical polar ring, towards the basal end of the parasite. Once formed, the subpellicular microtubules are nondynamic, tethered to the cytosolic face of the parasite inner membrane complex (IMC), a collection of flattened vesicles originating from the ER-Golgi network (157). In addition to replication, microtubules play critical roles in a variety of aspects of *Toxoplasma* biology, including parasite motility, host cell attachment, and invasion; consequently, microtubules have emerged as attractive targets for therapeutic intervention (152). In addition, the mechanisms by which *Toxoplasma* microtubules are regulated is an active area of inquiry.

Microtubule functions are regulated by a diverse collection of post-translational modifications (PTMs) that occur on the  $\alpha$ - and  $\beta$ -tubulin subunits that make up microtubule polymers (158–161). Most of these tubulin PTMs occur on the C-terminal tails that extend out from the surface of the microtubules to regulate interactions with effector microtubule associated proteins (MAPs) (162, 163). By contrast, acetylation of lysine 40 (K40) on  $\alpha$ -tubulin is a unique PTM that resides within the lumen of microtubules (164, 165).

Several studies have implicated Elp3 as the major  $\alpha$ -tubulin acetyltransferase. In *Arabidopsis*, tubulin affinity chromatography identified an Elp3 homolog (Elongata 3) which can bind to  $\alpha\beta$ -tubulin heterodimers (166). In 2009, Elp3 was identified as an  $\alpha$ -tubulin acetyltransferase required for radial migration and branching of mouse cortical projection neurons; similar neuronal migration defects were observed in an  $\alpha$ -tubulin (K40A) mutant (81). In the same year, Elp3 was identified in a microsatellite-based genetic association study of amyotrophic lateral sclerosis (ALS), a progressive motor neuron degeneration disease in humans and further mutational studies in *Drosophila* concluded Elp3 tubulin acetylation is critically important for the axonal biology of neurons (78, 93). Mutations in Elongator are present in a second neurologic disease, familial dysautonomia (FD) which is thought to be caused by impaired vesicle trafficking along microtubules due to defects in tubulin acetylation (89). Furthermore, incubation of  $\alpha$ -tubulin with a purified recombinant human ELP3 results in increased  $\alpha$ -tubulin acetylation (81). In summary, several independent studies have identified Elp3 as an important factor in neuronal health and mechanistic studies implicate Elp3 as an  $\alpha$ -tubulin acetyltransferase.

However, a second enzyme has been identified as a tubulin acetyltransferase, Mec17/ATAT (167, 168) which is responsible for K40 acetylation, a PTM conserved across eukaryotes. Mec17/ATAT was originally identified in the flagella of the unicellular green algae *Chlamydomonas reinhardtii* (169, 170), K40 acetylation was subsequently found to be enriched on long-lived microtubules throughout higher eukaryotes (171, 172). Recent studies in *C. elegans* suggest that K40 acetylation stabilizes microtubules by promoting the formation of a salt bridge that augments interactions between  $\alpha$ -tubulin subunits in adjacent protofilaments (173). Despite the mounting evidence supporting a role of K40 acetylation in microtubule stability, the biological function of this PTM *in vivo* remains unclear, as evidenced by the variety of phenotypes observed across numerous systems when K40 acetylation is manipulated (168, 174–176).

Numerous tubulin PTMs, including acetylation of K40, have been catalogued in *Toxoplasma* (55, 177–179), but the functional importance of these



modifications on microtubule dynamics and parasite biology remains largely undefined. In these studies, we establish the role of  $\alpha$ -tubulin K40 acetylation by generating point mutants in endogenous  $\alpha$ -tubulin and identified the *Toxoplasma*  $\alpha$ -tubulin acetyltransferase orthologue (named TgATAT), not TgElp3, as the enzyme responsible for acetylating  $\alpha$ -tubulin. Together, these approaches reveal that K40 acetylation is critical for stabilizing tachyzoite microtubules, which is required for daughter cell formation and karyokinesis. The discovery that TgATAT-mediated acetylation of  $\alpha$ -tubulin is necessary for *Toxoplasma* replication establishes the importance of tubulin PTMs in apicomplexan parasites and uncovers a new opportunity for potential therapeutic exploitation.

## **3.2 Materials and Methods**

### **3.2.1 Antibodies**

The following primary antibodies were used at the indicated dilutions: rabbit anti-*T. gondii*- $\beta$ -tubulin (1:2,000; (156)), mouse anti-acetyl-K40- $\alpha$ -tubulin (1:2,000; Sigma 6-11-B-1), rabbit anti-acetyl-K40- $\alpha$ -tubulin (1:2,000; EMD Millipore ABT241), mouse anti-SAG1 (1:2,000; Genway), rat anti-IMC3 (1:2,000; (180)), rat anti-ISP1 (1:1,000; (181)), rabbit anti-Centrin 1 (1:1,000; (182)), mouse anti-Atrx1 (1:2,000; 11G8 (183)) and rat anti-HA (1:1,000; Roche). Secondary antibodies used for immunoblots include donkey anti-rabbit (1:2,000; GE Healthcare), sheep anti-mouse (1:5,000; GE Healthcare), and goat anti-rat (1:2,000; GE Healthcare) conjugated to horseradish peroxidase. Fluorophore-conjugated secondary antibodies (AlexaFluor, ThermoFisher) were used for immunofluorescence assays at 1:2,000 dilutions (1:1,000 for TgATAT<sup>HA</sup>).

### **3.2.2 Parasite culture and transfection**

*Toxoplasma* parasites were maintained in HFFs with DMEM supplemented with 10% heat-inactivated FBS at 37°C and 5% CO<sub>2</sub> (113). To assess parasite doubling time, purified tachyzoites were allowed to invade HFF monolayers in 12-well plates for 2 hours. Extracellular parasites were removed and infected monolayers were incubated for an additional 22 hours before being

fixed in methanol for staining with Differential Quick Staining Kit (Polysciences, Inc). For generation of TgTUBA1 K40 mutants, wild-type RH parasites were electroporated with 100 µg of linearized plasmid and selection medium containing 2.5 µM oryzalin was added 24 hours following transfection. Similarly, TgATAT<sup>HA</sup> parasites were generated by transfection of RHΔ*hxΔku80* parasites (102, 103) with 75 µg of linearized plasmid and were selected with medium containing 1 µM pyrimethamine. Following 3 passages under drug selection, resistant parasites were cloned by limiting dilution in 96-well plates.

### 3.2.3 Generation of TgTUBA1 K40 mutant parasites

The plasmid construct described in (184) containing the *TgTUBA1* genomic sequence carrying T239I oryzalin-resistance mutation was used as template for site-directed mutagenesis using the QuikChange II Kit (Agilent) to introduce K40K silent, K40R and K40Q mutations using the primers 1-6 in Appendix B. This construct was then linearized by digestion with *NotI-HF* and *HindIII-HF* and transfected into RH strain parasites by electroporation as described above. Transfected parasites were selected by growth in media containing 2.5 µM oryzalin, and surviving parasites were cloned out by limiting dilution into 96-well plates. For the generation of V252L strains, T239I was restored to T239T and the V252L mutation was introduced using the Q5 Site Directed Mutagenesis Kit (New England Biolabs) using primers 7-10, and stable clones were selected as described above. Single clones were confirmed by PCR amplification of the *TgTUBA1* locus from gDNA purified using the DNeasy Blood and Tissue Kit (Qiagen) and sequencing with primers 11 and 12.

### 3.2.4 Endogenous tagging of TgATAT

Genomic DNA was isolated from RHΔ*hxΔku80* parasites and primers 13 and 14 (Appendix B) were used to amplify ~1.2kb of the *TgATAT* gene just upstream of the stop codon. The In-Fusion HD cloning kit (Clontech) was used to clone the amplified *TgATAT* sequence into the *PacI* restriction site of pLIC.HA3.DHFR (121). Prior to transfection, 75 µg of plasmid DNA was

linearized by *NcoI* and electroporated into RH $\Delta$ *hx* $\Delta$ *ku80* parasites. Following three passages under 1.0  $\mu$ M pyrimethamine selection, parasites were cloned by limiting dilution, and positive clones were identified by immunoblotting.

### 3.2.5 Immunoblotting

Freshly egressed parasites were passed through 3.0 micron filters to remove host cell debris and then washed in PBS. Parasites were lysed in RIPA buffer supplemented with complete protease inhibitor cocktail (Roche), sonicated twice for 10s each using a microtip sonicator, and centrifuged at 21,000 x g for 10 min at 4°C to remove insoluble debris. Cleared lysate was subjected to SDS-PAGE electrophoresis using pre-cast 4-20% Mini-PROTEAN TGX gels (BioRad) and resolved proteins were transferred to nitrocellulose membranes using Trans-blot SD semi-dry transfer system (BioRad). Membranes were blocked in 5% milk/TBST, and probed with primary antibodies for 1.5 hours at room temperature or overnight at 4°C. Membranes were washed 3x 10 min in TBST and probed with secondary antibodies for 45 min at room temperature. Membranes were washed again 3x 10 min in TBST and proteins were detected using SuperSignal West Femto substrate (ThermoFisher) and imaged on a FluorChem R imager (Bio-Techne).

### 3.2.6 IFAs

Confluent HFF monolayers grown on coverslips in 24-well plates were infected with freshly lysed parasites. For all images of microtubules, cells were fixed with cold methanol, washed with PBS, and blocked for 30 min with 3% BSA in PBS. For imaging TgATAT<sup>HA</sup>, cells were fixed with 4% paraformaldehyde in PBS, blocked for 30 min in 3% BSA/PBS, and permeabilized with PBS with 0.2% Triton X-100 (PBS-T) for 10 min. Primary antibodies diluted in 3% BSA/PBS were applied for 1.5 hours at room temperature or (for TgATAT<sup>HA</sup>) overnight at 4°C in BSA/PBS-T. Coverslips were washed 3x 15 min with PBS and secondary antibodies were added in 3% BSA/PBS for 45 min. Following 3x 15 min washes

in PBS, coverslips were mounted using Vectashield antifade mounting medium (Vector Labs) containing 4',6-diamidino-2-phenylindole (DAPI) to visualize nuclei.

### **3.2.7 CRISPR-mediated disruption of *TgATAT***

Plasmid described in (24825012) (GFP-Cas9/sgUPRT) was used for site-directed mutagenesis using the Q5 Kit to mutate the single guide RNA sequence to target the *TgATAT* locus using primers 15 and 16. *TgATAT*<sup>HA</sup> parasites were transfected with 50 µg of purified *TgATAT*- or UPRT-targeted GFP-Cas9 plasmid and 50 µg of 90 bp dsDNA oligos 17 and 18. Transfected populations were used to inoculate coverslips and were fixed at timepoints as indicated in figures.

## **3.3 Results**

### **3.3.1 K40 acetylation is dispensable only if tubulin is stabilized through another mutation**

*Toxoplasma* α-tubulin can be acetylated at lysine-40 (K40), but the functional significance of this post-translational modification (PTM) has yet to be addressed. Three α-tubulin isotypes are present in the *Toxoplasma* genome: TGME49\_316400 (*TgTUBA1*), TGME49\_231770 (putative alpha-tubulin I), and TGME49\_231400 (tubulin/Ftsz family). *TgTUBA1* is the only isotype expressed in tachyzoites and the only one that contains the conserved K40 residue reported as acetylated (177). To address the role of α-tubulin K40 acetylation in tachyzoites, we generated three parasite clones with different K40 mutations in the endogenous *TgTUBA1* genomic locus: (i) lysine to arginine (K40R), which conserves the positive charge of lysine but prevents acetylation, (ii) lysine to glutamine (K40Q), which is an acetyl-lysine mimic (185), or (iii) a silent mutation as a control (K40K). To select for positive clones harboring mutant K40, our construct included a second mutation that confers resistance to the microtubule-disrupting drug oryzalin (184, 186). Since studies in other species suggest that K40 acetylation stabilizes microtubules, we chose to generate oryzalin resistance by mutating valine-252 to lysine (V252L), a mutation known to have no effect on microtubule stability (187).

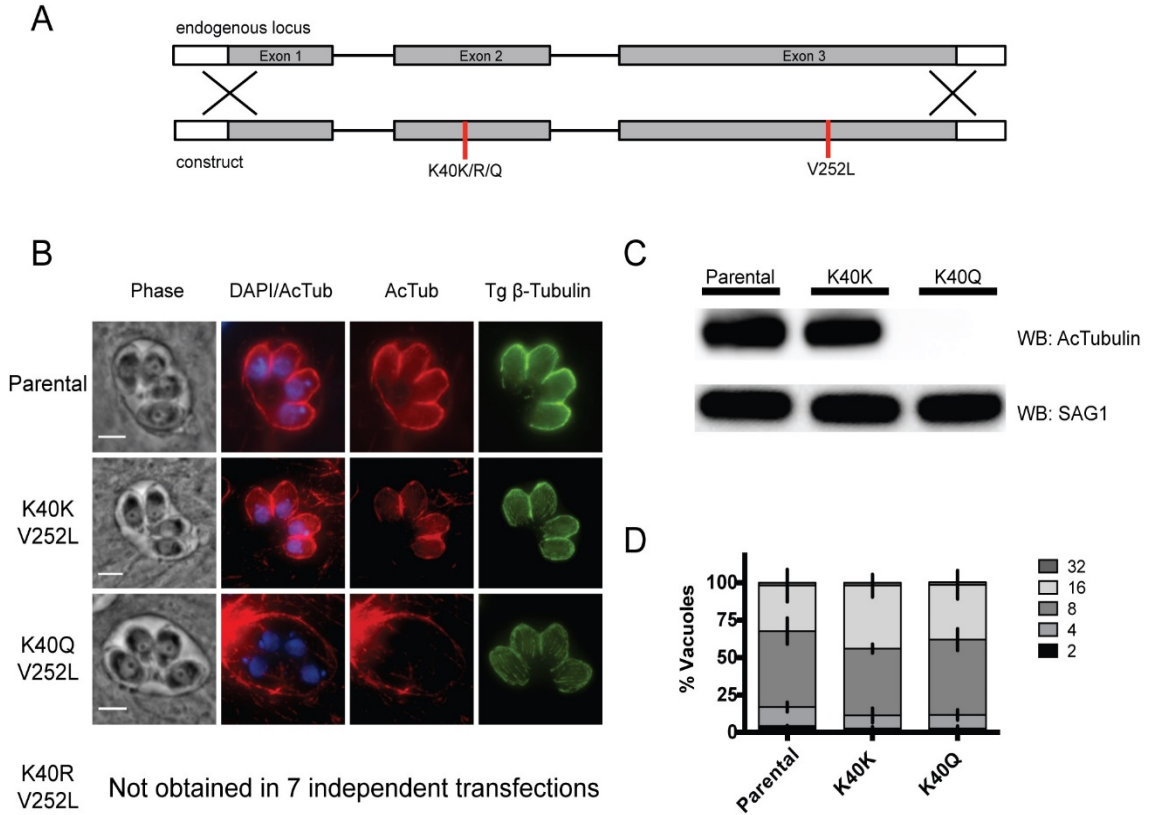


Figure 20. Ablation of K40 acetylation is not tolerated unless replaced by the K40Q acetyl-lysine mimic. Reprinted from reference (188).

A. Diagram of TgTUBA1 genomic locus aligned with the construct used to replace the endogenous locus by double homologous recombination. The construct contains the nonstabilizing V252L oryzalin resistance mutation and the K40K, K40R, or K40Q mutation. B. IFAs of K40 mutants stained for acetyl-K40- $\alpha$ -tubulin (red) or  $\beta$ -tubulin (specific to *Toxoplasma*, green). The K40Q mutation results in complete loss of K40 acetylation in the parasite but not its host cell. Images were merged with the DNA stain DAPI (blue). Scale bars, 3  $\mu$ m. C. Western blot (WB) assay of parental RH and mutant parasites showing loss of K40 acetylation in K40Q mutants. The blot was probed with anti-acetyl-K40- $\alpha$ -tubulin and anti-SAG1 antibodies as a loading control. D. Doubling assays performed to assess the growth of parental RH and mutant parasites. Replication rates were determined by counting the parasites within 100 random vacuoles at 24 h post-infection. Three independent trials were conducted, and the average percentage of vacuoles with the indicated number of parasites  $\pm$  the standard error of the mean is shown (no significant difference between mean percentages of vacuoles at each stage between strains as determined by two-way analysis of variance).

We used an allelic replacement strategy to make K40 mutants using the non-stabilizing V252L mutation to confer oryzalin resistance (Figure 20). The *TgTUBA1* gene was amplified from genomic DNA isolated from oryzalin-resistant clones and the presence of the expected mutations in each established line was confirmed by sequencing. While both K40K and K40Q mutations were readily obtained, K40R mutant parasites were never obtained despite seven independent attempts. The acetylation status of  $\alpha$ -tubulin K40 was assessed using both immunofluorescence assays (IFA) and Western blot (Figure 20). K40Q mutant parasites show a complete loss of K40 acetylation (as expected, the glutamine acetyl-lysine mimic does not cross-react with the anti-K40-acetyl  $\alpha$ -tubulin antibody), but no obvious defects in any microtubule structures, as visualized using a *Toxoplasma*-specific  $\beta$ -tubulin antibody (Figure 20). Parasite growth assays further show that replacement of K40 with the glutamine acetyl-lysine mimic (K40Q) did not affect replication rate (Figure 20).

Some mutations in the oryzalin pocket stabilize microtubules by promoting protofilament interactions and tubulin polymerization (187). Given the reported role of K40 acetylation in microtubule stability, we hypothesized that an oryzalin-resistant mutation in this binding pocket might allow for the generation of K40R mutants. We therefore generated constructs containing K40K, K40R, and K40Q using the T239I oryzalin binding pocket mutation (Figure 21), chosen for its similar levels of drug resistance as V252L (189). Sequencing of the *TgTUBA1* gene confirmed the presence of both mutations in the oryzalin-resistant clones. In the T239I oryzalin-resistant background, all K40 mutants including K40R were readily obtained. Both K40Q and K40R parasites showed a complete loss of K40 acetylation as visualized by both IFA and Western blot (Figure 21), yet displayed no difference in replication relative to the silent mutation or wild-type (Figure 21).

Our mutational analyses show that ablation of  $\alpha$ -tubulin K40 acetylation is only possible when a second, stabilizing mutation is present (e.g., T239I), or when K40 is mutated to a residue (glutamine) that mimics an acetylated lysine. These results suggest that K40 acetylation is required in tachyzoites and likely contributes to the stabilization of microtubules.

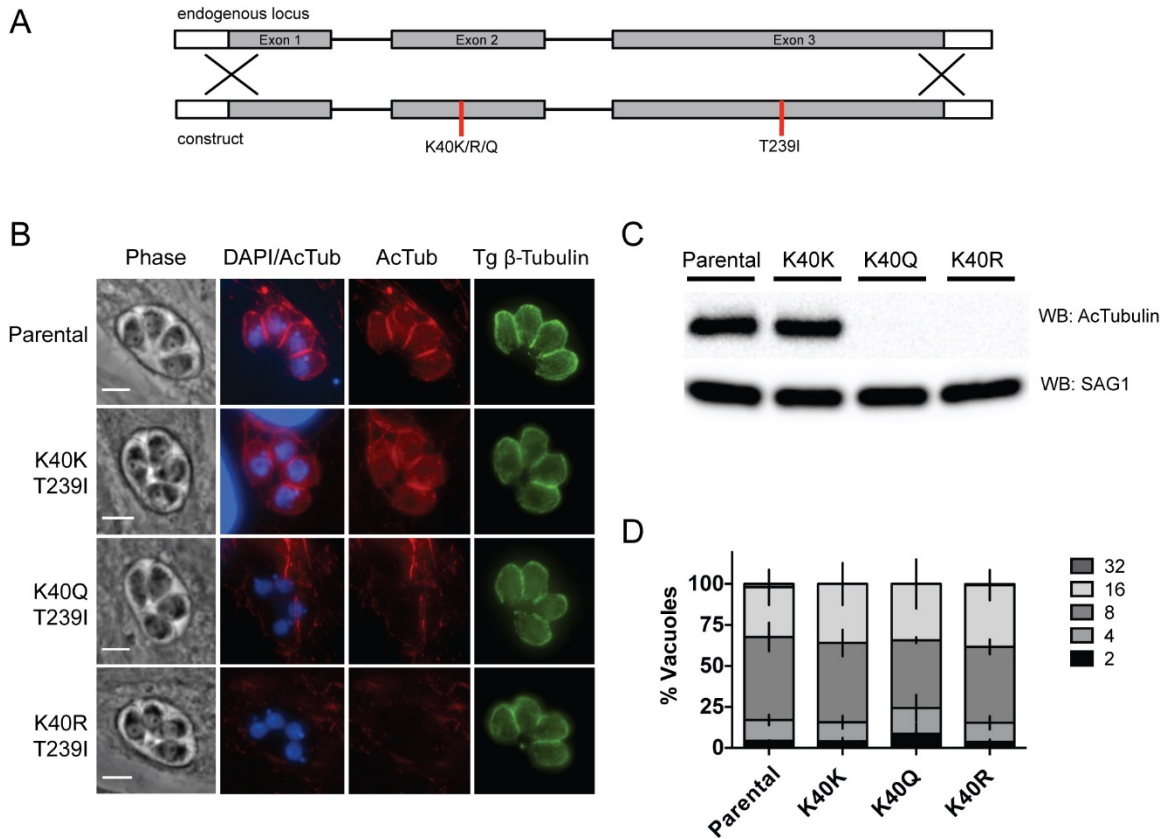


Figure 21. K40 acetylation is dispensible in the presence of the T239I oryzalin resistance mutation. Reprinted from reference (188).

A. Diagram of the TgTUBA1 genomic locus aligned with the allelic replacement construct containing the oryzalin resistance mutation T239I and the K40K, K40R, or K40Q mutation. B. IFAs of mutant parasite lines stained for acetyl-K40- $\alpha$ -tubulin (red) or  $\beta$ -tubulin (green). Images were merged with the DNA stain DAPI (blue). Scale bars, 3  $\mu$ m. C. Western blot (WB) assay of parental RH and mutants confirms the loss of K40 acetylation in K40Q and K40R parasites. The blots were probed with anti-acetyl-K40- $\alpha$ -tubulin and anti-SAG1 antibodies as a loading control. D. Doubling assays performed as described in the legend to Fig. 1D to assess the growth of parental RH and mutant parasites.

### 3.3.2 Identification of an acetyltransferase that co-localizes with acetylated tubulin during tachyzoite division

To further characterize the role of  $\alpha$ -tubulin K40 acetylation in tachyzoites, we sought to identify the enzyme delivering this PTM. In other species, Alpha-Tubulin AcetylTransferase (ATAT, also known as Mec17) has been implicated as the primary enzyme acetylating tubulin (167, 168, 190, 191). A bioinformatics

survey of ToxoDB.org v.24 (192) revealed a single gene containing a Mec17-domain belonging to the Gcn5-related superfamily, TGME49\_319600, which we will refer to as *TgATAT*. *TgATAT* is located on chromosome IV and contains two exons encoding a predicted protein of 907 amino acids (Figure 22). We aligned the lysine acetyltransferase (KAT) domains of ATAT homologues from several representative species using Clustal Omega (192, 193) (Figure 22). Interestingly, while the Mec-17 domain is highly conserved, including the key residues critical for enzymatic activity (Figure 22), the predicted *TgATAT* protein is considerably larger compared to all previously characterized ATAT/Mec17 proteins (Figure 22) (168, 189). *TgATAT* transcripts are expressed in tachyzoites, peaking in the early stages of mitosis, waning during cytokinesis, and remaining at basal levels during interphase, suggesting that *TgATAT* is a cell-cycle regulated protein (194).



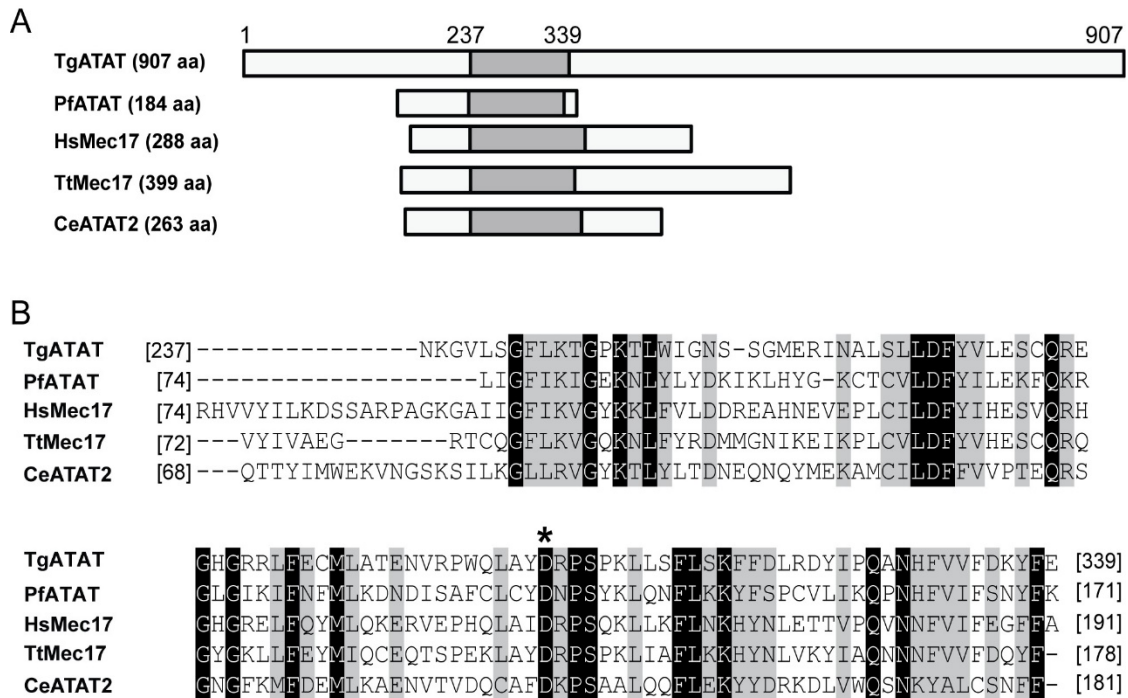


Figure 22. Comparison of ATAT/Mec-17 homologues. Reprinted from reference (188).  
 A. Depiction of ATAT protein sequences from *T. gondii* (TgATAT, TGME49\_31600), *Plasmodium falciparum* (PfATAT, PF3D7\_0924900), Homo sapiens (HsMec17, XP\_005249477.1), *Tetrahymena thermophila* (TtMec17, TTHERM\_00355780), and *C. elegans* (CeATAT2, CELE\_W06B11.1), with the number of amino acids (aa) in parentheses. Gray boxes represent the lysine acetyltransferase domain. B. Amino acid sequence alignment of the KAT domain of the indicated ATAT homologues with identical residues highlighted in black and similar residues highlighted in gray. The asterisk denotes an aspartic acid residue previously shown to be important for ATAT activity (189).

To confirm the unusual size and assess the expression patterns of TgATAT, we introduced three C-terminal hemagglutinin (3xHA) epitope tags at the endogenous *TgATAT* locus using single-crossover homologous recombination in the RH $\Delta ku80\Delta hxxprt$  parasites (102, 121). TgATAT<sup>HA</sup> resolves as a single band migrating at the predicted size of 98 kDa, and the C-terminal 3xHA tag had no effect on K40 acetylation (Figure 23). IFAs show that TgATAT<sup>HA</sup> exhibit cell-cycle regulated expression, with low-levels appearing during S phase and mitosis and peak levels occurring during early cytokinesis (Figure 23). In agreement with the mRNA expression data (194), TgATAT<sup>HA</sup> protein levels

decrease as tachyzoites complete division and then remain undetectable throughout interphase (Figure 23). In agreement with other studies (178, 179), we observe that  $\alpha$ -tubulin K40 acetylation occurs at both spindle and subpellicular microtubules during early daughter formation (Figure 23). Collectively, these findings suggest that TgATAT is expressed during the early stages of tachyzoite replication, when acetylation of nascent microtubule structures occurs. These findings strongly support that K40 acetylation is mediated by TgATAT and there is little evidence that TgElp3 functions as a tubulin acetyltransferase in *Toxoplasma*.

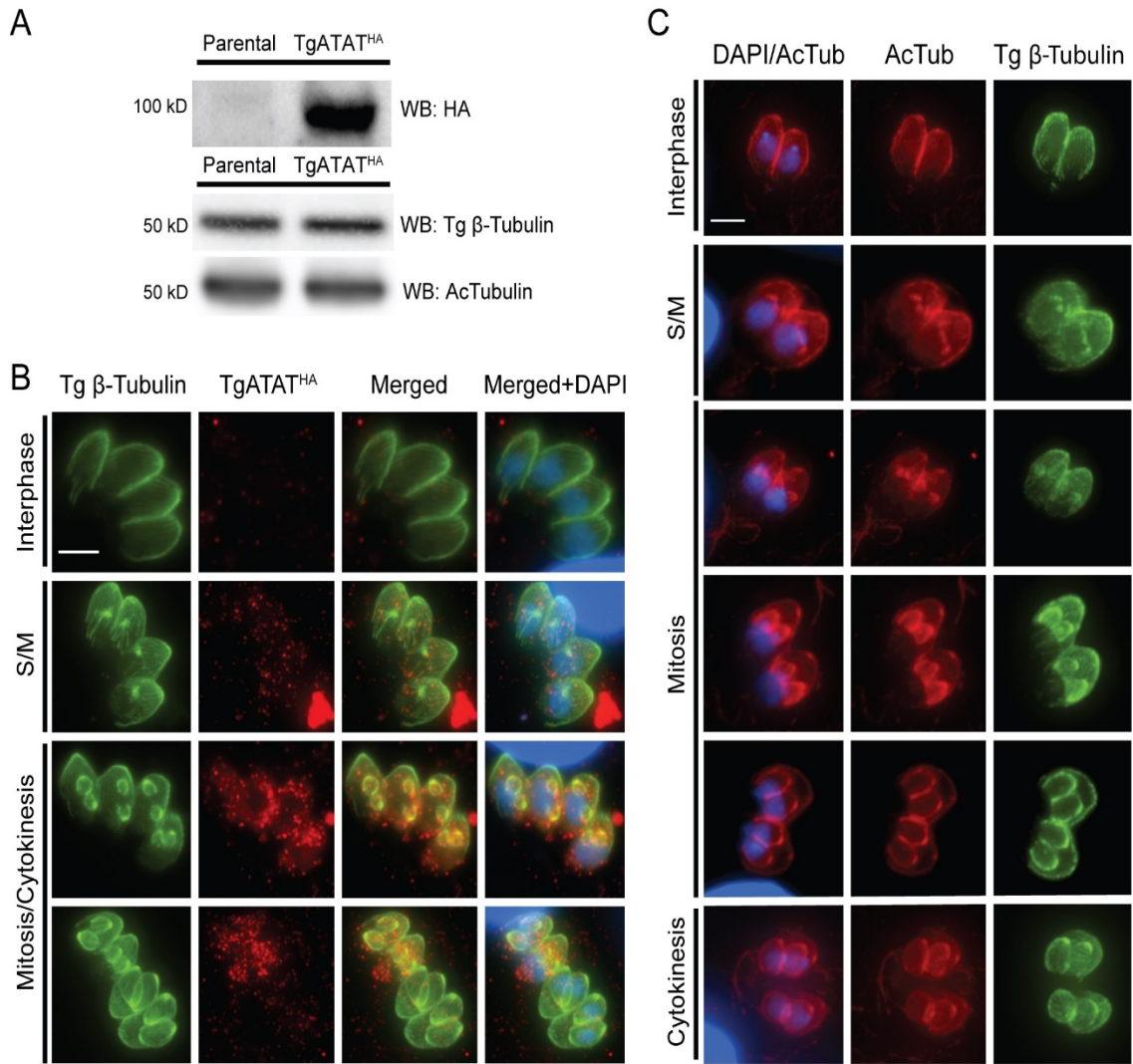


Figure 23. Expression of TgATAT and acetylated  $\alpha$ -tubulin during the tachyzoite cell cycle. Reprinted from reference (188).

A. Western blot (WB) assay of lysates from the parental strain (RH $\Delta$ hx $\Delta$ ku80) and parasites containing endogenously HA-tagged TgATAT (TgATAT<sup>HA</sup>). The blot was probed with antibodies recognizing the HA epitope or acetyl-K40- $\alpha$ -tubulin.  $\beta$ -Tubulin was also probed as a loading control. B. IFAs of TgATAT<sup>HA</sup> parasites stained for HA (red, TgATAT<sup>HA</sup>) or  $\beta$ -tubulin (green) at the indicated stages of the parasite cell cycle. Images were merged with the DNA stain DAPI (blue). C. IFAs of RH parasites stained for acetyl-K40- $\alpha$ -tubulin (red) or  $\beta$ -tubulin (green) at the indicated stages of the parasite cell cycle. Note that K40 acetylation is present on both spindle microtubules during mitosis and in the daughter subpellicular microtubules throughout replication. Scale bar, 3  $\mu$ m.

### 3.3.3 Disruption of *TgATAT* leads to loss of $\alpha$ -tubulin K40 acetylation

To determine the impact of *TgATAT* on  $\alpha$ -tubulin K40 acetylation, we attempted to knockout the genomic locus using double homologous recombination but could not isolate viable clones, suggesting that *TgATAT* may be essential in tachyzoites. We then employed the CRISPR/Cas9 system recently reported for *Toxoplasma* (195, 196) by transfecting a plasmid encoding a GFP-Cas9 fusion and a *TgATAT*-targeting single guide RNA (sgRNA) into our *TgATAT*<sup>HA</sup> parasites. Along with the GFP-Cas9/sgRNA plasmid, we co-transfected a dsDNA oligomer containing four stop codons flanked by short regions of homology to the *TgATAT* Cas9 cleavage site to ensure disruption of the gene, and the loss of *TgATAT*<sup>HA</sup> protein was subsequently confirmed by IFA (Figure 24). A control transfection was performed using the aforementioned dsDNA oligomer and the GFP-Cas9 plasmid containing sequences encoding a sgRNA targeting the unrelated and nonessential uracil phosphoribosyltransferase (*UPRT*) gene (196). Transfected parasites were inoculated onto human foreskin fibroblasts (HFF) and the infected monolayers were fixed after 20 hours so that the expression of GFP-Cas9 could be observed by fluorescence microscopy (Figure 24). In parasites transfected with the *UPRT* targeting construct, we observed 13% (30/231) expressing GFP-Cas9; in contrast, GFP-Cas9 expression was observed at a lower frequency in parasites transfected with *TgATAT*-targeting sgRNA (2.89 $\pm$ 0.93% SEM, n=3). Importantly,  $\alpha$ -tubulin K40 acetylation was completely abolished in the majority of the GFP-Cas9 positive parasites transfected with the *TgATAT*-targeting sgRNA (57.8 $\pm$ 4.97% SEM, n=3) but never diminished in GFP-Cas9 positive parasites transfected with the control *UPRT*-targeting sgRNA (Figure 24). At 40 hours post-transfection, the number of GFP-Cas9 positive parasites lacking  $\alpha$ -tubulin K40 acetylation increased to 76.1 $\pm$ 2.01% (SEM, n=3) in *TgATAT*-sgRNA transfected populations. The inability to detect  $\alpha$ -tubulin K40 acetylation when the *TgATAT* locus is selectively targeted for CRISPR/Cas9-mediated disruption strongly suggests that *TgATAT* is the major  $\alpha$ -tubulin K40 acetyltransferase in *Toxoplasma* and not *TgElp3*.

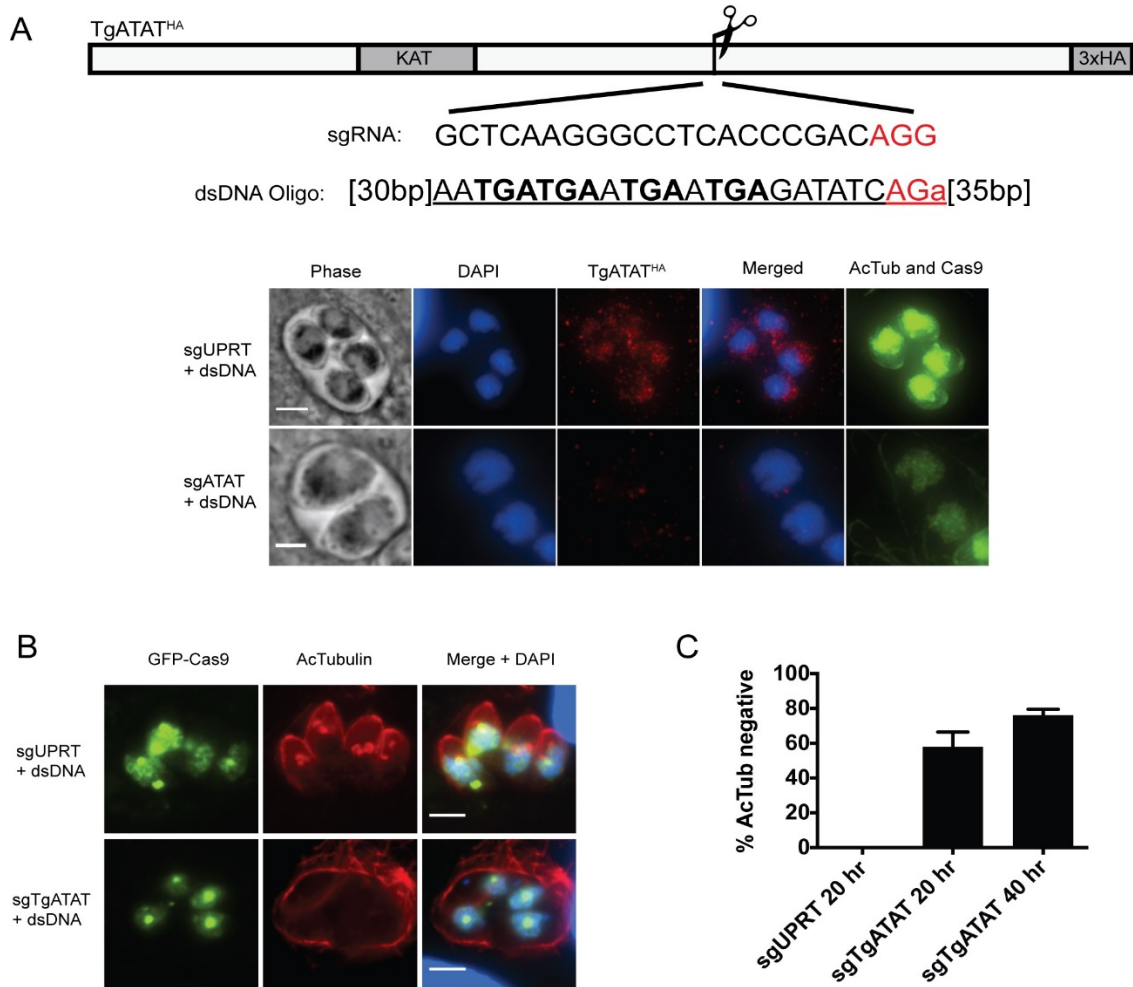


Figure 24. Selective targeting of GFP-Cas9 to the TgATAT locus eliminates K40 acetylation. Reprinted from reference (188).

A. Diagram showing the site on TgATAT targeted by GFP-Cas9. The 20-bp TgATAT sgRNA sequence is shown; it is immediately upstream of the protospacer adjacent motif sequence (PAM, red). The dsDNA oligomer used for recombination is shown, and in brackets are the numbers of bases of homology flanking the PAM site. Underlined is the exogenous sequence introduced, including the four stop codons in bold.

IFAs of dividing parasites expressing GFP-Cas9 confirm that disruption of TgATAT and loss of K40 acetylation occur only when Cas9 is targeted to the TgATAT locus (sgTgATAT). B. IFA of TgATAT<sup>HA</sup> parasites 40 h posttransfection with dsDNA oligomers and GFP-Cas9 targeted to either the UPRT (sgUPRT) or the TgATAT (sgTgATAT) locus. Scale bar, 3  $\mu$ m. C. Bar graph showing the percentage of GFP-Cas9-positive vacuoles that are acetyl-K40 negative in parasites in which GFP-Cas9 was targeted to UPRT (sgUPRT) versus TgATAT (sgTgATAT) 20 or 40 h after transfection. Error bars show the standard errors of the means (n = 3).

### 3.3.4 Loss of K40 acetylation causes microtubule defects and impairs replication.

GFP-Cas9 expressing parasites transfected with the *UPRT* targeting control retained acetylated  $\alpha$ -tubulin and displayed normal microtubule structures 40 hours post-transfection, as did *TgATAT*-sgRNA transfectants that lacked GFP-Cas9 expression (Figure 25). In contrast, *TgATAT*-sgRNA transfectants expressing GFP-Cas9 that lost  $\alpha$ -tubulin acetylation exhibited abnormal morphology (Figure 25, phase, compare acetyl-K40 positive parasites in inset *i* with acetyl-K40 negative parasites in inset *ii*). DAPI-staining revealed that the parasites lacking K40 acetylation possessed nuclei that were grossly deformed, as if they failed to complete karyokinesis (Figure 25, inset *ii*, asterisks). *TgATAT*-sgRNA transfectants that retained acetylated  $\alpha$ -tubulin contain nuclei of uniform shape and area (as measured in pixels), whereas parasites lacking acetylated  $\alpha$ -tubulin possess a wide variety of DAPI-staining structures that are abnormal in size and shape (Figure 25). Of note, while large nuclei that appeared to have undergone genomic duplication were frequently observed, the classic horseshoe shape of the nucleus routinely seen during cytokinesis was largely absent in parasites lacking K40 acetylation. Further, many of the parasites lacking K40 acetylation contained daughter parasites that were devoid of nuclear material (Figure 25, inset *i*, arrowheads). Parasites lacking K40 acetylation were also observed to possess numerous additional cytoplasmic  $\beta$ -tubulin-containing structures, many of which resembled caps of budding daughter cells (Figure 25, inset *ii*, arrows); in these parasites, the mother's microtubules and cytoskeleton fail to undergo recycling to the residual body and instead appear to remain intact while the formation of multiple daughter parasites seems to have been initiated. Despite this evidence of early daughter bud initiation, proper formation of the mature cytoskeleton appears to be impaired upon loss of K40 acetylation, as a variety of abnormal parasite sizes and shapes are observed (Figure 25, phase and  $\beta$ -tubulin channels). Together, these defects in cytokinesis and cytoskeleton formation suggest that K40 acetylation likely impacts both spindle and subpellicular microtubule populations.



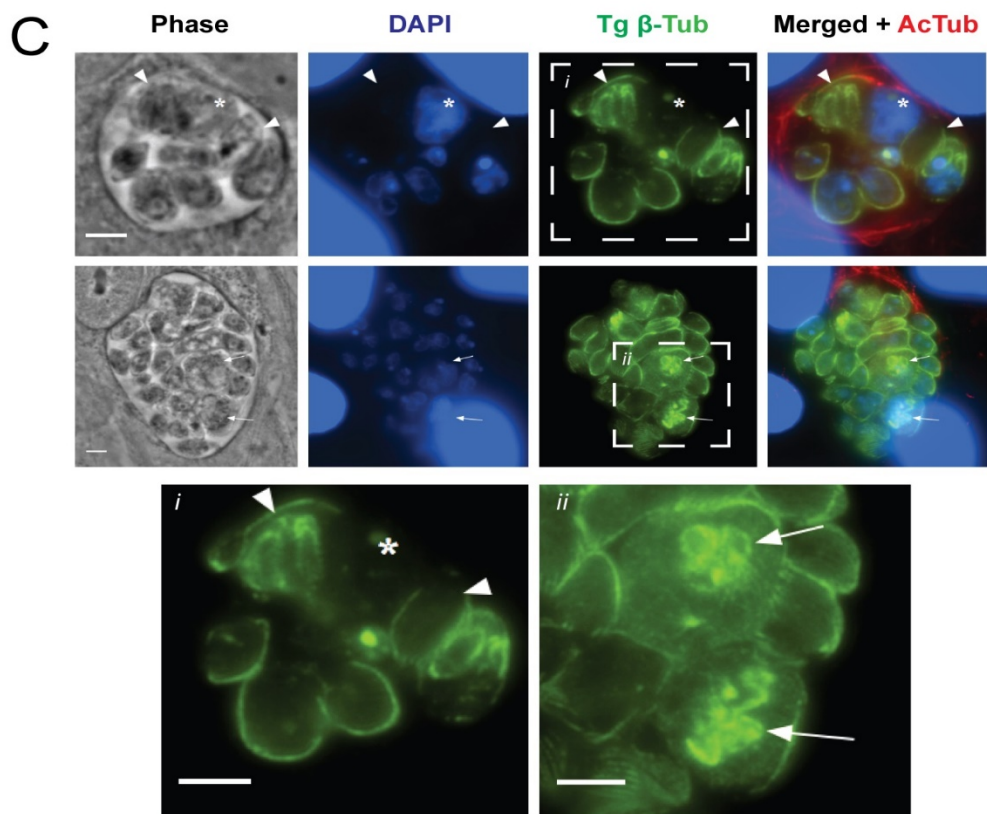
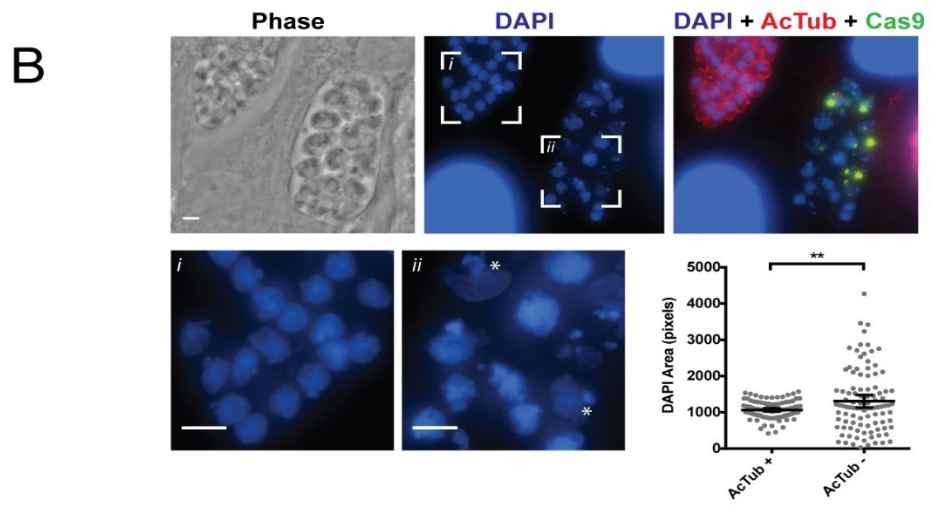
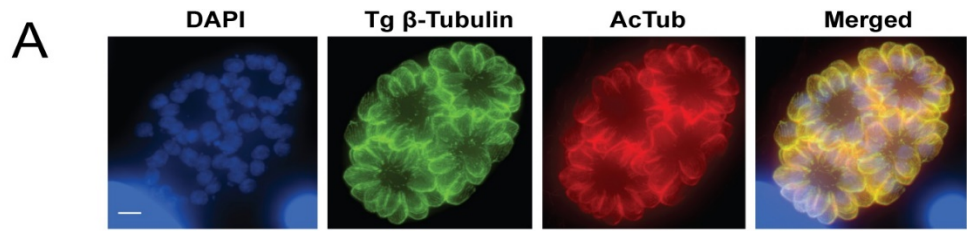


Figure 25. Defects in nuclear division and segregation in parasites lacking  $\alpha$ -tubulin K40 acetylation. Reprinted from reference (188).

A. TgATAT<sup>HA</sup> parasites were transfected with GFP-Cas9-sgTgATAT and imaged at 40 h post-transfection. Shown are transfectants lacking GFP-Cas9 expression, which display normal replication and have microtubules containing K40 acetylation, as visualized with anti- $\beta$ -tubulin (green) and acetyl-K40- $\alpha$ -tubulin (red) antibodies, with DAPI co-stain in blue. B. Parasites expressing GFP-Cas9 lose K40 acetylation and contain abnormal nuclear morphology compared to that of parasites possessing K40 acetylation. Nuclei were visualized by DAPI staining (blue). Insets of acetyl-K40-positive (i) and -negative (ii) parasites are shown and expanded in the lower panels. The DAPI-stained structures was measured with ImageJ (n = 100 nuclei). Double asterisks indicate a significant difference in mean area, as determined by unpaired t test with Welch's correction for unequal variance (P = 0.0085). C. Vacuoles containing parasites lacking acetylated microtubules (red) and showing aberrant phenotypes detected by staining all of the microtubules (green) and DNA (blue) are shown. Inset i shows that parasites lacking K40 acetylation have defects in microtubule structures and fail to partition nuclear material into daughter parasites. Anucleate parasites are marked by arrowheads, while the improperly segregated nuclear mass is indicated by the asterisk. Inset ii shows parasites containing multiple  $\beta$ -tubulin structures resembling daughter cell conoids (arrows). Scale bar, 3  $\mu$ m.

To explore these replication defects more closely, we examined early steps in *Toxoplasma* endodyogeny when the duplication of the centrosome and subsequent division of the apicoplast occur (197). Control parasites containing K40 acetylation have either a single or duplicated centrosome per nucleus (Figure 26, arrowhead), as well as a single apicoplast (Figure 26, arrowhead). Parasites lacking K40 acetylation can still duplicate centrosomes; however, those with defects in nuclear division often had >2 centrosomes per nucleus (Figure 26, arrows). Additionally, parasites lacking K40 acetylated  $\alpha$ -tubulin often contained large, irregular apicoplasts, suggesting a role for acetylated  $\alpha$ -tubulin in the proper division of this organelle (Figure 26, arrows).



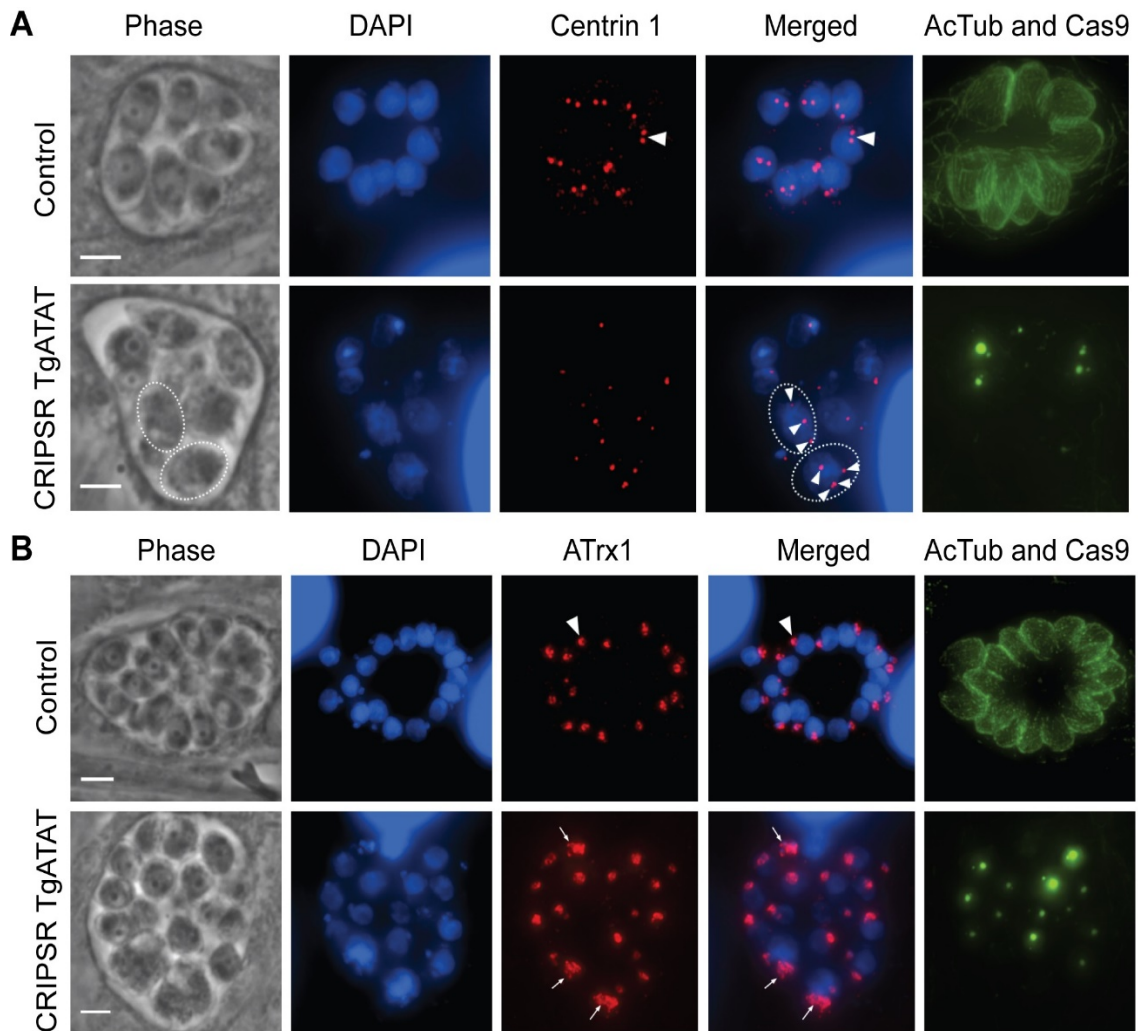


Figure 26. Centrosome duplication and apicoplast division in parasites lacking K40 acetylation. Reprinted from reference (188).  
 A. Duplication of the centrosomes occurs in the presence (top row, arrowhead) or absence of K40  $\alpha$ -tubulin acetylation (bottom row, arrowheads), as visualized by IFA staining for centrin 1 (red), acetyl-K40- $\alpha$ -tubulin (green), and DNA (DAPI, blue). K40-acetylated  $\alpha$ -tubulin and GFP-Cas9 (localized to the nucleus) were detected in the same channel (green). Note the loss of acetylated  $\alpha$ -tubulin and GFP-Cas9-expressing parasites. Dotted lines encircle individual parasites with arrowheads indicating multiple centrosomes. B. IFAs of parasites stained for apicoplast membrane protein Atrx1 (red), acetyl-K40- $\alpha$ -tubulin (green), DNA (DAPI, blue), and GFP-Cas9 (green, nuclear). Apicoplasts that underwent normal division are visible in acetyl-K40-positive parasites (top row, arrowhead). Apicoplasts that failed to divide in parasites lacking K40 acetylation (bottom row) are indicated by arrows. Scale bars, 3  $\mu$ m.

Centrosome duplication is followed by formation of the daughter bud apical complex. As we observed evidence of apical conoid formation in the absence of K40 acetylation (Figure 25, arrowheads), we investigated whether K40 acetylation was required to recruit the IMC and IMC subcompartment proteins (ISPs) to the nascent daughter cytoskeleton. During interphase, ISP1 localizes to the apical cap of each parasite (Figure 27), and is recruited to the apical regions of the daughter buds during bud formation (181). While parasites containing acetylated  $\alpha$ -tubulin showed two ISP1-labeled apical caps per dividing parasite, loss of  $\alpha$ -tubulin acetylation resulted in parasites containing multiple ISP1 structures per nucleus (Figure 27, arrowhead). In parasites lacking acetylated  $\alpha$ -tubulin, IFAs staining for IMC3, which localizes to the IMC following recruitment of ISP1 to daughter caps, revealed the presence of multiple IMC structures forming within a single parasite (Figure 27, arrowheads). Taken together, these results suggest that acetylation of  $\alpha$ -tubulin at K40 is dispensable for initiation of mitosis and the early steps of daughter cell formation, but is required for karyokinesis, apicoplast division, and completion of *Toxoplasma* replication.

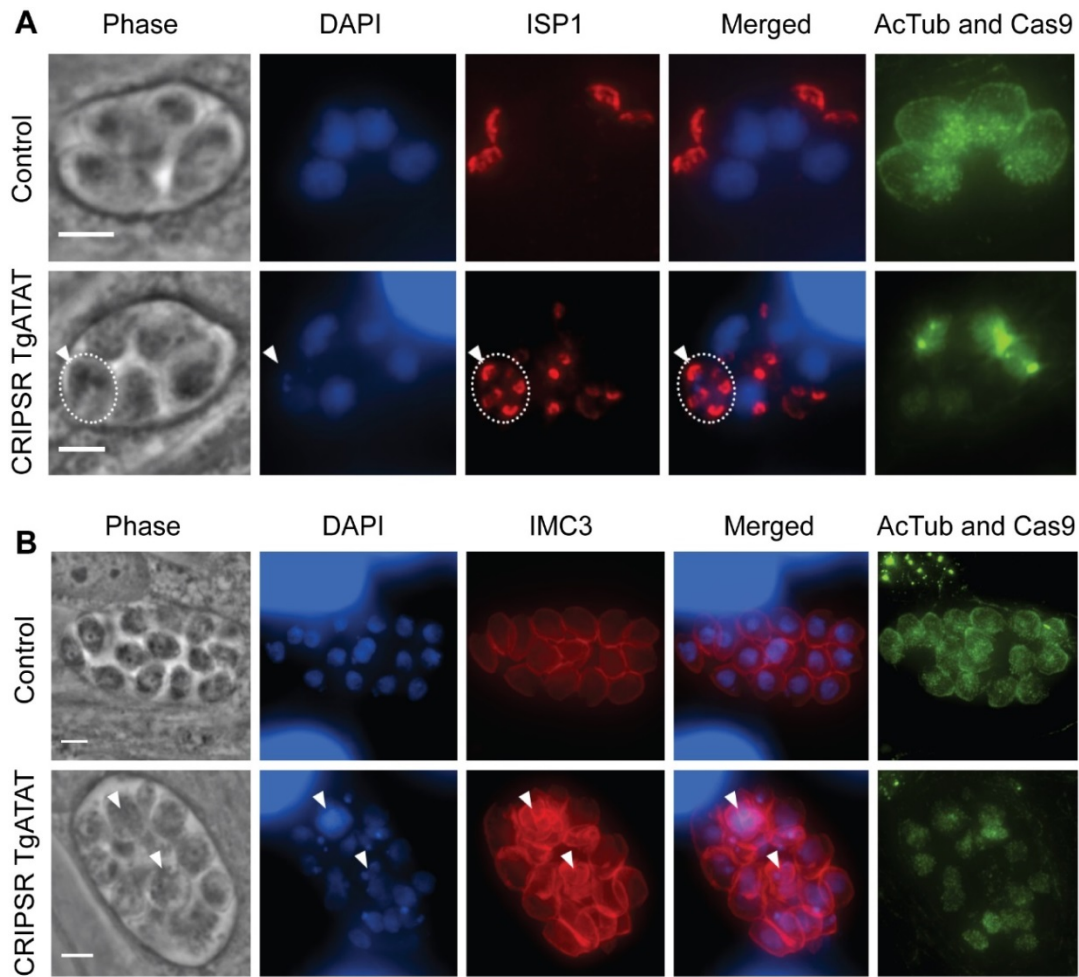


Figure 27. Daughter cytoskeleton completion is impaired upon loss of K40 acetylation. Reprinted from reference (188).  
 A. IFA visualizing ISP1 (red), acetyl-K40- $\alpha$ -tubulin (green), DNA (DAPI, blue), and GFP-Cas9 (green, nuclear) in normal parasites (top) versus those lacking acetylated  $\alpha$ -tubulin (bottom). Dotted lines encircle an individual parasites containing excess daughter buds (bottom row, arrowhead), as visualized by numerous ISP1-positive apical cap structures. B. IFA stained for IMC3 (red), acetyl-K40- $\alpha$ -tubulin (green), DNA (DAPI, blue), and GFP-Cas9 (green, nuclear). Arrowheads indicate multiple IMC3-positive structures in parasites lacking K40  $\alpha$ -tubulin acetylation, indicative of partially formed daughter cells that failed to complete division. Scale bars, 3  $\mu$ m.

### 3.4 Discussion

In this study, we addressed the biological role of  $\alpha$ -tubulin K40 acetylation in the protozoan pathogen *Toxoplasma* using two independent genetic approaches that ablated either the modifying enzyme or the substrate. Our

mutational analyses of *TgTUBA1* show that mutation of K40 to glutamine, an acetyl-lysine mimic, is tolerated, while mutation to arginine is inviable unless a secondary mutation that stabilizes microtubules is made. Additionally, we have identified that the KAT responsible for mediating K40-acetylation is TgATAT (not TgEIp3). Loss of K40 acetylation following CRISPR/Cas9-mediated disruption of the *TgATAT* locus severely impairs nuclear division and parasite replication.

Interestingly, many of the phenotypes we observed upon the disruption of K40  $\alpha$ -tubulin acetylation parallel the effects observed when microtubules are destabilized with oryzalin (155, 156, 186, 198, 199). Treatment of intracellular parasites with oryzalin prevents completion of the daughter budding process, although nuclei size increased and centriole replication occurred (187). Additional studies show that destabilization of the spindle microtubules by oryzalin results in the formation of anuclear “zoids”, similar to what we observed in parasites lacking K40 acetylation (Figure 25) (156). Importantly, EM analysis of oryzalin-treated parasites showed that numerous daughter conoids form within mother parasites when nuclear division failed. This bears a striking resemblance to the defects we observed in parasites lacking K40 acetylation, as we detect numerous structures resembling daughter caps that stain positive for  $\beta$ -tubulin, ISP1, and IMC3 (Figure 25, Figure 27). Early stages of parasite division, including replication of genomic DNA, duplication of the centrosomes, and daughter bud initiation, remain intact following loss of K40 acetylation, again mirroring what is seen in oryzalin-treated parasites. In addition to defects in nuclear division, we also see evidence that apicoplast division is impaired in parasites without K40 acetylation (Figure 26, arrows). This agrees with studies showing that apicoplast division is a microtubule-dependent process that occurs temporally with nuclear division and is disrupted by oryzalin treatment (200). Together, these results suggest that acetylation of  $\alpha$ -tubulin at K40 plays an important role in stabilizing both the subpellicular and mitotic spindle populations of microtubules in *Toxoplasma*, and that this microtubule stabilization is especially critical for proper tachyzoite replication.

Our mutational analyses of *TgTUBA1* showed that the function of K40 acetylation can be mimicked by substitution of K40 with glutamine (Figure 20), in agreement with findings in both *C. elegans* and *R. norvegicus* (167, 201). Molecular dynamics simulations provide a plausible explanation for the ability of the K40Q substitution to effectively mimic K40 acetylation. In those simulations, acetylation of K40 on  $\alpha$ -tubulin disrupts an intra-monomeric salt bridge between  $\alpha$ -tubulin residues K40 and E55, a residue conserved in *Toxoplasma*  $\alpha$ -tubulin. This disruption allows for the acetyl-group on K40 to form a new salt bridge with H283 (also conserved in *Toxoplasma*) of an  $\alpha$ -tubulin monomer in an adjacent protofilament (173). Mutation of K40 to arginine would chemically allow for salt bridge formation with the carboxyl-group of E55 while preventing inter-protofilament salt bridge formation through H283. Conversely, mutation of K40 to glutamine would constitutively promote salt bridge formation between the glutamine carboxyl group (Q40) with the imidazole group (H283) located on the adjacent protofilament. Therefore, our ability to generate parasites expressing only Q40 in the non-stabilizing V252L background suggests that salt bridge formation between protofilaments is important for microtubule structure and stability.

The ability to generate K40R mutants in the T239I background further speaks to the role of K40 acetylation in *Toxoplasma* microtubule stability. T239I resides in the H7 helix of  $\alpha$ -tubulin and is within the oryzalin binding pocket (202). Mutation of another binding pocket residue (L136F) stabilized microtubules by promoting interactions between  $\alpha$ -tubulin subunits within the microtubule lattice (187). Together, these data suggest that oryzalin-resistance generated by mutating binding pocket residues may also lead to increased inter-protofilament interactions, which is similar to the proposed mechanism by which K40 acetylation promotes microtubule stability discussed above. Therefore, it is plausible that like L136F, the T239I mutation stabilizes microtubules and compensates for the loss of stability when K40 acetylation is nullified.

To further determine the biological importance of  $\alpha$ -tubulin K40 acetylation in *Toxoplasma*, we identified and disrupted the  $\alpha$ -tubulin acetyltransferase,

*TgATAT*. Endogenous tagging of the *TgATAT* locus revealed a cell-cycle expression pattern that correlated temporally with enriched regions of  $\alpha$ -tubulin acetylation during parasite replication. These results agree with a recent report noting that  $\alpha$ -tubulin K40 acetylation occurs after spindle microtubule assembly in early daughter formation (179). *TgATAT* is considerably larger than all previously characterized ATAT/Mec17 proteins, possessing highly divergent sequences flanking the conserved Mec17-domain (Figure 22). Further bioinformatic analysis revealed that select species within the coccidian subclass of the Apicomplexa phylum also possess a large *TgATAT* homologue, 89 kDa in *Neospora caninum* (NCLIV\_010560) and 98 kDa in *Hammondia hammondia* (HHA\_319600). Our CRISPR-mediated disruption of *TgATAT* indicates that it is the primary  $\alpha$ -tubulin acetyltransferase in *Toxoplasma*. As *TgATAT* is essential for parasite replication and has divergent features, it may make an attractive potential drug target.

While mammalian ATAT has been shown to localize to the lumen of the microtubule where it exerts its KAT activity (203), the considerably larger size of the apicomplexan orthologues may seem to preclude their access to this site. However, recent *in vitro* studies using polymerized microtubules have shown that large macromolecules, such as the full-length 6-11B-1 anti-acetyl-K40- $\alpha$ -tubulin antibody (~150 kDa), are able to enter the lumen of microtubules (203). Other studies have also reported that ATAT/Mec17 can bind to the exterior surface of microtubules; if microtubules undergo lateral opening between protofilaments, the K40 substrate could be exposed for acetylation (204, 205). Further studies are required to address exactly how *TgATAT* gains access to its substrate. Whether *TgATAT* has additional substrates is also an intriguing question for future study. Outside of ATAT/Mec17 itself (206), no other substrates have been reported for this family of KATs to date.

Our analysis of K40 acetylation provides the first detailed look at the functional role and importance of tubulin modifications in *Toxoplasma* biology. Given that many other tubulin PTMs have been reported for *Toxoplasma* (177), it is likely that these modifications may also contribute to regulating microtubule function in the parasite. While dissecting the biological role of these PTMs in

other species is complicated by the expression of multiple  $\alpha$ -tubulin isotypes, their function in *Toxoplasma* tachyzoites may be easier to determine as only *TgTUBA1* is expressed in this stage. The identification and characterization of the enzymes responsible for mediating these PTMs provides an exciting new field of study for the development of novel therapeutics to treat toxoplasmosis.

### **3.5 Concluding Remarks**

Unlike higher eukaryotes, Elp3 in *Toxoplasma* does not function as an alpha-tubulin acetyltransferase. Instead, we identified TgATAT as the enzyme responsible for K40 acetylation. Our experimental findings determined that K40 acetylation is essential for parasite replication, making this an exciting new avenue to explore for future drug development. However, we still do not know the enzymatic function of TgElp3. Despite strong sequence homology of the KAT and rSAM domains of TgElp3 with higher eukaryotes, our data suggests that it may function differently in *Toxoplasma*. Supporting this idea, TgElp3 contains a transmembrane domain which is only found in the phylum Apicomplexa and a few select species. Seeing that this transmembrane domain is not present in higher eukaryotes and that parasite viability is dependent on TgElp3 localization to the outer mitochondrial membrane, in the next chapter we explore this trafficking mechanism.

## **CHAPTER 4: Targeting of TgElp3 and other tail-anchored proteins to subcellular organelles in *Toxoplasma gondii***

### **4.1 Introduction**

In *Toxoplasma gondii*, selective permeabilization experiments determined TgElp3 is positioned at the OMM with the N-terminal domains facing the cytoplasm (83). Proteins like TgElp3 with a single TMD positioned within 30 amino acids of the C-terminus and uniquely positioned with the N-terminal domain protruding into the cytosol are classified as tail-anchored (TA) proteins (207, 208). Interestingly, only Elp3 homologues identified in the Apicomplexa phylum and a few select species possess a C-terminal TMD, suggesting Elp3 may have functions pre-dating the evolution of the Elongator complex. Moreover, localization of TgElp3 to the parasite mitochondrion is essential for *Toxoplasma* viability signifying a possible role specific to this organelle.

Organellar localization and lipid membrane integration are highly dependent on the TA protein TMD sequence (208). Numerous biological processes including vesicle-mediated trafficking, protein translocation and the regulation of apoptosis are reliant on correct TA protein localization (209–211). Due to the notable position of the C-terminal TMD sequence, translation termination must occur prior to the exit of the TMD sequence from the ribosome (212, 213). Thus, the localization of TA proteins to their target membranes must ensue in a post-translational dependent manner (212).

Post-translational targeting of TA proteins to the ER is well characterized in some species, with 4 distinct targeting mechanisms: Hsc70/Hsp40 (214–216), TRC40/Asna1/Get1 (217–219), SRP assisted insertion (212, 220) and unassisted insertion (221–223). TA proteins residing in the Golgi apparatus first insert into the ER and then are trafficked to the Golgi (210). Less well-characterized is the trafficking and targeting of TA proteins to the mitochondria and other organelles. Compared to ER-targeted TA proteins, mitochondrial TA proteins tend to possess TMDs that are shorter and moderately hydrophobic (207). Additionally, studies in *Saccharomyces cerevisiae* have shown that low levels of ergosterol present in the OMM can strongly influence unassisted TMD



integration (224). Most recently, a dibasic targeting motif was identified in many OMM-TA targeted proteins in *Arabidopsis thaliana* (225). Despite the identification of several TA trafficking mechanisms, localization to distinct subcellular organelles is complex and needs further study. The discovery of TA proteins in the early-branching eukaryote *Toxoplasma* speaks to the antiquity of this trafficking system in eukaryotic cells and to date, no detailed studies of TA proteins have been performed in protozoa.

Previous bioinformatics surveys have identified putative TA proteins in several species including *Saccharomyces cerevisiae* (55 TA proteins) (226), *Arabidopsis thaliana* (454 TA proteins) (227), and *Homo sapiens* (325 TA proteins) (228). To identify how TgEIp3 localizes to the parasite mitochondrion, we followed a similar approach to identify and characterize other potential TA proteins in *Toxoplasma*. In collaboration with Dr. Gustavo Arrizabalaga we identified 59 putative TA proteins, 9 of which contained representative features we dissected further. The results revealed novel TA proteins trafficking to specific subcellular organelles in *Toxoplasma*, including the parasite ER, mitochondrion and Golgi apparatus. Domain-swapping strategies were also employed to gain insight into the targeting mechanisms of these *Toxoplasma* TA proteins, including TgEIp3.

## **4.2 Materials and Methods**

### **4.2.1 Parasite culture and transfection**

For all experiments the starting *Toxoplasma* strain was RH. Parasites were maintained in confluent human foreskin fibroblast (HFF) monolayers with Dulbecco's modified Eagle's medium supplemented with 1% heat-inactivated fetal bovine serum at 37°C and 5% CO<sub>2</sub> (113). Wild-type RH strain parasites were electroporated with 75µg of plasmid and allowed to infect fresh HFFs; 24 hours post-transfection, 1µM pyrimethamine was added to select for transgenic parasites (100).

## 4.2.2 Bioinformatics analyses

Annotated *Toxoplasma* proteins from strain ME49 in release 9.0 of the genome database (ToxoDB.org) were downloaded as a single FASTA file. The FASTA file was submitted to the TMHMM (version 2.0, <http://www.cbs.dtu.dk/services/TMHMM/>) (229) and DAS (<http://www.sbc.su.se/~miklos/DAS/>) (230) transmembrane prediction sites for batch analysis. With both prediction sites default parameters were used. Proteins that were predicted to possess a single transmembrane domain were analyzed for its position within the protein sequence. Those for which the transmembrane domain was followed by only 30 or less amino acids were considered as putative TA proteins.

Total hydrophobicity of each putative TA protein TMD was calculated using the Kyte and Doolittle hydrophobicity scale, default parameters were used (<http://web.expasy.org/protscale/>) (231).

## 4.2.3 Plasmid DNA construction

### 4.2.3.1 HA-tagging vectors

All generated DNA vectors are listed in Appendix E and all primers used are listed in Appendix F. To generate constructs for immunolocalization, a *Toxoplasma* expression vector was generated that fuses an N-terminal hemagglutinin (HA)-tag to the protein under study. The DHFR 3' UTR was amplified from the pHXGPRT:tub vector using primers F1 and R1 and inserted into the *Toxoplasma* expression vector pDHFR-TS at the HindIII restriction site (DHFR 3'UTR-pDHFR-TS) (99, 100). Next, the tubulin promoter-5'UTR-HA-tag (TubHA) was amplified from the <sup>HA</sup>TgEIp3 plasmid using primers F2 and R2 and inserted upstream into the Apal restriction site of the DHFR 3'UTR-pDHFR-TS plasmid (TubHA-EcorV-DHFR 3'UTR-pDHFR-TS) (83, 100). EcoRV restriction sites were inserted into both the TubHA and 3'UTR DHFR PCR fragments to generate in-frame restriction sites used for insertion of gene amplicons. RNA was extracted from RH $\Delta$ hxgpri (or Pru $\Delta$ ku80 $\Delta$ hxgpri for Cytb-5) parasites using the RNeasy Plus mini kit (Qiagen; #74134) and cDNA was prepared using the

Omniscript RT kit (Qiagen; #205111). Genes were amplified starting with the first nucleotide downstream of the start codon through the stop codon from cDNA. All primers are listed in Appendix F. PCR amplicons were inserted into the EcorV sites of the HA-tagging plasmid (TubHA-EcorV-DHFR 3'UTR-pDHFR-TS) using the in-Fusion HD cloning kit (Clontech; #011614).

#### **4.2.3.2 YFP-fusion vectors**

An N-terminal YFP-fusion construct was generated by amplifying the tubulin promoter-5'UTR-YFP (TubYFP) using primers F2 and R2-2 (Appendix F) from the previously published YFP-C construct (83). This fragment was inserted into the Apal restriction site of the DHFR 3'UTR-pDHFR-TS plasmid described above. Similarly, PCR was used to insert in-frame EcorV restriction sites downstream of the TubYFP and upstream of the 3'UTR-pDHFR to create the YFP-tagging plasmid, TubYFP-EcorV-DHFR3'UTR-pDHFR-TS. DNA fragments encoding the tail anchor signal for each gene including ten amino acids upstream of the predicted transmembrane domain, the transmembrane domain, and the flanking C-terminal sequence were amplified from the HA-tagging constructs using primers listed in Appendix F. These fragments were inserted into the EcorV restriction sites using the in-Fusion HD cloning kit (Clontech; #011614).

#### **4.2.3.3 Domain-swap vectors**

For constructs in which only the CTS was swapped, PCR amplification was performed using primers to insert the designated CTS mutations (See Appendices E and F for primers used and their sequences). Constructs containing the replacement of the TMD and CTS were created by fusing two different gene fragments that were each amplified from the gene-specific HA-tagging constructs described above. To generate the TMD replacement constructs, the cytoplasmic domain and TMD were amplified from the TMD-CTS domain swapping plasmids; primers were used to insert the CTS corresponding to the cytoplasmic domain. For all domain swapping constructs, amplicons were

inserted into the EcorV sites of the Tub<sub>HA</sub>-EcorV-DHFR 3'UTR-pDHFR-TS construct using the in-Fusion HD cloning kit (Clontech; #011614).

#### 4.2.4 Immunofluorescence Assays

Confluent HFF monolayers grown on coverslips in 24-well plates were infected with freshly lysed parasites. Infected host cells were fixed with 4% paraformaldehyde in PBS, blocked for 30 min in 3% BSA+PBS, and permeabilized with 0.2% Triton X-100 (PBS-T) for 10 min. Primary antibodies (see below) diluted in 3% BSA-PBS were applied overnight at 4°C. Cultures were washed three times for 10 min each with PBS. Secondary antibodies diluted in 3% BSA-PBS were applied for 1hr at room temperature. Coverslips were washed three times for 10 min and 4',6-Diamidino-2-phenylindole dihydrochloride (DAPI, Life Technologies; #D1306) diluted 1:1,000 in PBS was applied for 10 mins at room temperature. Following three 10 min washes, coverslips were mounted using Vectashield antifade mounting medium (Vector Labs; #H-1000).

The following primary antibodies were used at the dilutions indicated: rat anti-HA (1:2,000; Roche #11867423001), rabbit anti-HA (1:2,000; Cell Signaling Technology #3724), mouse anti-TgF1B-ATPase (1:4,000; (109)), rat anti-TgSORTLR (1:2,000; (232)) and mouse anti-TgSERCA (1:2,000; (233)). Secondary antibodies conjugated to a fluorophore (Alexa Fluor; Thermo Fisher #A11005, #A11006, #A11007, #A11034) were used for IFAs at a 1:5,000 dilution.

### 4.3 Results and Discussion

#### 4.3.1 Identification of TA membrane proteins in *Toxoplasma*

We previously identified TgElp3 as a TA membrane protein in *Toxoplasma* that resides at the outer membrane of the parasite's single mitochondrion (83). We performed a bioinformatics survey to identify other candidate TA proteins in the parasite in order to investigate targeting of this unusual protein family in an early-branching eukaryote. For this analysis, FASTA sequences for each annotated *Toxoplasma* protein were downloaded from ToxoDB.org v.9.0 (192) and analyzed for the presence of a single transmembrane within 30 amino acids

of the C-terminus using the prediction servers TMHMM (<http://www.cbs.dtu.dk/services/TMHMM/>) (229) and DAS (<http://www.sbc.su.se/~miklos/DAS/>) (234). Only proteins predicted to have a single transmembrane were analyzed using SignalP (<http://www.cbs.dtu.dk/services/SignalP/>) and proteins devoid of a signal sequence were included in our list of putative TA proteins (Figure 28, Table 2 and Appendix D). Of the 57 predicted *Toxoplasma* TA proteins, nearly half (25 out of 57) are annotated as hypothetical proteins with unknown function. A few proteins (5) appear to be parasite specific, and the remaining 27 proteins contain conserved domains that make them likely homologues that have been characterized in other species (Appendix D).

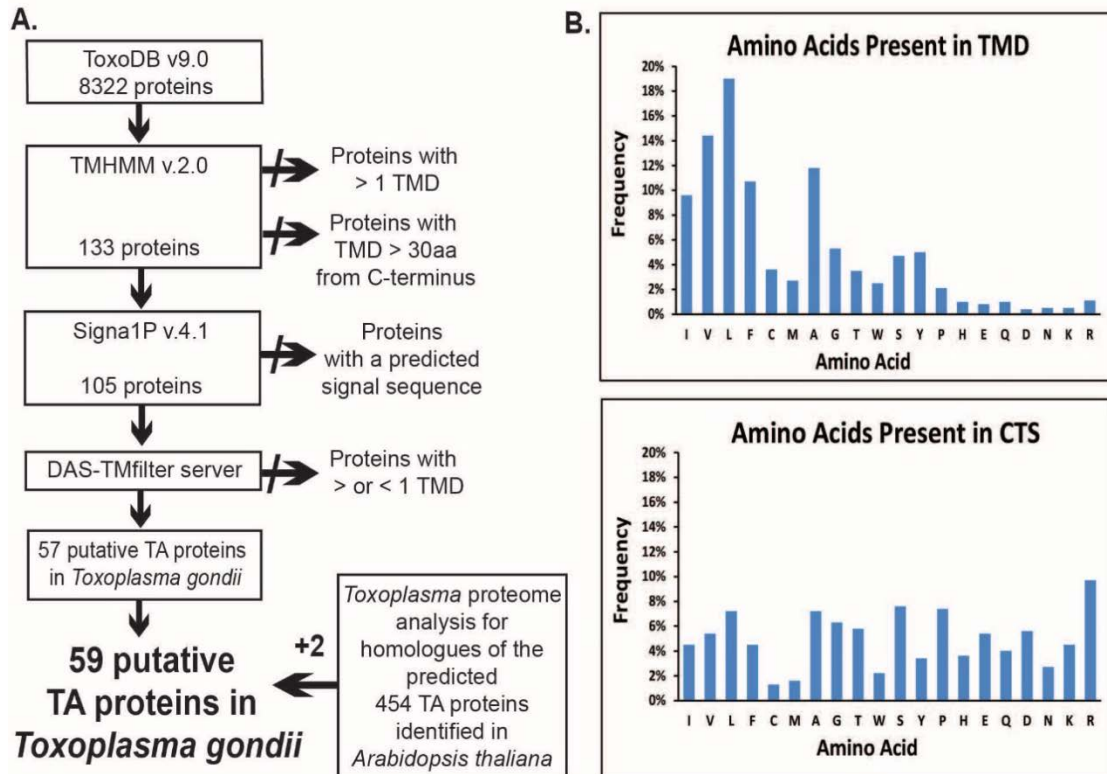


Figure 28. Identification of putative tail-anchored (TA) proteins in *Toxoplasma*. A. Flow diagram listing the bioinformatics steps performed to identify putative TA proteins is shown. The computational tools used and the number of proteins retained at each step are listed. B. Average amino acid frequencies were calculated for the predicted transmembrane domain (TMD) sequence and subsequent C-terminal sequence (CTS). Amino acids are listed in decreasing order of hydrophobicity according to the Kyte and Doolittle scale (231). Crossed out arrows represent excluded proteins. Plus sign represents addition of proteins. Reprinted from reference (119) with permission.

We also examined the *Toxoplasma* proteome for homologues of the predicted 454 TA proteins in *Arabidopsis thaliana* (227). Our search identified 57 *Toxoplasma* homologues, but only 11 of these proteins possess TA protein characteristics; the other 46 protein homologues were eliminated due to the lack of TMD (33 proteins), prediction of more than one TMD (10 proteins) or incorrect TMD location (3 proteins) (Appendix G). Of the 11, only two putative TA proteins were not detected in our original analysis (Appendix D). Together, these two independent approaches revealed 59 putative TA proteins in *Toxoplasma*.

Sequence composition and length for both the TMD and C-terminal sequence (CTS) influences TA protein localization in other species (235–239). The TMD sequence length among the 59 putative *Toxoplasma* TA proteins varies from 18 to 28 amino acids, with an average length of 22 amino acids (Appendix D). We used ProtParam (<http://web.expasy.org/protparam>) (240) to determine whether certain amino acids were enriched in the TMD and CTS domains for each *Toxoplasma* TA protein. Our findings show that the TMD contains a bias towards amino acids with hydrophobic side chains, as expected; in contrast, there was no clear preference for any particular type of amino acid in the CTS (Figure 28), which has an average sequence length of 8 amino acids. Collectively, these TMD characteristics are consistent with previously validated TA proteins in other species, underscoring the fidelity of our bioinformatics approach to identify TA proteins in *Toxoplasma*.

Table 2. The 9 putative TA proteins selected for experimental validation. Reprinted from reference (119) with permission. Assigned protein names along with their functional description are listed. Protein attributes including the TMD and CTS amino acid sequences along with the TMD length and hydrophobicity according to the Kyte and Doolittle scale are listed (231). Localization of each TA protein is shown. Abbreviations: CTS, C-terminal sequence; ER, endoplasmic reticulum; F1S1, fission 1 protein; TA, tail-anchored; KD, Kyte and Doolittle; RBD, RNA-binding domain protein; TMD, transmembrane domain; UBC, ubiquitin-conjugating enzyme.

Gene	Gene Description	TMD Sequence	CTS	Sequence Length	KD Hydro.	Organelle Localization
Cyt-b5	cytochrome B Fam heme/steroid binding domain-containing protein	GSVGAALVVLAAAAVFYILNL	S	23	2.06	ER
RBD	RNA binding domain-containing protein	WTLAIVLGFVAYLAACKFFV	EA	20	1.97	ER
UBC	ubiquitin-conjugating enzyme subFAMILY protein	VAAADLVLLLLVLASVLLADLF	VNPPKVTMYG SSGAGGKL	23	2.57	ER
R-SNARE1	synaptobrevin protein	YFIVFGMIVLVIIILASFFCGGL	TFQTCLRIN	23	2.62	Golgi
R-SNARE2	synaptobrevin protein	LTVMLCIAFAATLAYLIYVVVNL	LSDSKK	23	2.25	Golgi
Qa-SNARE	SNARE domain-containing protein	GRAAQCIVLVTIFFLLVLLIM	KHT	23	2.47	Golgi
Elp3	elongator complex protein	PLWLGVVGLGAAAVVTLFASVAV	RRRR	23	2.04	Mito
FIS1	tetratricopeptide repeat protein 11	LIGSVLLGLAVGGCVWYLTRLWT	LSK	23	1.43	Mito
RImN	radical SAM domain-containing protein	AVLAASLAAFAGVAAAGVTHWIL	RRARV	23	1.79	Mito

### 4.3.2 Hydrophobicity of the TMDs in *Toxoplasma*

Localization of TA proteins is influenced by the hydrophobic properties of the TMD. It has been reported that TMD hydrophobicity may have predictive value in determining where a TA protein traffics in the cell (213, 228, 241). In general, mitochondrial TA proteins tend to cluster toward lower hydrophobicity values compared to ER-localizing TA proteins, and TA proteins that ultimately localize to the Golgi apparatus tend to possess TMDs with higher hydrophobicity values (228, 241–243).

We examined the hydrophobicity of the TMDs for each of the predicted 59 putative TA proteins in *Toxoplasma*. For each protein, the TMD was analyzed using the Kyte and Doolittle (KD) scale (231). This widely used hydrophobicity scale uses a numerical value assigned to each amino acid type. A more hydrophobic region of amino acids is represented by a more positive numerical value (231); in *Toxoplasma*, TMD hydrophobicity values ranged from 0.434 to 3.195 with the 3 most hydrophobic TA proteins classified as putative soluble N-ethylmaleimide-sensitive factor attachment protein receptor (SNARE) proteins (Table 2 and Appendix D). SNARE proteins are involved in vesicle-mediated trafficking and are often localized to the Golgi apparatus (244). In HeLa cells, TA proteins that ultimately traffic to the Golgi apparatus typically possess TMDs with high hydrophobicity values (228), similar to the *Toxoplasma* putative SNARE protein hydrophobicity values, suggesting the KD hydrophobicity scale might have predictive value in *Toxoplasma*.

### 4.3.3 Localization of *Toxoplasma* TA proteins to various organelles

We selected 9 representatives from the putative TA proteins that exhibit diverse attributes with respect to TMD length, CTS composition and hydrophobicity, for localization studies. Names were assigned to these selected proteins based on the descriptive function provided by ToxoDB (Table 2).

All but two (RNA-binding domain protein (RBD) and radical S-adenosyl-L-methionine (SAM) domain-containing protein (RImN)) of the *Toxoplasma* TA proteins selected for experimental validation were homologues of proteins



previously localized to various organelles in other species. Ubiquitin-conjugating enzyme (UBC) (245, 246) and cytochrome b5 (Cyt-b5) (245, 247–250) are putative homologues of known ER TA proteins in other species. We also examined 3 predicted SNARE proteins: R-SNARE1, R-SNARE2, and QaSNARE, all of which are expected to traffic to the Golgi apparatus based on studies in other species (228, 251). In addition to the previously characterized TgElp3 (83), we chose to examine a putative *Toxoplasma* homologue of mitochondrial fission 1 protein (Fis1) as a candidate TA protein targeting the parasite's mitochondrion (83, 226, 252, 253).

To determine the subcellular localization of each of the 9 selected TA proteins in Table 2, we generated a series of constructs to ectopically express each protein fused to an HA-tag at the N-terminus. The constructs drive expression of the fusion protein using the *Toxoplasma* tubulin promoter and 5'UTR (99) (Figure 29). Using these tagging constructs, each of the 9 genes were transiently expressed in RH strain parasites and protein localization was assessed by immunofluorescence assays (IFAs) that included established markers for the parasite ER (TgSERCA, (233)), Golgi apparatus (TgSORTLR, (232)), and mitochondrion (TgF1B-ATPase, (108, 109)) (Figure 29).

As shown in Figure 29 and listed in Table 2, each of the *Toxoplasma* TA protein homologues localized to a single, subcellular organelle. In addition to the expected presence of R-SNARE2 at the Golgi apparatus, we observed a strong localization of this protein at the plasma membrane along with some vesicle-like structures, suggesting this protein may be involved in membrane vesicle trafficking. Notably, our studies revealed the localization of two previously uncharacterized proteins: RBD was found at the ER and RImN at the mitochondrion. RBD contains an RNA-binding domain that is likely to be involved in stabilizing RNA; its localization at the ER could signify a functional role in protein synthesis. Interestingly, RImN contains a radical SAM domain and is a mitochondrial TA protein, like TgElp3 (83). Proteins with a radical SAM domain are associated with the delivery of diverse methylation modifications; Elp3 and RImN in particular have been shown to have tRNA methyltransferase activity (84,

254, 255). In *Escherichia coli*, RlmN is responsible for the m<sup>2</sup>A synthesis at purine 37 in tRNA (256) and in *Saccharomyces cerevisiae*, Elp3 was found to modify uridine 34 located in the tRNA wobble position (86). Interestingly, a TMD on Elp3 or RlmN homologue is only found in the phylum Apicomplexa and select species within the Chromalveolata supergroup; it is not present in *E. coli*, *S. cerevisiae*, or higher eukaryotes (83). Why these radical SAM domain proteins uniquely localize to the mitochondrion through a TA-mediated trafficking mechanism, and whether or not RlmN and Elp3 possess tRNA methyltransferase activity in *Toxoplasma*, are important questions for future investigation.

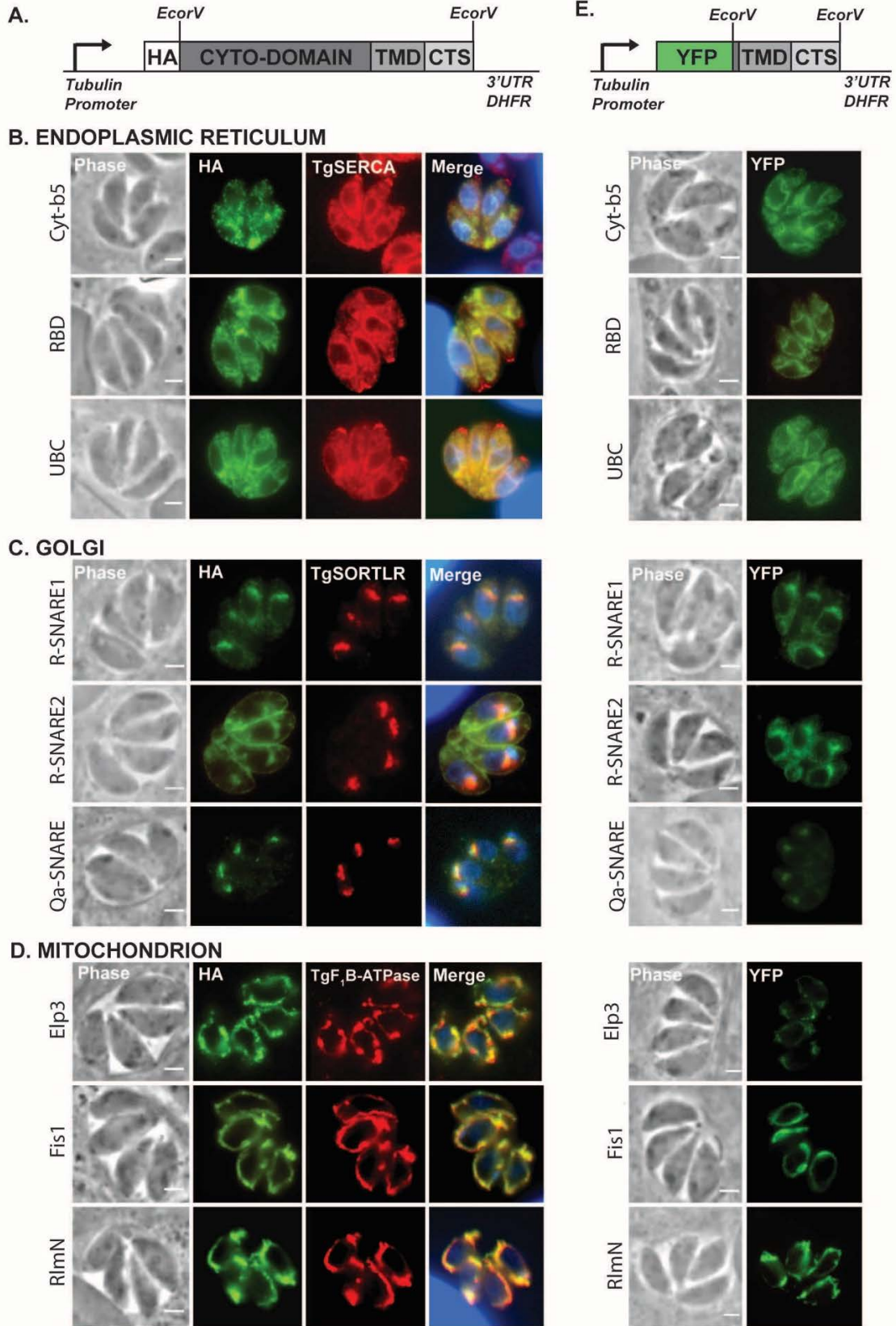


Figure 29. Subcellular localization of tail-anchored (TA) proteins. Reprinted from reference (119) with permission.

A. Schematic of constructs introduced into parasites to express HA-tagged versions of the putative TA proteins. Cyto-domain: Cytoplasmic region of the protein, TMD: transmembrane domain; CTS: C-terminal Sequence. B-D, HA-tagged full-length proteins stained with  $\alpha$ -HA (green). The following markers of designated parasite organelles were used for colocalization: B. Endoplasmic reticulum (ER) stained with  $\alpha$ -TgSERCA (red). C. Golgi apparatus stained with  $\alpha$ -TgSORTLR (red). D. Mitochondrion stained with  $\alpha$ -TgF<sub>1</sub>B-ATPase (red). E. Localization of ectopically expressed yellow fluorescent protein (YFP) fused with the TMD (including 10 amino acids upstream) and CTS for each protein. YFP-C-terminal fusion proteins are visualized using YFP (green). All images merged with the DNA stain DAPI (blue). Scale bar = 2  $\mu$ m.

#### **4.3.4 TMD and CTS are sufficient to target *Toxoplasma* TA proteins to the proper subcellular organelle**

To begin deciphering the mechanism of TA protein trafficking, we tested whether the C-terminal TMD and CTS were sufficient for specific organellar targeting. We generated 9 additional constructs engineered to ectopically express Yellow Fluorescence Protein (YFP) fused to the TMD (including 10 amino acids upstream) and CTS of each protein (Figure 29). Following transient transfection, the localization of each of the YFP-fusion proteins was assessed by IFA. As shown in Figure 29, the full-length, HA-tagged proteins and their corresponding YFP-TMD-CTS fusion protein localized to the same organelle. These data show that targeting to the proper subcellular organelle requires only the TMD and CTS, the signature feature confirming that these are indeed TA proteins.

#### **4.3.5 Targeting of TA proteins to the mitochondrion**

Positively charged residues located immediately downstream of the TMD in the CTS are critical for targeting TA proteins to the mitochondria in other species (211, 241, 257, 258). In accordance, positively charged residues are strongly enriched within the CTS region of two of the *Toxoplasma* TA proteins that we found to target the mitochondrion: RImN and Elp3 (Table 2, Figure 29). In contrast, the 3 amino acids comprising the Fis1 CTS only include one

positively charged residue (lysine). To examine the contribution of the CTS to TA protein localization, we ectopically expressed each of these 3 TA proteins using the previously described HA-tagging construct containing a premature stop codon immediately downstream of the TMD (Figure 30). Elp3 and RimN share a similar CTS (RRRR and RRARV, respectively), and its removal ablated mitochondrial targeting (Figure 30). However, removal of the CTS from Fis1 (LSK) did not perturb localization to the parasite's mitochondrion (Figure 30).

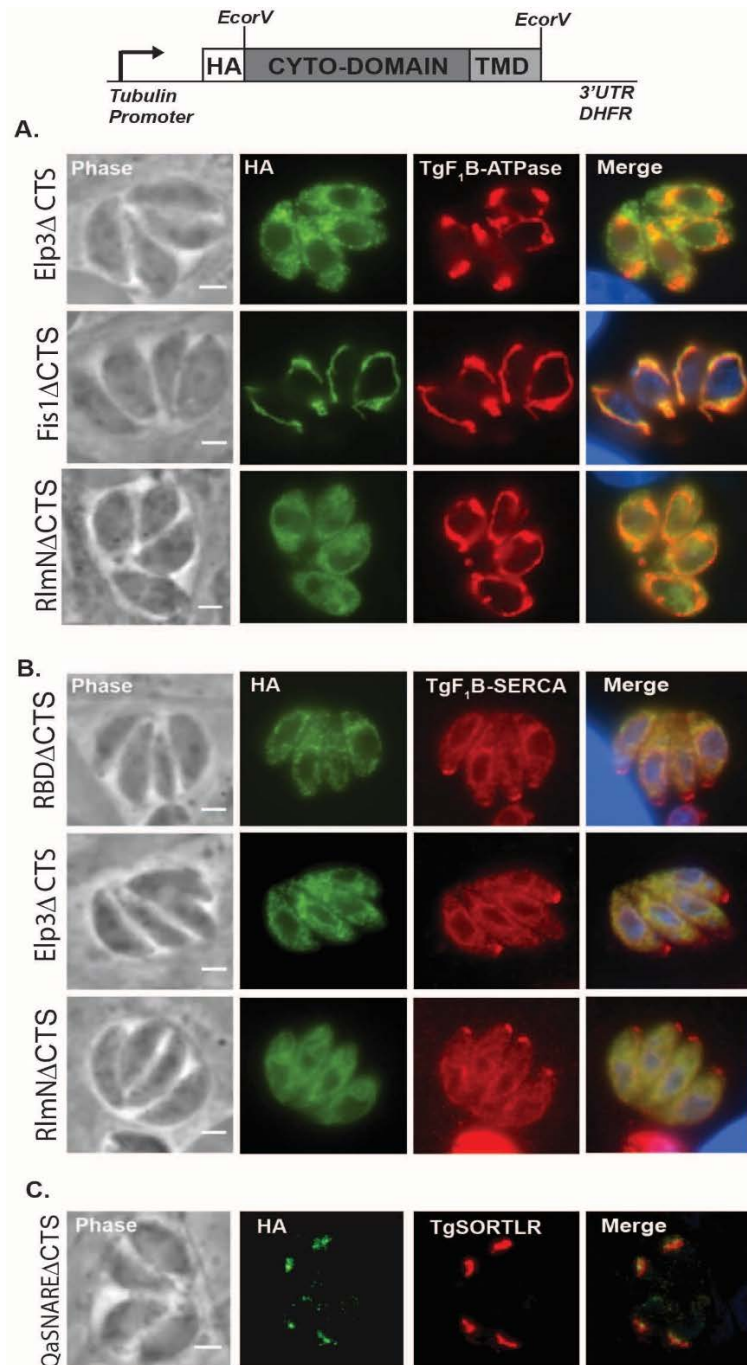


Figure 30. Role of the C-terminal sequence (CTS) in subcellular localization of tail-anchored (TA) proteins. Reprinted from reference (119) with permission. Immunofluorescence assays (IFAs) of intracellular parasites expressing HA-tagged TA-proteins containing the transmembrane domain (TMD) sequence and lacking the CTS. Parasites were stained with  $\alpha$ -HA (green), DNA stain DAPI (blue) and either (A)  $\alpha$ -TgF<sub>1</sub>B-ATPase (red) to detect the mitochondrion, (B)  $\alpha$ -TgSERCA (red) to detect the ER or (C)  $\alpha$ -TgSORTLR to detect the Golgi apparatus stained with (red). Scale bar = 2  $\mu$ m.

These data suggest that there may be at least two pathways in *Toxoplasma* for targeting mitochondrial TA proteins (225): one pathway relies on the established dibasic targeting motif (-R-R/K/H-X (X≠E)) found in both Elp3 and RImN (225, 250), and a second pathway responsible for the mitochondrial localization of Fis1. This is reminiscent of two distinct mechanisms of Fis1 isoform targeting in *Arabidopsis thaliana*; Fis1a contains the dibasic motif (VAAMSRKK) while Fis1b does not (LRS) (225). The mitochondrial targeting of Fis1 varies between species. The *S. cerevisiae* Fis1 CTS contains the dibasic mitochondrial targeting motif (259, 260), but human Fis1 (hFis1) does not contain the dibasic motif (SKSKS) (261). Rather than the dibasic motif, the *Toxoplasma* Fis1 CTS (LSK) has an amino acid sequence more similar to that found in hFis1 and *Arabidopsis* Fis1b. Some evidence also exists that Fis1 can also target to the peroxisome in mammalian cells (262); evidence for membrane-bound peroxisomes in *Toxoplasma* is contradictory (263, 264) and our data indicates that *Toxoplasma* Fis1 is only at the mitochondrion.

Since the CTS is required for Elp3 localization to the mitochondrion, we tested whether the CTS alone could operate as a mitochondrial targeting sequence by replacing the RBD CTS (which targets ER) with the Elp3 CTS. Replacing the RBD CTS (just two amino acids, EA) with the Elp3 CTS (RRRR) was sufficient to mislocalize RBD from the ER to the cytoplasm, but it did not target the protein to the mitochondrion (Figure 31). We then replaced both the TMD and CTS of RBD with those of Elp3, which was able to redirect RBD from the ER to the mitochondrion (Figure 31). To further explore the signal contribution of the TMD versus the CTS, we replaced the RBD TMD with the similarly hydrophobic Elp3 TMD (RBD TMD: 1.97; Elp3 TMD: 2.04). While the fusion protein levels were too low to discern localization with confidence, there appears to be little overlap with the mitochondrion (Figure 31). Collectively, these studies show that the Elp3 CTS is necessary but not sufficient to target the mitochondrion; however, the combination of TMD and CTS are all that is required to redirect a heterologous protein to the mitochondrion.



**A.**

Construct	Gene	TMD	CTS	Localization
RBD   TMD   CTS	RBD	WTLAIVLGFVAYLAAKCFV	EA	Endoplasmic Reticulum
QaSNARE   TMD   CTS	QaSNARE	GRAAQCVFLVITIFFLLVLLIM	KHT	Golgi
Elp3   TMD   CTS	Elp3	PLWLGVVGLGAAAVVTLFASVAV	RRRR	Mitochondrion

**B.**

Gene-TMD-CTS	IFA Localization	Phase	HA	TgF <sub>1</sub> B-ATPase	Merge
(i) RBD-RBD TMD-RRRR RBD   TMD   CTS	Cytoplasmic				
(ii) RBD-Elp3 TMD-RRRR RBD   TMD   CTS	Mitochondrion				
(iii) RBD-Elp3 TMD-EA RBD   TMD   CTS	Indeterminate				
(iv) Elp3-Elp3 TMD-EA Elp3   TMD   CTS	Endoplasmic Reticulum				
(v) Elp3-RBD TMD-EA Elp3   TMD   CTS	Endoplasmic Reticulum				
(vi) Elp3-RBD TMD-RRRR Elp3   TMD   CTS	Mitochondrion				
(vii) Elp3-Elp3 TMD-KHT Elp3   TMD   CTS	Cytoplasmic & Mitochondrion				
(viii) Elp3-QaSNARE TMD-KHT Elp3   TMD   CTS	Golgi				
(ix) Elp3-QaSNARE TMD-RRRR Elp3   TMD   CTS	Golgi				



Figure 31. C-terminal sequence swap of tail-anchored (TA) proteins alters subcellular localization. Reprinted from reference (119) with permission. A, Schematic of RNA-binding domain protein (RBD), QaSNARE, and Elp3 with sequences of their transmembrane domain (TMD) and C-terminal sequence (CTS) shown. B, CTS, TMD-CTS and TMD were swapped between HA-tagged TA proteins as depicted in schematic on the left, (i)-(ix) denote specific construct designs. Gray shades match those in A to indicate origin of domain. Fusion constructs are listed with the gene name, the TMD (bold), and CTS (italicized). Immunofluorescence assays (IFAs) showing the localization of swapping mutants stained with  $\alpha$ -HA (green),  $\alpha$ -TgF<sub>1</sub>B-ATPase (red) and merged with DAPI (blue). Scale bar = 2  $\mu$ m.

#### 4.3.6 Targeting of TA proteins to the ER and Golgi apparatus

Our findings have uncovered the first TA proteins in phylum Apicomplexa that target the ER, as well as those that traffic to the Golgi apparatus. It has been established that TA proteins destined for the Golgi apparatus are first inserted into the ER and then delivered via vesicular transport, whereas ER TA proteins are targeted directly to the ER upon release from the ribosome (210, 265). To gain insight into the specificity of these targeting mechanisms in *Toxoplasma*, we performed additional domain swap experiments. To determine if the CTS is required for TA protein localization for either RBD (ER) or QaSNARE (Golgi apparatus), we used the previously described HA-tagging construct containing a premature stop codon immediately downstream of the TMD. Removal of the CTS did not alter protein localization for either RBD or QaSNARE, suggesting the TMD sequence is sufficient for the targeting of these proteins (Figure 30).

To further explore protein localization to the ER, we generated fusion constructs to identify which sequences are necessary for ER localization (Figure 31). For these experiments we used the mitochondrial localizing protein TgElp3 and swapped the TgElp3 CTS, TMD and TMD-CTS sequences with those of RBD (ER). Replacement of the TgElp3-TMD with the similarly hydrophobic RBD-TMD resulted in protein localization to the mitochondrion, while replacement of the TgElp3 TMD-CTS with the RBD TMD-CTS or even just the RBD CTS (EA) resulted in targeting of TgElp3 to the ER instead of the mitochondrion (Figure 31). As observed in other species, proteins lacking clear mitochondrial targeting

sequences are often inserted into the more permissive ER membrane, which is able to accept TMDs of different lengths and sequences (207, 211, 257, 260, 266–268). In *Toxoplasma*, replacement of the TgElp3 CTS dibasic motif was enough to reroute TgElp3 to the ER, suggesting that without a strong mitochondrial targeting sequence the ER is likely the default destination for TA protein localization.

Given that we were able to mislocalize TgElp3 to the ER by simply replacing the CTS with a sequence from RBD, we examined whether it was possible to mislocalize TgElp3 to the Golgi apparatus by replacing the CTS from QaSNARE (KHT). Replacement of just the CTS of TgElp3 with the CTS of QaSNARE resulted in some mislocalization from the mitochondrion, but no clear trafficking to the ER or Golgi apparatus (Figure 31). We then swapped the TgElp3 TMD and TMD-CTS sequences with those from QaSNARE, which resulted in a striking redirection of TgElp3 to the Golgi apparatus (Figure 31). The more hydrophobic QaSNARE TMD (2.47 compared to 2.04) may prevent protein insertion into the mitochondrial membrane or may act as a robust signal sequence overriding the TgElp3 CTS dibasic mitochondrial targeting motif. Generally, these data suggest that optimal TA protein targeting in early-branching eukaryotes like *Toxoplasma* is determined by both the TMD and CTS sequences.

#### **4.4 Concluding Remarks**

Our findings represent the first characterization of TA proteins in the phylum Apicomplexa using the early-branching protozoan parasite *Toxoplasma* as a model. Our bioinformatics analysis identified 59 putative TA proteins in the *Toxoplasma* proteome. Nine representatives were chosen for experimental analyses, localizing to various subcellular compartments including the parasite ER, mitochondrion, or Golgi apparatus. As in other species, at least two pathways appear to direct mitochondrial TA protein localization, one of which employs an established dibasic targeting motif which is required for Elp3 and RImN mitochondrial localization; removal of this motif results in mislocalization of

the TA protein to the ER membrane. TA protein localization to ER (or subsequently the Golgi apparatus) appear to be solely dependent on the TMD sequence; however, addition of a CTS containing a mitochondrial targeting dibasic motif results in TA protein mislocalization, suggesting the dibasic motif may prevent membrane integration or signal removal from the ER.

Based on the experimentally localized *Toxoplasma* TA proteins described here, the Kyte and Doolittle hydrophobicity scale appears to have some predictive power, similar to what is observed in other species. Domain swapping experiments confirmed that the combination of the TMD and CTS are all that is required to redirect a heterologous protein to a destined organelle. Interestingly, when only the TMD was swapped to form a heterologous TMD-CTS sequence, localization of fusion proteins varied, indicating protein targeting may occur in a context dependent manner. Further mechanistic studies and exploration of potential chaperones are required to resolve how the TMD and CTS mediate organelle-specific targeting. As in other species, it is likely that *Toxoplasma* TA proteins interact with chaperone proteins, integrate in an unassisted manner, or recognize docking proteins present in their target organelle. Based on sequence homology analyses of the ToxoDB, putative homologues for components of the Hsc70/Hsp40, SRP54, and some members of the GET complex appear to be present in *Toxoplasma*.

## CHAPTER 5: Conclusions

### 5.1 Summary of Findings

Disruption of lysine acetylation is detrimental to *Toxoplasma*, and previous studies identified that the putative lysine acetyltransferase TgElp3 is essential for parasite viability. Our laboratory determined that TgElp3 possesses KAT activity and its localization to the OMM is essential for parasite viability. However, a key question remained unanswered, “What is the function of TgElp3 at the mitochondrion?” The work in this thesis describes various investigative approaches to determine TgElp3’s enzymatic function and how it localizes to the parasite mitochondrion.

Using a targeted mutational approach, we were unable to generate viable parasites with defective KAT or rSAM domains in TgElp3, suggesting that both of these domains are essential for protein function. Moreover, overexpression of TgElp3 resulted in a significant replication defect while overexpression of mutant rSAM and TMD domains were tolerated. These findings highlight the importance of the rSAM domain and further confirm that TgElp3 activity is dependent on its localization to the OMM.

Since studies in other species have determined that the rSAM in Elp3 is important for the synthesis of tRNA modifications ( $mcm^5$  and  $ncm^5$ ), we investigated TgElp3 as a potential tRNA modification enzyme. In collaboration with Dragony Fu’s lab at the University of Rochester, we identified the first tRNA modification in *Toxoplasma*, tRNA<sup>Glu</sup>  $mcm^5s^2U35$ . However, we were unable to attribute the TgElp3<sup>OE</sup> replication defect to changes in the tRNA<sup>Glu</sup>  $mcm^5s^2U35$  modification. Knowing that the  $mcm^5s^2$  modification requires two independent enzymes and that Elp3 has been shown to modify 11 different tRNAs, we cannot eliminate the possibility that TgElp3 is a tRNA modification enzyme.

Elp3 was initially characterized as a lysine acetyltransferase and several studies have implicated  $\alpha$ -tubulin as a substrate. Recently, a second  $\alpha$ -tubulin acetyltransferase (ATAT) was identified in *C. elegans*. When we genetically ablated the *Toxoplasma* homologue, TgATAT, we observed a complete loss of  $\alpha$ -tubulin acetylation in the parasite. Since there was no detectable  $\alpha$ -tubulin

acetylation when TgATAT was knocked out and assuming TgElp3 was still present, we can conclude that TgElp3 is not the primary  $\alpha$ -tubulin acetyltransferase in *Toxoplasma*. In support of these findings, a recent study in *C. elegans* analyzed the lysine codon usage of ATAT and found that there is a strong codon bias for –G ending codons (33% AAA/67% AAG) compared to the average lysine codon usage preferring –A ending codons (61% AAA/39%AAG); the authors speculate that Elongator may regulate the protein expression level of ATAT through its elevated AAA codon content, and thus the decrease in  $\alpha$ -tubulin acetylation in Elongator mutants may be through an indirect tRNA modification pathway (269).

Furthermore, since TgElp3 localization to the OMM is essential for parasite viability, we sought to determine the factors required for protein trafficking. TgElp3 is classified as a tail-anchored (TA) protein as it contains a single TMD positioned within 30 amino acids of the C-terminus. To gain insight into how TgElp3 is targeted to the OMM, we used a bioinformatics approach and identified an additional 59 putative TA proteins in *Toxoplasma*. Of these proteins, a second rSAM domain containing protein was identified, RImN. Experiments determined that RImN and TgElp3 share a similar positively charged C-terminal sequence motif required for OMM localization. Interestingly, RImN in *Escherichia coli* has been characterized as a tRNA modification enzyme, but its function in *Toxoplasma* is not known.

Considering that our mutational studies identified the rSAM domain critical for TgElp3 function and we identified a second putative tRNA modification enzyme that similarly localizes to the OMM, the data presented in this thesis suggest that TgElp3 is likely a tRNA modification enzyme. However, we cannot rule out TgElp3's potential role as a lysine acetyltransferase. Moreover, why this enzyme localizes to the parasite's mitochondrion is puzzling. Therefore future experimental studies are needed to determine the molecular function of TgElp3 and the significance of its localization at the mitochondrion.

## 5.2 Future Directions

The data presented in this thesis have broadened our focus from not only exploring TgElp3 a KAT but also investigating its potential role as a tRNA modification enzyme. In addition to determining the enzymatic function of TgElp3, determining why it localizes to the mitochondrion is another important facet of parasite biology to explore. Our findings have led to a number of new questions to be answered.

### 5.2.1 Does Elp3 bind tRNA?

Immunoprecipitation studies in yeast have determined that Elp3 can bind tRNA. We could follow a similar approach to determine if TgElp3 can bind tRNA in *Toxoplasma*. The endogenously tagged (<sup>HA</sup>TgElp3) or overexpressing (<sup>HA</sup>TgElp3<sup>OE</sup>) parasite lines can be subjected to formaldehyde treatment (or ultra violet light) to cross-link TgElp3 to tRNA substrates. Using anti-HA conjugated beads, TgElp3 can be immunoprecipitated. The immunoprecipitated complex can be resolved on a polyacrylamide gel and stained with SYBR gold to detect associated tRNAs. To specifically determine which tRNA pulled down with the TgElp3-RNA complex, subsequent Northern blot or sequencing analysis could be performed.

An alternative approach is to perform an *in vitro* TgElp3-tRNA binding assay. In this case, TgElp3 protein is immunoprecipitated and incubated with a radio-labeled (or biotin-labeled) tRNA. This RNA-protein complex can be assessed as described above.

### 5.2.2 Does TgElp3 modify tRNA *in vitro*?

An *in vitro* tRNA modification assay was recently developed by Raven Huang at the University of Illinois (84). This assay requires a minimum of 1 mg of purified protein. Despite employing multiple approaches we were unable to generate enough soluble protein to perform this assay. Recently, there have been numerous reports stating radical SAM domain containing proteins are very sensitive to oxygen, and thus must be purified within an anaerobic chamber.

Since the recombinant protein expression constructs are already made, repeating the recombinant protein expression experiments in either the SF21 or *E. coli* cells, and then using an anaerobic chamber for protein purification may yield enough soluble recombinant TgElp3 protein to perform the *in vitro* tRNA modification assay.

### **5.2.3 Does overexpression of tRNA<sup>Lys</sup> and/or tRNA<sup>Glu</sup> rescue the <sup>HA</sup>TgElp3<sup>OE</sup> growth phenotype?**

Several independent studies show that overexpression of specific tRNAs especially tRNA<sup>Lys</sup> can overcome Elongator mutant stress phenotypes. There is some evidence that stress response genes possess a higher number of lysine – AA ending codons and therefore disruption of Elongator results in preferential translation of –AG ending codons (270). Elongator mutants may not be able to translate stress response genes as efficiently resulting in a slow growth phenotype. Exactly how overexpression of unmodified tRNA<sup>Lys</sup> overcomes the Elongator mutant phenotype is not understood. Our <sup>HA</sup>TgElp3<sup>OE</sup> parasites may have the opposite problem in which they have hyper-modified tRNAs that promote translation of a subset of genes (potentially stress response genes). Overexpression of tRNA<sup>Lys</sup> may shift the tRNA pool and promote homeostatic translation.

### **5.2.4 Does overexpression of TgElp3 affect protein synthesis?**

We previously used polyribosome profiling and the SUnSET method to assess protein synthesis in our TgElp3 overexpression mutants. Using these methods we did not detect any difference in protein synthesis. However, these approaches assess translation at a global level and likely miss small changes in protein synthesis. Since Elp3 tRNA modifications affect anticodon-codon binding, (mcm<sup>5</sup> efficiently binding –G and mcm<sup>5</sup>s<sup>2</sup> efficiently binding –A ending codon), ribosomal footprint profiling could be used to monitor protein synthesis at higher resolution. This method essentially produces a “global snapshot” of all the active ribosomes in a cell. Briefly, cycloheximide is applied to “freeze” the ribosomes to

mRNA transcripts. RNA not protected by the ribosome is digested, followed by purification of the mRNA-ribosome complex using a sucrose gradient. The mRNA can be purified, reverse-transcribed and then sequenced. Alignment of the sequence reads will determine the translational profile. From these data, the ribosome distributions could be determined at the codon level and, through comparison with the parental strain, biases in codon frequency could be detected.

To further assess translation regulation, luciferase (renilla vs firefly) or fluorescent (CFP vs YFP) reporter constructs containing various stretches of cognate codons (e.g. 5 x AAA vs 5 x AAG) could be expressed in the TgElp3 mutant parasite lines we developed. Following transfection, quantitative measurements of protein output will determine if overexpression of TgElp3 alters protein synthesis. Depending on the promoter used to express the reporter genes, there is a chance for protein saturation. Therefore, ribosomal profiling followed by qRT-PCR on the collected fractions could be used as a second method to assess translation. Early fractions indicate less ribosome association (less translation) while the later fractions contain transcripts highly decorated with ribosomes (more translation). If TgElp3 overexpressing parasites exhibit a change in protein synthesis as a result of inefficient anticodon-codon base pairing, we would expect to see the reporter construct mRNA enriched in different polyribosome fractions compared to the parental strain. A second method, ribosomal footprinting, can be used to determine the precise position of ribosomes on any given transcript and calculation of the codon occupancy will unveil any codon usage biases.

Additionally, a quantitative proteomics approach could be used to determine if overexpression of TgElp3 alters protein levels. The proteins identified as differentially expressed between the parental and TgElp3 strains will be subjected to codon frequency analysis to determine if there is a codon bias. However, any changes detected in protein levels and subsequent codon bias could be a result of indirect mechanisms, so additional studies are needed. Since our TgElp3 overexpressing parasites have a severe replication defect, analysis of



protein expression will also give us insight into the cellular state of these parasites.

### **5.2.5 Does TgEIp3 overexpression alter parasite mitochondrial function?**

We did not detect any obvious mitochondrial abnormalities, however since overexpression of TgEIp3 is detrimental only when the protein resides at the parasite's mitochondrion, a more detailed analysis of mitochondrial function is needed. Mitochondrial membrane potential can be assessed using the fluorescent MitoTracker probe or JC-1, a membrane potential dependent cationic dye that accumulates in the mitochondria and changes from green to red as it accumulates. Moreover, we can assess mitochondrial function by measuring mitochondrial respiration, ATP and reactive oxygen species (ROS) to determine if TgEIp3 overexpression disrupts mitochondrial function. In addition, treating our TgEIp3 overexpressing parasites with mitochondrial inhibitors such as atovaquone, antimycin A and myxothiazol may unveil differences in susceptibility or resistance. In addition, perturbing the cellular energy pathways in the parasite through alterations in media composition (low or high glucose) and assessing parasite growth may also give insight into the function of TgEIp3 at the mitochondrion. Collectively, these studies will determine if TgEIp3 overexpression alters mitochondrial function.

## APPENDICES

### Appendix A. Constructs and primers used in chapter 2.

<b>PROJECT AND CONSTRUCT NAME</b>	<b>BACKGROUND PARASITE STRAIN</b>	<b>SELECTION CASSETTE</b>
<b>BioID</b>		
<i>TubHX-myc-BirA-HA-TgElp3</i>	RHΔ <i>hx</i>	HXGPRT
<b>Endogenous Replacement</b>		
<sup>HA</sup> <i>TgElp3</i>	RHΔ <i>hxΔku80</i>	DHFR
<sup>HA</sup> <i>TgElp3-rSAMmut (C284A)</i>	RHΔ <i>hxΔku80</i>	DHFR
<sup>HA</sup> <i>TgElp3-KATmut(Y715/716A)</i>	RHΔ <i>hxΔku80</i>	DHFR
<b>Destabilization Domain</b>		
<i>TubHX-DD-<sup>HA</sup>TgElp3</i>	RHΔ <i>hx</i>	HXGPRT
<i>TubHX-DD-<sup>HA</sup>TgElp3-rSAM(C284A)</i>	RHΔ <i>hx</i>	HXGPRT
<i>TubHX-DD-<sup>HA</sup>TgElp3-KATmut(Y715/716A)</i>	RHΔ <i>hx</i>	HXGPRT
<b>Ectopic Overexpression</b>		
<i>TubHX<sup>HA</sup>TgElp3<sup>OE</sup></i>	RHΔ <i>hx</i>	HXGPRT
<i>Tub<sup>HA</sup>TgElp3<sup>OE</sup></i>	ME49	DHFR
<i>TubHX<sup>HA</sup>TgElp3-KAT(Y715/716A)<sup>OE</sup></i>	RHΔ <i>hx</i>	HXGPRT
<i>TubHX<sup>HA</sup>TgElp3-KAT(Y716A)<sup>OE</sup></i>	RHΔ <i>hx</i>	HXGPRT
<i>TubHX<sup>HA</sup>TgElp3-KAT(Y715F/Y716F)<sup>OE</sup></i>	RHΔ <i>hx</i>	HXGPRT
<i>TubHX<sup>HA</sup>TgElp3-rSAM(C284A/C287A)<sup>OE</sup></i>	RHΔ <i>hx</i>	HXGPRT
<i>TubHX<sup>HA</sup>TgElp3-rSAM(C284A/C287A)/KAT(Y716A)<sup>OE</sup></i>	RHΔ <i>hx</i>	HXGPRT
<i>TubHX<sup>HA</sup>TgElp3-rSAM(C284A/C287A)/KAT(Y715F/Y716F)<sup>OE</sup></i>	RHΔ <i>hx</i>	HXGPRT
<i>TubHX<sup>HA</sup>TgElp3-ΔTMD<sup>OE</sup></i>	RHΔ <i>hx</i>	HXGPRT
<b>RECOMBINANT PROTEIN EXPRESSION CONSTRUCTS</b>		
<i>pET19b-10xHIS-EnzymaticElp3ΔTMD</i>	Rosetta	AMP
<i>pET30a-EnzymaticElp3ΔTMD</i>	Rosetta	KAN
<i>pGEX-4T-1-GST-EnzymaticElp3ΔTMD</i>	Rosetta	AMP
<i>6HIS-SUMO-Elp3ΔTMD</i>	Rosetta	KAN
<i>6HIS-SUMO-Elp3ΔTMDshort1</i>	Rosetta	KAN
<i>6HIS-SUMO-Elp3ΔTMDshort2</i>	Rosetta	KAN

*Insect Cells*

*BacPAK9-10xHIS-EnzymaticElp3ΔTMD*

*BacPAK9-EnzymaticElp3ΔTMD*

*BacPAK9-GST-EnzymaticElp3ΔTMD*

SF21

AMP

SF21

AMP

SF21

AMP

**PRIMERS:**

	<b>PRIMER DESCRIPTION</b>	<b>PRIMER SEQUENCE</b>
<b>F1</b>	BirA-Elp3F_step1a	GCTCGGTACCAAGCTTGTACCCGTACGACGTCC C
<b>R1</b>	BirA-Elp3R_step1a	GGATCGATCCACTAGCACGATTGGCAGCATT TTTTGACA
<b>F2</b>	BirAElp3-tubHX-F	ATCCCTTTTAGATCaccatggaacaaaaactcatctcagaa gag
<b>R2</b>	BirAElp3-tubHX-R	TGTAGTCCCTAGGATCACGATTGGCAGCATT TTTTGACA
<b>F3</b>	TubHX-SeqF1	CTTGCGGAAACTACTCGTTGG
<b>R3</b>	TubHX-SeqR1	GTCGTCGTCGTCCTTGTAGTC
<b>F4</b>	Knock-IN-Elp3-Prom	CCGCTCTAGAAGTACCGTTCTCGAACCAGTG CTTTCA
<b>R4</b>	Knock-IN-Elp3-Prom	gacgtcgtacgggtacatGGTGAAAAGAGAGATAGGTTG AGAGGGC
<b>F5</b>	Knock-IN-HA-Elp3	ATGTACCCGTACGACGTCCC
<b>R5</b>	Knock-IN-HA-Elp3	GGATCGATCCACTAGCACGATTGGCAGCATT TTTTGACA
<b>F6</b>	Knock-IN-Elp3- Downstream	CAGCCTGGCGAAGCTAAAAGATTTGCTGCAGAT GCAGC
<b>R6</b>	Knock-IN-Elp3- Downstream	CGGTATCGATAAGCTGACTGATTATGTCGGATGC AAAGTTCC
<b>F7</b>	TgELP3_rSAMC284A_F	TCTTGCCCTCACAACGCGCATTACTGCCCAAC
<b>R7</b>	TgELP3_rSAMC284A_R	GTTGGGGCAGTAATGCGCGTTGTGAGGGCAAGA
<b>F8</b>	TgElp3- KAT_Y715/716A_F	GGTGTCCGTACGCGGGAGGCTGCCCGAAAGAAT GGGTACG
<b>R8</b>	TgElp3- KAT_Y715/716A_R	CGTACCCATTCTTTCGGGCAGCCTCCCGCGTAC CGACACC
<b>F9</b>	pDHFR_SeqF1	GGGATCGATCCACTAGTTCTAGAG
<b>R9</b>	pDHFR_SeqR1	CCCTCGAGGTCGACGGTA
<b>F10</b>	K-IN-upstream_F1	CCAAGCATAAGGCTGGAAAA
<b>R10</b>	K-IN-construct_R1	TCGCGAATAAATTCCTCCTG
<b>F11</b>	K-IN-construct_F2	TTTCTGACGTTCTCGACGTG
<b>R11</b>	K-IN-downstream_R2	AAGAAACCCAAGCGCCTTAC
<b>F12</b>	TubHX_to_pDHFR_Hind III F	CGGTATCGATAAGCTTACGTGGTACGGCTATGA GCC
<b>R12</b>	TubHX_to_pDHFR_Hind	CAGCCTGGCGAAGCTTCTGCCGGAACACTTGT

	III R	CAACCG
<b>F13</b>	TgElp3-KAT_Y716A_F	TACGCGGGAGgcgctacCGAAAGAATGGGTACG
<b>R13</b>	TgElp3-KAT_Y716A_R	CCCATTCTTTTCGGTA <sub>cg</sub> cCTCCCGCGTACCGAC
<b>F14</b>	TgElp3_KAT_Y715F/Y716F_F	GTCGGTACGCGGGAGTtcTtCCGAAAGAATGGGTAC
<b>R14</b>	TgElp3_KAT_Y715F/Y716F_R	GTACCCATTCTTTTCGGTAATACTCCCGCGTACCGAC
<b>F15</b>	TgELP3_rSAMC287A_F	CACAACGCGCATTACGCGCCCAACGAGCCTGGC
<b>R15</b>	TgELP3_rSAMC287A_R	GCCAGGCTCGTTGGGCGCGTAATGCGCGTTGTG
<b>F16</b>	TgELP3_ΔTMD_F	CCCTCGCTGGCGAACTGACTCTGGCTTGGGGT
<b>R16</b>	TgELP3_ΔTMD_R	ACCCAAGCCAGAGTCAGTTCGCCAGCGAGGG
<b>F17</b>	pET19b_EnzymaticElp3-F	ACGACGACAAGCATAATCAGCGGAACCGCGT
<b>R17</b>	pET19b_EnzymaticElp3-R	GGATCCTCGAGCATATCATAGTGAGGAAGACCGACC
<b>F18</b>	pET30a_EnzymaticElp3_F	AAGGAGATATACATAACCATGCAGCGGAACCG
<b>R18</b>	pET30a_EnzymaticElp3_R	TGCTCGAGTGCGGCCTCATAGTGAGGAAGACCGACC
<b>F19</b>	pGEX-4T-1_EnzymaticElp3_F	ATCCCCGGAATTCCCACAGCGGAACCGCGT
<b>R19</b>	pGEX-4T-1_EnzymaticElp3_R	CGCTCGAGTCGACCCTCATAGTGAGGAAGACCGACC
<b>F20</b>	6HIS-SUMO-Elp3_F1	tacttccaatccaatATGGAACACACTTCTCCTTCTCTTCT
<b>F20.1</b>	6HIS-SUMO-Elp3_F2	tacttccaatccaatTCTTCGGACCGGTGTGC
<b>F20.2</b>	6HIS-SUMO-Elp3_F3	tacttccaatccaatCAGCGGAACCGCGTACT
<b>R20</b>	6HIS-SUMO-Elp3_R1	ttatccactccaatTCATGGGTTCCGCCAGCG
<b>F21</b>	BacPak9-EnzymaticElp3#87_F	ATAAATACGGATCCCACCATGCAGCGGAACCG
<b>R21</b>	BacPak9-EnzymaticElp3#87_R	CGAGCTCGAATTCCCTCATTCCGTGAATGCGTCCGG
<b>F22</b>	GST-EnymaticElp3_F	ATAAATACGGATCCCACCATGTCCCCTATACTAGGTTATTGGA
<b>R22</b>	GST-EnymaticElp3_R	CGAGCTCGAATTCCCTCATAGTGAGGAAGACCGACC
<b>F23</b>	BacPak9 Seq_F1	AACCATCTCGCAAATAAATA
<b>R23</b>	BacPak9 Seq_R1	ACGCACAGAATCTAGCGCTT

**Appendix B. Primers used in chapter 3.**

	Primer	Name	Primer Sequence Used
<b>TUBA1 Site-irected</b>	1	K40K F	GCAGATGCCCTCTGACAAAACCATTGGAGG TGG
	2	K40K R	CCACCTCCAATGGTTTTGTCAGAGGGCATCT GC
	3	K40R F	GCAGATGCCCTCTGACCGCACCATTGGAGG TGG
	4	K40R R	CCACCTCCAATGGTGCGGTCAGAGGGCATC TGC
	5	K40Q F	GCAGATGCCCTCTGACCAGACCATTGGAGG TGG
	6	K40Q R	CCACCTCCAATGGTCTGGTCAGAGGGCATC TGC
<b>Oryzalin Mutation</b>	7	I239T F	gagagacgcggtcagggaggagatgacctg
	8	I239T R	caggctcatctcctccctgaccgcgtctctc
	9	V252L F	cgctcaacgtcgactgactgagtccagac
	10	V252L R	gtctggaactcagcaagtcgacgttgagcg
<b>TgTUBA1 Sequencing</b>	11	<i>TgTUBA1</i> F	ATGAGAGAGGTTATCAGCATC
	12	<i>TgTUBA1</i> R	TTAGTACTCGTCACCATAGCC
<b>TgATAT tagging</b>	13	<i>TgATAT_F</i>	ttccaatccaatttaATTTCTACGTCCTCGAGAGCTG T
	14	<i>TgATAT_R</i>	ccactccaattttaaaCGACCAGTTGAGGAGAGAC G
<b>Deletion of HA tag in GFP-Cas9/sgU PRT</b>	15	CRISPR HA del F	AGCCTGGGCAGCGGCTCC
	16	CRISPR HA del R	GGCGTCGCCTCCCAGCTG
<b>TgATAT CRISPR sgRNA</b>	17	<i>TgATAT</i> sgRNA F	ctcaccgcgacGTTTTAGAGCTAGAAATAGCAAG
	18	<i>TgATAT</i> sgRNA R	gcccttgagcAACTTGACATCCCCATTTAC
<b>TgATAT CRISPR Oligos</b>	19	<i>TgATAT</i> Oligo F	tccactccgagctcaagggcctcaccgcgacAATGATGAAT GAATGAGATATCagAccgcctccaccggctcctgccga cgctccagctg
	20	<i>TgATAT</i> Oligo R	cgactggagcgtcggcaggagccgggtggaaggcggTctGA TATCTCATTATTATCATTgtcgggtgaggccctg agctcggagtga

**Appendix C. Copyright permission for chapter 4.**

JOHN WILEY AND SONS LICENSE  
TERMS AND CONDITIONS

Apr 13, 2017

This Agreement between Leah R Padgett ("You") and John Wiley and Sons ("John Wiley and Sons") consists of your license details and the terms and conditions provided by John Wiley and Sons and Copyright Clearance Center.

License Number: 4057650159663

License date

Licensed Content Publisher: John Wiley and Sons

Licensed Content Publication: Traffic

Licensed Content Title

Targeting of tail-anchored membrane proteins to subcellular organelles in  
Toxoplasma gondii

Licensed Content Author

Leah R. Padgett, Gustavo Arrizabalaga, William J. Sullivan

Licensed Content Date: Jan 17, 2017

Licensed Content Pages: 10

Type of use: Dissertation/Thesis

Requestor type: Author of this Wiley article

Format: Print and electronic

Portion: Full article

Will you be translating? No

Title of your thesis / dissertation

INVESTIGATIONS INTO THE FUNCTION OF ELP3 IN TOXOPLASMA GONDII

Expected completion date: May 2017

Expected size (number of pages): 250

#### Appendix D. Identification of 59 putative TA proteins in *Toxoplasma*.

List of the 59 predicted TA proteins in *Toxoplasma*. Proteins highlighted in grey were used for experimental validation and localization. Column (A) lists the gene ID for the ME49 strain (ToxoDB v9.0). Gene product description (column B) with names assigned listed in bold parenthesis. The TMD (column C) and CTS (column D) sequences are listed for each of the putative TA proteins. Various C-terminal characteristics are listed: TMD length (column E), CTS length (column F) and TMD hydrophobicity (column G), KD=Kyte and Doolittle (227).

GENE ID	Product Description	TM	CTS	TMD length	CTS length	KD
TGME49_207150	SAG-related sequence SRS49C (SAG2D)	EAETPATPEPSRGEQGVVLGSAFMIAFISC	F	28	1	0.43
TGME49_326100	dynamain gtpase	VYTQYIHSDTVVMYIYIYIYIY	MLIC	23	4	0.62
TGME49_295472	C2 domain-containing protein	VAYLNLVVGQQTICALIKASTACF	CGVLF LVIIA FVVAV IVIAA RMP	23	23	1.10
TGME49_254030	zinc finger CDGSH-type domain-containing protein	NTPLACVASFAAAFSVGVASTYL	HG	23	2	1.24
TGME49_269130	EGF family domain-containing protein	VAMLLICIVHTLLGKTPAGE	SPFLP	20	5	1.31
TGME49_247770	hypothetical protein	VSLVYFCWGLILFLYPMAMYARS	YATEHGHPFAPARTDGSRGHG PLWWFIE	23	29	1.34
TGME49_278290	<i>Toxoplasma gondii</i> family A protein	GWSSAGGVGGVSGLLLTMAALF	QVYQLY	23	6	1.37
TGME49_210255	hypothetical protein	LFHYGVIPALFVVGLAYTGELTL	DPTSLFQKIVIN	23	12	1.38
TGME49_261300	hypothetical protein	GVFVYMLTYIYIYIMCIYMDIY	L	23	1	1.39
TGME49_263323	(FIS1) tetratricopeptide repeat protein 11, putative	LIGSVLLGLAVGGCVWYLTRLWT	LSK	23	3	1.43

TGME49_236550	hypothetical protein	PWPFYIWSFWAFSMVVVPIGLLF	QSNYYFSGRILPKVNGNTQLCED SW	23	25	1.45
TGME49_238530	hypothetical protein	SSAVRAGLAMSAAVVGVVASLLQF	A	23	1	1.48
TGME49_242840	membrane protein	AWFVLSGQIMFTFFWSFALYSVI	ERWYVNGKIDTFSKWQDRATD	23	21	1.50
TGME49_220310	hypothetical protein	LPPASTAFSCFACVYIFLF	REI	19	3	1.64
TGME49_207170	hypothetical protein	VYFPLTAVLVTLGPLYMF	SKAFF	18	5	1.64
TGME49_278370	Toxoplasma gondii family A protein	AWSVAGGISTLSVFLSAAAVTLL	PTF	23	3	1.64
TGME49_246230	hypothetical protein	YSYRLLALIVPFLSVAAL	P	18	1	1.66
TGME49_270070	synaptobrevin family protein	LQQYAPLVMCLFFAILIFWKLF	L	23	1	1.68
TGME49_318160	MSP (Major sperm protein) domain- containing protein	LWHIPVYIFIGVVIWYFFG	RSAEITK	19	7	1.73
TGME49_209790	(RImN) radical SAM domain-containing protein	AVLAASLAAFAGVAAAGVTHWIL	RRARV	23	5	1.79
TGME49_301355	hypothetical protein	YACAHAYICIIYICVYVLIHIF	F	23	1	1.83
TGME49_231991	hypothetical protein	IGCIRLAWIHLGCLAICSPIFV	SGTLGRPM	23	8	1.91
TGME49_301996	ORF D	YIYSQILFFLISSFIFFWIL	KQFYLRIFIY	20	10	1.93
TGME49_223620	golgi SNARE, putative	LWGGMFLTLLFFFLYRLV	HRSREVDADGSDALNSEQ	20	20	1.95
TGME49_260470	heat shock protein DNAJ pfj4, putative	WYWVRVAADVFLSIWIFVAFLY	PSLLG	23	5	1.96



TGME49_212980	(RBD) hypothetical protein (RNA binding domain-containing protein)	WTLAIVLGFVAYLAAKCFV	EA	20	2	1.97
TGME49_279360	hypothetical protein	SLMMLGALVALFLFFFMPTSPIL	PLLFW LHGES PPPAP PVA	23	18	2.00
TGME49_263810	hypothetical protein	AVPTWCVFLLAYSVLAVFGV	C	20	1	2.01
TGME49_305480	(ELP3) elongator complex protein ELP3	PLWLGVVGLGAAVVTLFASVAV	RRRR	23	4	2.04
TGME49_276110	(Cyt-b5) cytochrome b5 family heme/steroid binding domain-containing protein	GSVGAAALVVLAAAAVFYILNL	S	23	1	2.06
TGME49_211040	Sec61beta family protein	IGPQTVLILTLCFMASVLLHIV	GKVHQTYGGEN	23	11	2.06
TGME49_268630	YagE family protein	LEWIVIYLICVEVLIDLWVNILI	KDILKWV	23	7	2.10
TGME49_278890	hypothetical protein	ATRLFALFYFVLLHFLVFLVLFY	LQSRG QADQA GSHQP RYHYY LNEHA D	23	26	2.11
TGME49_251710	hypothetical protein	LILALVIAACVCLSLWVMRGHA	SAVDPGPG	23	8	2.12
TGME49_214330	DnaJ domain-containing protein	VFFPAVAGAVVLAVSCFSLFAAT	PT	23	2	2.12
TGME49_293400	hypothetical protein	LLSVALGCGAVTVSIAGLVYVVA	TWYEQ PLIRV GETTR ETENR REPTT VVA	23	28	2.17
TGME49_257520	(R-SNARE2) synaptobrevin protein	LTVMLCIAFAATLAYLIYVVVNL	LSDSKK	23	6	2.25
TGME49_205150	ACR, YagE family COG1723 domain-containing protein	MTWIIVLLLVAQVVAAAVKYVVL	DEP	23	3	2.28

TGME49_239640	hypothetical protein	ILEGSIVCLTALFFLLLWL	M	19	1	2.28
TGME49_220380	hypothetical protein	AIVRSLICYILICASLVLWL	RRAVHD	20	6	2.29
TGME49_205030	hypothetical protein	TCYLALFVVVIFIIIFYFLYG	DEP	20	3	2.40
TGME49_247930	(Qa-SNARE) SNARE domain-containing protein	GRAAQCIVFLVITIFFLLVLLIM	KHT	23	3	2.47
TGME49_275870	tubulin/FtsZ family, GTPase domain-containing protein	FLFFFSLFFALFVFAFSAFLAGI	STNDD DWRRER RHDFQ SGRAE TREKE MCIR	23	29	2.48
TGME49_278670	(UBC) ubiquitin-conjugating enzyme subfamily protein	VAAADLVLLLLVLASVLLADLF	VNPPK VTMYG SSGAG GKL	23	18	2.57
TGME49_309420	ferlin family protein	GVWMTVAGIIALVIFVMFLL	K	20	1	2.62
TGME49_248100	(R-SNARE1) synaptobrevin protein	YFIVFGMIVVLVILASFFCGGL	TFQTCLRIN	23	9	2.62
TGME49_246610	hypothetical protein	LYCLVAGAVVVFVFAWV	L	18	1	2.66
TGME49_208010	hypothetical protein	FYAMALLLIGCILFVMVMSFILF	TPG	23	3	2.67
TGME49_216680	ankyrin repeat-containing protein	LLGFVVVAIIFLLLYFGLELFIA	RDSRKRR	23	7	2.69
TGME49_253360	hypothetical protein	FFTRLLLIVILLFLVCFVLSIVY	ARYIKRA	23	7	2.75
TGME49_262980	hypothetical protein	AVYVALVCFCMVGPLVIALIMLI	SQMLQ	23	5	2.76
TGME49_306640	hypothetical protein	FSQCLCLFIFLFLVIAIVLVCVP	R	23	1	2.78
TGME49_242080	hypothetical protein	LILVAIIVFLSLAIVCVLIHRLL	RLVRDV	23	6	2.88
TGME49_278630	tetratricopeptide repeat-containing protein	IIVFIVLPVLLLLMVLLGCAHFF	ASLASPAPSIHPFADPSHHSEL	23	22	2.88
TGME49_226600	syntaxin 5, putative	LILKVFAILFTFIVFFVFFL	S	20	1	2.91

TGME49_300290	SNARE domain-containing protein	ACLLFTALALLVVLIFLVVA	TA	20	1	3.13
TGME49_300240	syntaxin 6, n-terminal protein	LCLILWLSCIALLLFLLLI	T	20	1	3.20
TGME49_235680	peptidase M16 inactive domain-containing protein	LLLLSSLAALGALIWLSRL	RQR	19	3	1.90
TGME49_276940	ribosome associated membrane protein RAMP4, putative	VGPLILALFLFVVVGSAILQIIF	SAQRGTIL	23	8	2.57

## Appendix E. Constructs used in chapter 4.

A list of all the constructs and the primers used to create each construct.

Construct Name	Primers Used
<b>HA-tagging:</b> Tub <sub>HA</sub> - <b>EcorV</b> -DHFR3'UTR-pDHFR-TS	F1 & R1; F2 & R2
Tub <sub>HA</sub> - <b>RlmN</b> -DHFR3'UTR-pDHFR-TS	F3 & R3
Tub <sub>HA</sub> - <b>Cyt-b5</b> -DHFR3'UTR-pDHFR-TS	F4 & R4
Tub <sub>HA</sub> - <b>R-SNARE1</b> -DHFR3'UTR-pDHFR-TS	F5 & R5
Tub <sub>HA</sub> - <b>R-SNARE2</b> -DHFR3'UTR-pDHFR-TS	F6 & R6
Tub <sub>HA</sub> - <b>QaSNARE</b> -DHFR3'UTR-pDHFR-TS	F7 & R7
Tub <sub>HA</sub> - <b>FIS1</b> -DHFR3'UTR-pDHFR-TS	F8 & R8
Tub <sub>HA</sub> - <b>RBD</b> -DHFR3'UTR-pDHFR-TS	F9 & R9
Tub <sub>HA</sub> - <b>UBC</b> -DHFR3'UTR-pDHFR-TS	F10 & R10
<b>YFP fusion:</b> Tub <sub>YFP</sub> - <b>EcorV</b> -DHFR3'UTR-pDHFR-TS	F1 & R1; F2 & R2-2
Tub <sub>YFP</sub> - <b>RlmN</b> -DHFR3'UTR-pDHFR-TS	F16 & R3
Tub <sub>YFP</sub> - <b>Cyt-b5</b> -DHFR3'UTR-pDHFR-TS	F14 & R4
Tub <sub>YFP</sub> - <b>R-SNARE1</b> -DHFR3'UTR-pDHFR-TS	F12 & R5
Tub <sub>YFP</sub> - <b>R-SNARE2</b> -DHFR3'UTR-pDHFR-TS	F13 & R6
Tub <sub>YFP</sub> - <b>QaSNARE</b> -DHFR3'UTR-pDHFR-TS	F18 & R7
Tub <sub>YFP</sub> - <b>FIS1</b> -DHFR3'UTR-pDHFR-TS	F15 & R8
Tub <sub>YFP</sub> - <b>RBD</b> -DHFR3'UTR-pDHFR-TS	F17 & R9
Tub <sub>YFP</sub> - <b>UBC</b> -DHFR3'UTR-pDHFR-TS	F19 & R10

	Tub <sub>YFP</sub> - <b>Elp3</b> -DHFR3'UTR-pDHFR-TS	F11 & R11
<b><i>ΔCTS:</i></b>	Tub <sub>HA</sub> - <b>RImNACTS</b> -DHFR3'UTR-pDHFR-TS	F3 & R12
	Tub <sub>HA</sub> - <b>FIS1ΔCTS</b> -DHFR3'UTR-pDHFR-TS	F8 & R13
	Tub <sub>HA</sub> - <b>Elp3ΔCTS</b> -DHFR3'UTR-pDHFR-TS	F20 & R14
	Tub <sub>HA</sub> - <b>QaSNAREΔCTS</b> -DHFR3'UTR-pDHFR-TS	F7 & R15
	Tub <sub>HA</sub> - <b>RBDΔCTS</b> -DHFR3'UTR-pDHFR-TS	F9 & R16
<b><i>Domain Swap:</i></b>	Tub <sub>HA</sub> - <b>RBD_RBD TMD_RRRR</b> -DHFR3'UTR-pDHFR-TS	F9 & R21
	Tub <sub>HA</sub> - <b>RBD_Elp3 TMD_RRRR</b> -DHFR3'UTR-pDHFR-TS	F9 & R22; F23 & R11
	Tub <sub>HA</sub> - <b>Elp3_Elp3 TMD_EA</b> -DHFR3'UTR-pDHFR-TS	F20 & R17
	Tub <sub>HA</sub> - <b>Elp3_RBD TMD_EA</b> -DHFR3'UTR-pDHFR-TS	F20 & R18; F21 & R9
	Tub <sub>HA</sub> - <b>Elp3_Elp3 TMD_KHT</b> -DHFR3'UTR-pDHFR-TS	F20 & R19; F22 & R11
	Tub <sub>HA</sub> - <b>Elp3_QaSNARE TMD_KHT</b> -DHFR3'UTR-pDHFR-TS	F20 & R20; F22 & R11
	Tub <sub>HA</sub> - <b>RBD_Elp3 TMD_EA</b> -DHFR3'UTR-pDHFR-TS	F9 & R24
	Tub <sub>HA</sub> - <b>Elp3_RBD TMD_RRRR</b> -DHFR3'UTR-pDHFR-TS	F20 & R25
	Tub <sub>HA</sub> - <b>Elp3_QaSNARE TMD_RRRR</b> -DHFR3'UTR-pDHFR-TS	F20 & R26

## Appendix F. Primers used in chapter 4.

A list of all primer names, primer numbers as referred to within the text and primer sequences used in this study.

No.=number

Construct Design	Primer Name	Primer No.	Sequence
<b>Tagging Constructs:</b>			
	Step1-EcoV-3'UTR-pDHFR	F1	CGGTATCGATAAGCTGATATCCTAGGGACTACAAGGACGAC
	Step1-EcoV-3'UTR-pDHFR	R1	CAGCCTGGCGAAGCTCGCGGCTTATCTAGTTAAGGGAG
	Step2-TubHA-EcorV-pDHFR	F2	CAAAAGCTGGTACCGGGAGAAAAACGCTGTTTGCAGAAAC
	Step2-TubHA-EcorV-pDHFR	R2	TCGACCTCGAGGGGGGATATCCGCGTAGTCCGGGAC
	Step2-TubYFP-EcorV-pDHFR	R2-2	TCGACCTCGAGGGGGGATATCCTTGTACAGCTCGTCCATG
<b>Gene Amplification:</b>			
	RlmN	F3	CCGGACTACGCGGATGCGCGCCGTCCG
		R3	TGTAGTCCCTAGGATCTACACTCGAGCGCGCC
	Cyt-b5	F4	CCGGACTACGCGGATTTTCTTCAGGAGATCTGGCCGT
		R4	TGTAGTCCCTAGGATCAAGAAAGATTCAGAATGTAGAAGACAGCTG
	R-SNARE1	F5	CCGGACTACGCGGATTGGGCGGCCCGTG
		R5	TGTAGTCCCTAGGATTTAGTTGATTGGAAGGCATGTTTGAAATGTAAG
	R-SNARE2	F6	CCGGACTACGCGGATAAGGGGTCAACGAGCACAG
		R6	TGTAGTCCCTAGGATCTACTTTTTCGAATTGGAAAGGAGGTTGAC
	Qa-SNARE	F7	CCGGACTACGCGGATGCGGCTACACTAGCAGCG
		R7	TGTAGTCCCTAGGATTTAGGTGTGTTTCATGATCAGCAGAACG
	FIS1	F8	CCGGACTACGCGGATGAAGACTCCAACCTTCAGTCTCCAAG
		R8	TGTAGTCCCTAGGATTTATTTTGATAGCGTCCACAAACGCG

RBD	F9	CCGGACTACGCGGATGAAGAGCTCTCTCACGCCTCT
	R9	TGTAGTCCCTAGGATTCACGCTTCGACGAAAAAACATTT
UBC	F10	CCGGACTACGCGGATCAGGGAGTGAGCAATCCCG
	R10	TGTAGTCCCTAGGATTCAGAGTTTTCTCCAGCCCC
Elp3	R11	TGTAGTCCCTAGGATTCACCTACGTCTTCTTACAGCCAC
<b>TMD Amplification:</b>		
Elp3-TMD	F11	GAGCTGTACAAGGATGGACAATGGAAATCCCCCTCG
R-SNARE1-TMD	F12	GAGCTGTACAAGGATCAGCACGTCTGGTGGTCG
R-SNARE2-TMD	F13	GAGCTGTACAAGGATAACCAGTCCATGCGGTGG
Cyt-b5-TMD	F14	GAGCTGTACAAGGATACTGCGACAAAGGGCGC
FIS1-TMD	F15	GAGCTGTACAAGGATCTAATCATAGACCGGGCTTCCCA
RImN-TMD	F16	GAGCTGTACAAGGATGAAACCGATGTAGAGCTTCAGCG
RBD-TMD	F17	GAGCTGTACAAGGATGATGAAGGCTTTTTGACGTTTCATGAAGA
Qa-SNARE-TMD	F18	GAGCTGTACAAGGATCTTCGCAAAGCTGAGGAAAATCAGAG
UBC-TMD	F19	GAGCTGTACAAGGATCAAACCCCTTTCACGAGGGG
<b><math>\Delta</math>CTS:</b>		
RImN $\Delta$ RRRARV	R12	TGTAGTCCCTAGGATCTACAAAATCCAGTGAGT
FIS1 $\Delta$ LSK	R13	TGTAGTCCCTAGGATCTACGTCCACAAACGCGTGAGA
Elp3 $\Delta$ RRRR	F20	CCGGACTACGCGGATGAACACACTTCTCTCTTCTTCTTCTCT
Elp3 $\Delta$ RRRR	R14	TGTAGTCCCTAGGATTCATACAGCCACGGATGCG
QaSNARE $\Delta$ KHT	R15	TGTAGTCCCTAGGATTTACATGATCAGCAGAACG
RBD $\Delta$ EA	R16	TGTAGTCCCTAGGATTCAGACGAAAAAACATTT

---

**Domain Swap:**

Elp3-EA	R17	TGTAGTCCCTAGGATTCACGCTTCTACAGCCACGGATGCGAACAG
Elp3-RBD_TMD_frag1	R18	AGAGTCCAGTTCGCCAGCGAGGGG
Elp3-RBD_TMD_frag2	F21	GGCGAACTGGACTCTCGCCATCGTCT
Elp3-KHT	R19	TGTAGTCCCTAGGATTCAGGTGTGTTTTACAGCCACGGATGCGAAC
Elp3-SNARE_Frag1	R20	GCGCGTCCGTTCCGCCAGCGAGGGG
Elp3-SNARE_Frag2	F22	GGCGAACGGACGCGCTGCGC
RBD-RRRR	R21	TGTAGTCCCTAGGATTCACCTACGTCTTCTGACGAAAAACATTTTCGC
RBD-Elp3_Frag1	R22	CAGAGTGGCATCTTCATGAACGTCAAAAAGCCTTCA
RBD-Elp3_Frag2	F23	GAAGATGCCACTCTGGCTTGGGGT
Elp3-RBD_TMD-RRRR	R24	TGTAGTCCCTAGGATTCACCTACGTCTTCTGACGAAAAACA
RBD-Elp3_TMD-EA	R25	TGTAGTCCCTAGGATTCACGCTTCTTACAGCCACG
Elp3-SNARE TM-RRRR	R26	TGTAGTCCCTAGGATTCACCTACGTCTTCTCATGATCAGC

---

**Sequencing Primers:**

Sequencing 1	F24	CTTGCGAAAACTACTCGTTGG
Sequencing 2	R23	GTCGTCGTCGTCCTTGTAGTC
Sequencing 3	F26	TTTCTGACGTTCTCGACGTG

---



### Appendix G. Comparison of *Toxoplasma* and *Arabidopsis* TA proteins.

List of 59 putative TA proteins in *Arabidopsis* (Arab.) with the corresponding *Toxoplasma* (Toxo) homologue. Homologues are highlighted in grey. SP: Signal Peptide, TMD: Transmembrane Domain.

Arab.	Description	Toxo	TM prediction	<i>Toxoplasma</i> annotation
AT5G4 6860.1	VAM3 (syntaxin 22); SNAP receptor	TGME49_ 204060	1 TM 100 aa from C term	SNARE domain-containing protein
AT1G7 9450.2	LEM3 (ligand-effect modulator 3) family protein / CDC50 family protein	TGME49_ 239540	1 TM besides C term TM	LEM3 (ligand-effect modulator 3) family / CDC50 family protein
AT4G0 8590.1	zinc finger (C3HC4-type RING finger) family protein	TGME49_ 203510	2 TMs besides C term TM	zinc finger, C3HC4 type (RING finger) domain-containing protein
AT4G2 4920.1	protein transport protein SEC61 gamma subunit	TGME49_ 230380	2 TMs besides C term TM	protein translocation complex, SEC61 gamma subunit
AT3G4 8570.1	protein transport protein SEC61 gamma subunit	TGME49_ 230380	2 TMs besides C term TM and SP	protein translocation complex, SEC61 gamma subunit
AT1G0 4760.1	ATVAMP726 (VESICLE-ASSOCIATED MEMBRANE PROTEIN) member of Synaptobrevin -like protein family	TGME49_ 230430	2 TMs besides C term TM and SP	vesicle-associated membrane protein, putative
AT5G5 0460.1	protein transport protein SEC61 gamma subunit	TGME49_ 230380	3 TM	
AT1G0 8560.1	SYP111 (syntaxin 111); SNAP receptor, identical to Syntaxin-related protein KNOLLE	TGME49_ 209820	3 TMs besides C term TM and SP	syntaxin protein
AT3G0 3800.1	SYP131 (syntaxin 131); SNAP receptor	TGME49_ 209820	3 TMs besides C term TM and SP	syntaxin protein
AT5G0 8080.1	SYP132 (syntaxin 132); SNAP receptor member of SYP13 Gene Family	TGME49_ 209820	3 TMs besides C term TM and SP	syntaxin protein
AT1G1 1250.1	SYP125 (syntaxin 125); SNAP receptor member of SYP12 gene family	TGME49_ 209820	3 TMs besides C term TM and SP	syntaxin protein
AT1G4 3310.1	triose phosphate/phosphate translocator-related	TGME49_ 261070	5 TM besides C term TM	apicoplast triosephosphate translocator APT1 (APT1)
AT2G3	PGP1/PGPS1/PGS1 (PHOSPHATIDYLGLYCEROLPHOSPHATE	TGME49_	7 TMs besides C	CDP-alcohol phosphatidyltransferase

9290.1	SYNTHASE 1); CDP-alcohol phosphatidyltransferase	254540	term TM	superfamily protein
AT1G1 9310.1	zinc finger (C3HC4-type RING finger) family protein	TGME49_ 205600	a possible second TM	zinc finger, C3HC4 type (RING finger) domain-containing protein
AT4G0 3510.1	RMA1 (Ring finger protein with Membrane Anchor 1); protein binding / ubiquitin-protein ligase/ zinc ion binding	TGME49_ 205600	a possible second TM	zinc finger, C3HC4 type (RING finger) domain-containing protein
AT4G2 8270.1	zinc finger (C3HC4-type RING finger) family protein	TGME49_ 205600	a possible second TM	zinc finger, C3HC4 type (RING finger) domain-containing protein
AT5G5 0430.1	UBC33 (UBIQUITIN-CONJUGATING ENZYME 33)	TGME49_ 251640	a possible second TM	ubiquitin-conjugating enzyme subfamily protein
AT1G7 2090.1	radical SAM domain-containing protein / TRAM domain- containing protein	TGME49_ 273140	SP and 1 TM in N term	radical SAM methylthiotransferase, MiaB/RimO family protein
AT4G1 1970.1	YT521-B-like family protein	TGME49_ 201200	SP no TM	zinc finger (CCCH type) motif- containing protein
AT1G5 1740.1	SYP81 (SYNTAXIN 81); protein binding member of SYP8 Gene Family	TGME49_ 267530	SP no TM	hypothetical protein
AT3G5 6300.1	tRNA synthetase class I (C) family protein	TGME49_ 299810	SP no TM	cysteine-tRNA synthetase (CysRS)
AT3G2 2920.1	peptidyl-prolyl cis-trans isomerase, putative / cyclophilin, putative / rotamase	TGME49_ 205700	TM in center of protein	cyclophilin precursor
AT4G0 9350.1	DNAJ heat shock N-terminal domain-containing protein	TGME49_ 244350	TM app. 80 aa from C term	DnaJ domain-containing protein
AT3G6 0540.1	Sec61beta family protein	TGME49_ 211040	TA protein	Sec61beta family protein
AT3G2 4350.1	SYP32 (syntaxin 32); SNAP receptor member of Glycoside Hydrolase Family 17	TGME49_ 226600	TA protein	syntaxin 5, putative
AT5G0 5760.1	SYP31 (T-SNARE SED 5); SNAP receptor A SNARE protein	TGME49_ 226600	TA protein	syntaxin 5, putative
AT5G3 9510.1	ATVTI11/ATVTI1A/SGR4/VTI11/VTI1A/ZIG (VESICLE TRANSPORT V-SNARE 11); receptor	TGME49_ 242080	TA protein	hypothetical protein
AT1G2 6670.1	ATVTI12/VTI12/VTI1B (VESICAL TRANSPORT V-SNARE 12)	TGME49_ 242080	TA protein	

AT5G1 6830.1	SYP21 (syntaxin 21); SNAP receptor	TGME49_ 247930	TA protein	SNARE domain-containing protein
AT3G0 5710.1	SYP43 (syntaxin 43); SNAP receptor	TGME49_ 247930	TA protein	SNARE domain-containing protein
AT4G0 2195.1	SYP42 (SYNTAXIN OF PLANTS 41); SNAP receptor	TGME49_ 247930	TA protein	SNARE domain-containing protein
AT5G2 6980.1	SYP41 (SYNTAXIN OF PLANTS 41); SNAP receptor	TGME49_ 247930	TA protein	SNARE domain-containing protein
AT1G1 1890.1	SEC22 (secretion 22); transporter member of SEC22 Gene Family	TGME49_ 270070	TA protein	synaptobrevin family protein
AT1G2 6340.1	B5 #6 (cytochrome b5 family protein #6); heme / transition metal ion binding	TGME49_ 276110	TA protein	cytochrome b5 family heme/steroid binding domain-containing protein
AT2G3 2720.1	B5 #4 (cytochrome b5 family); heme binding / transition metal ion binding	TGME49_ 276110	TA protein	cytochrome b5 family heme/steroid binding domain-containing protein
AT5G4 8810.1		TGME49_ 276110	TA protein	cytochrome b5 family heme/steroid binding domain-containing protein
AT5G5 3560.1	ATB5-A (Cytochrome b5 A)	TGME49_ 276110	TA protein	cytochrome b5 family heme/steroid binding domain-containing protein
AT3G1 7000.1	UBC32 (UBIQUITIN-CONJUGATING ENZYME 32); ubiquitin-protein ligase	TGME49_ 278670	TA protein	ubiquitin-conjugating enzyme subfamily protein
AT1G2 8490.1	SYP61 (SYNTAXIN OF PLANTS 61)	TGME49_ 300240	TA protein	phosphotransferase enzyme family protein
AT1G0 8820.1	VAP27-2 (VAMP/SYNAPTOBREVIN-ASSOCIATED PROTEIN 27-2)	TGME49_ 318160	TA protein	MSP (Major sperm protein) domain-containing protein
AT5G4 7180.1	vesicle-associated membrane family protein / VAMP family protein	TGME49_ 318160	TA protein	MSP (Major sperm protein) domain-containing protein
AT2G4 5140.1	vesicle-associated membrane protein, putative / VAMP	TGME49_ 318160	TA protein	MSP (Major sperm protein) domain-containing protein
AT3G6 0600.1	VAP27-1 (VAMP/SYNAPTOBREVIN-ASSOCIATED PROTEIN 27-1);	TGME49_ 318160	TA protein	MSP (Major sperm protein) domain-containing protein
AT4G0	vesicle-associated membrane family protein / VAMP family	TGME49_	TA protein	MSP (Major sperm protein) domain-

0170.1	protein	318160		containing protein
AT5G5 6730.1	peptidase M16 family protein / insulinase family protein	TGME49_ 235680	TA protein missed	peptidase M16 inactive domain- containing protein
AT1G2 7330.1	similar to unknown protein (TAIR:AT1G27350.1), domain Ribosome associated membrane RAMP4	TGME49_ 276940	TA protein missed	ribosome associated membrane protein RAMP4, putative
AT3G4 7550.2	zinc finger (C3HC4-type RING finger) family protein	TGME49_ 202840	No TM	FHA domain-containing protein
AT5G4 2320.1	carboxypeptidase A	TGME49_ 202910	No TM	zinc carboxypeptidase superfamily protein
AT2G2 5470.1	leucine-rich repeat family protein similar to leucine-rich repeat family protein	TGME49_ 203180	No TM	leucine rich repeat-containing protein
AT3G5 8840.1	similar to myosin heavy chain-related [Arabidopsis thaliana] (TAIR:AT1G06530.1)	TGME49_ 207370	No TM	hypothetical protein
AT1G1 7280.1	UBC34 (UBIQUITIN-CONJUGATING ENZYME 34); ubiquitin- protein ligase	TGME49_ 208570	No TM	ubiquitin conjugating enzyme E2, putative
AT3G6 2190.1	DNAJ heat shock N-terminal domain-containing protein	TGME49_ 214530	No TM	DnaJ domain-containing protein
AT3G4 5540.1	zinc finger (C3HC4-type RING finger) family protein	TGME49_ 226050	No TM	hypothetical protein
AT1G3 0230.2	elongation factor 1-beta / EF-1-beta	TGME49_ 226410	No TM	EF-1 guanine nucleotide exchange domain-containing protein
AT5G1 9660.1	ATS1P/ATSBT6.1/S1P (SITE-1 PROTEASE); endopeptidase/ subtilase	TGME49_ 231060	No TM	subtilisin SUB9 (SUB9)
AT4G3 6690.2	ATU2AF65A; RNA binding	TGME49_ 234520	No TM	U2 snRNP auxilliary factor, large subunit, splicing factor subfamily protein
AT2G2 6130.1	zinc finger (C3HC4-type RING finger) family protein	TGME49_ 235980	No TM	ARIADNE family protein
AT1G0 1450.1	protein kinase-related similar to protein kinase family protein	TGME49_ 237210	No TM	Tyrosine kinase-like (TKL) protein
AT5G6	ATATH13 (ABC2 homolog 13)	TGME49_	No TM	ABC1 family protein

4940.1		246600		
AT3G6 3410.1	VTE3, APG1   APG1 (ALBINO OR PALE GREEN MUTANT 1); methyltransferase	TGME49_ 247920	No TM	methyltransferase domain-containing protein
AT5G1 5200.2	40S ribosomal protein S9	TGME49_ 248480	No TM	ribosomal protein RPS9 (RPS9)
AT3G4 6450.1	SEC14 cytosolic factor family protein / phosphoglyceride transfer family protein	TGME49_ 254390	No TM	CRAL/TRIO domain-containing protein
AT4G3 1980.1	similar to unknown protein (TAIR:AT5G11290.1) DUF862 and DUF247 domains	TGME49_ 256780	No TM	hypothetical protein
AT5G2 6030.1	FC1 (FERROCHELATASE 1); ferrochelatase	TGME49_ 258650	No TM	protoheme ferro-lyase, putative
AT3G1 3445.2	TBP1 (TRANSCRIPTION FACTOR IID-1); DNA binding / RNA polymerase II transcription factor	TGME49_ 258680	No TM	TATA-box binding protein TBP2 (TBP2)
AT3G5 3240.1	leucine-rich repeat family protein	TGME49_ 260480	No TM	leucine rich repeat-containing protein
AT1G7 2416.3	heat shock protein binding	TGME49_ 265310	No TM	heat shock protein 40, putative
AT1G6 5060.2	4CL3 (4-coumarate:CoA ligase 3)	TGME49_ 266640	No TM	Acetyl-coenzyme A synthetase 2, putative
AT3G2 1640.1	TWD1 (TWISTED DWARF 1); FK506 binding / peptidyl-prolyl cis-trans isomerase	TGME49_ 283850	No TM	peptidyl-prolyl cis-trans isomerase
AT3G5 4010.1	PAS1 (PASTICCINO 1); FK506 binding / peptidyl-prolyl cis-trans isomerase	TGME49_ 283850	No TM	peptidyl-prolyl cis-trans isomerase
AT5G0 1980.1	zinc finger (C3HC4-type RING finger) family protein	TGME49_ 285190	No TM	zinc finger, C3HC4 type (RING finger) domain-containing protein
AT5G2 7540.1	EMB2473 (EMBRYO DEFECTIVE 2473); GTP binding	TGME49_ 289680	No TM	Ras-related protein Rab11
AT4G0 9760.3	choline kinase	TGME49_ 306540	No TM	phosphotransferase enzyme family protein
AT1G7 8260.2	RNA recognition motif (RRM)-containing protein	TGME49_ 310050	No TM	RNA recognition motif-containing protein

AT3G1 3224.1	RNA recognition motif (RRM)-containing protein	TGME49_ 310050	No TM	RNA recognition motif-containing protein
AT4G0 8140.1	similar to AtRPN1a/RPN1A (26S proteasome regulatory subunit S2 1A)	TGME49_ 313410	No TM	proteasome 26S regulatory subunit
AT5G2 1990.1	tetratricopeptide repeat (TPR)-containing protein	TGME49_ 314100	No TM	tetratricopeptide repeat-containing protein
AT2G4 1910.1	protein kinase family protein	TGME49_ 316150	No TM	ULK kinase
AT3G4 9430.2	SRP34A (SER/ARG-RICH PROTEIN 34A)	TGME49_ 319530	No TM	splicing factor SF2 (SF2)

## REFERENCES

1. Meyer H, De Mendonca IA. 1955. Electron microscopic observations of toxoplasma Nicolle et Manceaux grown in tissue cultures. I. Parasitology 45:449–451.
2. Ferguson DJP. 2009. Toxoplasma gondii: 1908-2008, homage to Nicolle, Manceaux and Splendore. Mem Inst Oswaldo Cruz 104:133–148.
3. Tenter AM, Heckeroth AR, Weiss LM. 2000. Toxoplasma gondii: from animals to humans. Int J Parasitol 30:1217–1258.
4. Turner M, Lenhart S, Rosenthal B, Zhao X. 2013. Modeling effective transmission pathways and control of the world's most successful parasite. Theor Popul Biol 86:50–61.
5. Halonen SK, Weiss LM. 2013. Toxoplasmosis. Handb Clin Neurol 114:125–145.
6. Carlucci JG, Blevins Peratikos M, Cherry CB, Lopez ML, Green AF, González-Calvo L, Moon TD, Ogumaniha-SCIP Zambézia Consortium. 2017. Prevalence and determinants of malaria among children in Zambézia Province, Mozambique. Malar J 16:108.
7. Moreira NA, Bondelind M. 2017. Safe drinking water and waterborne outbreaks. J Water Health 15:83–96.
8. Mahon M, Doyle S. 2017. Waterborne outbreak of cryptosporidiosis in the South East of Ireland: weighing up the evidence. Ir J Med Sci.
9. Hall V, Taye A, Walsh B, Maguire H, Dave J, Wright A, Anderson C, Crook P. 2017. A large outbreak of gastrointestinal illness at an open-water swimming event in the River Thames, London. Epidemiol Infect 145:1246–1255.
10. Howe DK, Sibley LD. 1995. Toxoplasma gondii comprises three clonal lineages: correlation of parasite genotype with human disease. J Infect Dis 172:1561–1566.
11. Khan A, Jordan C, Muccioli C, Vallochi AL, Rizzo LV, Belfort R, Vitor RWA, Silveira C, Sibley LD. 2006. Genetic divergence of Toxoplasma gondii strains associated with ocular toxoplasmosis, Brazil. Emerging Infect Dis 12:942–949.

12. Howe DK, Honoré S, Derouin F, Sibley LD. 1997. Determination of genotypes of *Toxoplasma gondii* strains isolated from patients with toxoplasmosis. *J Clin Microbiol* 35:1411–1414.
13. Sullivan WJ, Jeffers V. 2012. Mechanisms of *Toxoplasma gondii* persistence and latency. *FEMS Microbiol Rev* 36:717–733.
14. Gjerde B. 2013. Characterisation of full-length mitochondrial copies and partial nuclear copies (numts) of the cytochrome b and cytochrome c oxidase subunit I genes of *Toxoplasma gondii*, *Neospora caninum*, *Hammondia heydorni* and *Hammondia triffittae* (Apicomplexa: Sarcocystidae). *Parasitol Res* 112:1493–1511.
15. McFadden DC, Tomavo S, Berry EA, Boothroyd JC. 2000. Characterization of cytochrome b from *Toxoplasma gondii* and Q(o) domain mutations as a mechanism of atovaquone-resistance. *Mol Biochem Parasitol* 108:1–12.
16. Hikosaka K, Watanabe Y-I, Tsuji N, Kita K, Kishine H, Arisue N, Palacpac NMQ, Kawazu S-I, Sawai H, Horii T, Igarashi I, Tanabe K. 2010. Divergence of the mitochondrial genome structure in the apicomplexan parasites, *Babesia* and *Theileria*. *Mol Biol Evol* 27:1107–1116.
17. Esseiva AC, Naguleswaran A, Hemphill A, Schneider A. 2004. Mitochondrial tRNA import in *Toxoplasma gondii*. *J Biol Chem* 279:42363–42368.
18. Lim L, McFadden GI. 2010. The evolution, metabolism and functions of the apicoplast. *Philos Trans R Soc Lond, B, Biol Sci* 365:749–763.
19. Waller RF, Keeling PJ, Donald RG, Striepen B, Handman E, Lang-Unnasch N, Cowman AF, Besra GS, Roos DS, McFadden GI. 1998. Nuclear-encoded proteins target to the plastid in *Toxoplasma gondii* and *Plasmodium falciparum*. *Proc Natl Acad Sci USA* 95:12352–12357.
20. Fichera ME, Roos DS. 1997. A plastid organelle as a drug target in apicomplexan parasites. *Nature* 390:407–409.
21. Dubey JP, Lindsay DS, Speer CA. 1998. Structures of *Toxoplasma gondii* tachyzoites, bradyzoites, and sporozoites and biology and development of tissue cysts. *Clin Microbiol Rev* 11:267–299.
22. Frenkel JK, Dubey JP, Miller NL. 1970. *Toxoplasma gondii* in cats: fecal stages identified as coccidian oocysts. *Science* 167:893–896.
23. Dumètre A, Dardé ML. 2003. How to detect *Toxoplasma gondii* oocysts in environmental samples? *FEMS Microbiol Rev* 27:651–661.



24. Black MW, Boothroyd JC. 2000. Lytic cycle of *Toxoplasma gondii*. *Microbiol Mol Biol Rev* 64:607–623.
25. Robinson SA, Smith JE, Millner PA. 2004. *Toxoplasma gondii* major surface antigen (SAG1): in vitro analysis of host cell binding. *Parasitology* 128:391–396.
26. Friedrich N, Santos JM, Liu Y, Palma AS, Leon E, Saouros S, Kiso M, Blackman MJ, Matthews S, Feizi T, Soldati-Favre D. 2010. Members of a novel protein family containing microneme adhesive repeat domains act as sialic acid-binding lectins during host cell invasion by apicomplexan parasites. *J Biol Chem* 285:2064–2076.
27. Besteiro S, Dubremetz J-F, Lebrun M. 2011. The moving junction of apicomplexan parasites: a key structure for invasion. *Cell Microbiol* 13:797–805.
28. Blackman MJ, Carruthers VB. 2013. Recent insights into apicomplexan parasite egress provide new views to a kill. *Curr Opin Microbiol* 16:459–464.
29. Suzuki Y, Orellana MA, Schreiber RD, Remington JS. 1988. Interferon-gamma: the major mediator of resistance against *Toxoplasma gondii*. *Science* 240:516–518.
30. Jones TC, Alkan S, Erb P. 1986. Spleen and lymph node cell populations, in vitro cell proliferation and interferon-gamma production during the primary immune response to *Toxoplasma gondii*. *Parasite Immunol* 8:619–629.
31. Suzuki Y, Wang X, Jortner BS, Payne L, Ni Y, Michie SA, Xu B, Kudo T, Perkins S. 2010. Removal of *Toxoplasma gondii* cysts from the brain by perforin-mediated activity of CD8+ T cells. *Am J Pathol* 176:1607–1613.
32. Montoya JG, Liesenfeld O. 2004. Toxoplasmosis. *Lancet* 363:1965–1976.
33. Flegr J. 2013. Influence of latent *Toxoplasma* infection on human personality, physiology and morphology: pros and cons of the *Toxoplasma*-human model in studying the manipulation hypothesis. *J Exp Biol* 216:127–133.
34. Hsu P-C, Groer M, Beckie T. 2014. New findings: depression, suicide, and *Toxoplasma gondii* infection. *J Am Assoc Nurse Pract* 26:629–637.

35. Yazar S, Arman F, Yalçın S, Demirtaş F, Yaman O, Sahin I. 2003. Investigation of probable relationship between *Toxoplasma gondii* and cryptogenic epilepsy. *Seizure* 12:107–109.
36. Celik T, Kamişli O, Babür C, Cevik MO, Oztuna D, Altınayar S. 2010. Is there a relationship between *Toxoplasma gondii* infection and idiopathic Parkinson's disease? *Scand J Infect Dis* 42:604–608.
37. Miman O, Mutlu EA, Ozcan O, Atambay M, Karlidag R, Unal S. 2010. Is there any role of *Toxoplasma gondii* in the etiology of obsessive-compulsive disorder? *Psychiatry Res* 177:263–265.
38. Berdoy M, Webster JP, Macdonald DW. 2000. Fatal attraction in rats infected with *Toxoplasma gondii*. *Proc Biol Sci* 267:1591–1594.
39. House PK, Vyas A, Sapolsky R. 2011. Predator cat odors activate sexual arousal pathways in brains of *Toxoplasma gondii* infected rats. *PLoS ONE* 6:e23277.
40. Remington JS. 1974. Toxoplasmosis in the adult. *Bull N Y Acad Med* 50:211–227.
41. Burnett AJ, Shortt SG, Isaac-Renton J, King A, Werker D, Bowie WR. 1998. Multiple cases of acquired toxoplasmosis retinitis presenting in an outbreak. *Ophthalmology* 105:1032–1037.
42. Montoya JG, Jordan R, Lingamneni S, Berry GJ, Remington JS. 1997. Toxoplasmic myocarditis and polymyositis in patients with acute acquired toxoplasmosis diagnosed during life. *Clin Infect Dis* 24:676–683.
43. Desmonts G, Couvreur J. 1974. Toxoplasmosis in pregnancy and its transmission to the fetus. *Bull N Y Acad Med* 50:146–159.
44. Many A, Koren G. 2006. Toxoplasmosis during pregnancy. *Can Fam Physician* 52:29–30, 32.
45. Hyde JE. 2005. Exploring the folate pathway in *Plasmodium falciparum*. *Acta Trop* 94:191–206.
46. Neville AJ, Zach SJ, Wang X, Larson JJ, Judge AK, Davis LA, Vennerstrom JL, Davis PH. 2015. Clinically Available Medicines Demonstrating Anti-*Toxoplasma* Activity. *Antimicrob Agents Chemother* 59:7161–7169.

47. van der Ven AJ, Schoondermark-van de Ven EM, Camps W, Melchers WJ, Koopmans PP, van der Meer JW, Galama JM. 1996. Anti-toxoplasma effect of pyrimethamine, trimethoprim and sulphonamides alone and in combination: implications for therapy. *J Antimicrob Chemother* 38:75–80.
48. Tabbara KF, O'Connor GR. 1980. Treatment of ocular toxoplasmosis with clindamycin and sulfadiazine. *Ophthalmology* 87:129–134.
49. Madi D, Achappa B, Rao S, Ramapuram JT, Mahalingam S. 2012. Successful treatment of cerebral toxoplasmosis with clindamycin: a case report. *Oman Med J* 27:411–412.
50. Katlama C, De Wit S, O'Doherty E, Van Glabeke M, Clumeck N. 1996. Pyrimethamine-clindamycin vs. pyrimethamine-sulfadiazine as acute and long-term therapy for toxoplasmic encephalitis in patients with AIDS. *Clin Infect Dis* 22:268–275.
51. Fung HB, Kirschenbaum HL. 1996. Treatment regimens for patients with toxoplasmic encephalitis. *Clin Ther* 18:1037–1056; discussion 1036.
52. Van Delden C, Hirschel B. 1996. Folinic acid supplements to pyrimethamine-sulfadiazine for *Toxoplasma* encephalitis are associated with better outcome. *J Infect Dis* 173:1294–1295.
53. Avci ME, Arslan F, Çiftçi Ş, Ekiz A, Tüten A, Yildirim G, Madazli R. 2016. Role of spiramycin in prevention of fetal toxoplasmosis. *J Matern Fetal Neonatal Med* 29:2073–2076.
54. Gras L, Gilbert RE, Ades AE, Dunn DT. 2001. Effect of prenatal treatment on the risk of intracranial and ocular lesions in children with congenital toxoplasmosis. *Int J Epidemiol* 30:1309–1313.
55. Jeffers V, Sullivan WJ. 2012. Lysine acetylation is widespread on proteins of diverse function and localization in the protozoan parasite *Toxoplasma gondii*. *Eukaryotic Cell* 11:735–742.
56. Dixon SE, Stilger KL, Elias EV, Naguleswaran A, Sullivan WJ. 2010. A decade of epigenetic research in *Toxoplasma gondii*. *Mol Biochem Parasitol* 173:1–9.
57. Sullivan WJ, Hakimi M-A. 2006. Histone mediated gene activation in *Toxoplasma gondii*. *Mol Biochem Parasitol* 148:109–116.

58. Darkin-Rattray SJ, Gurnett AM, Myers RW, Dulski PM, Crumley TM, Allocco JJ, Cannova C, Meinke PT, Colletti SL, Bednarek MA, Singh SB, Goetz MA, Dombrowski AW, Polishook JD, Schmatz DM. 1996. Apicidin: a novel antiprotozoal agent that inhibits parasite histone deacetylase. *Proc Natl Acad Sci USA* 93:13143–13147.
59. Bougdour A, Maubon D, Baldacci P, Ortet P, Bastien O, Bouillon A, Barale J-C, Pelloux H, Ménard R, Hakimi M-A. 2009. Drug inhibition of HDAC3 and epigenetic control of differentiation in Apicomplexa parasites. *J Exp Med* 206:953–966.
60. Jeffers V, Gao H, Checkley LA, Liu Y, Ferdig MT, Sullivan WJ. 2016. Garcinol Inhibits GCN5-Mediated Lysine Acetyltransferase Activity and Prevents Replication of the Parasite *Toxoplasma gondii*. *Antimicrob Agents Chemother* 60:2164–2170.
61. Vanagas L, Jeffers V, Bogado SS, Dalmaso MC, Sullivan WJ, Angel SO. 2012. *Toxoplasma* histone acetylation remodelers as novel drug targets. *Expert Rev Anti Infect Ther* 10:1189–1201.
62. Otero G, Fellows J, Li Y, de Bizemont T, Dirac AM, Gustafsson CM, Erdjument-Bromage H, Tempst P, Svejstrup JQ. 1999. Elongator, a multisubunit component of a novel RNA polymerase II holoenzyme for transcriptional elongation. *Mol Cell* 3:109–118.
63. Wittschieben BO, Otero G, de Bizemont T, Fellows J, Erdjument-Bromage H, Ohba R, Li Y, Allis CD, Tempst P, Svejstrup JQ. 1999. A novel histone acetyltransferase is an integral subunit of elongating RNA polymerase II holoenzyme. *Mol Cell* 4:123–128.
64. Winkler GS, Petrakis TG, Ethelberg S, Tokunaga M, Erdjument-Bromage H, Tempst P, Svejstrup JQ. 2001. RNA polymerase II elongator holoenzyme is composed of two discrete subcomplexes. *J Biol Chem* 276:32743–32749.
65. Krogan NJ, Greenblatt JF. 2001. Characterization of a six-subunit holo-elongator complex required for the regulated expression of a group of genes in *Saccharomyces cerevisiae*. *Mol Cell Biol* 21:8203–8212.
66. Li Y, Takagi Y, Jiang Y, Tokunaga M, Erdjument-Bromage H, Tempst P, Kornberg RD. 2001. A multiprotein complex that interacts with RNA polymerase II elongator. *J Biol Chem* 276:29628–29631.

67. Winkler GS, Kristjuhan A, Erdjument-Bromage H, Tempst P, Svejstrup JQ. 2002. Elongator is a histone H3 and H4 acetyltransferase important for normal histone acetylation levels in vivo. *Proc Natl Acad Sci USA* 99:3517–3522.
68. Wittschieben BO, Fellows J, Du W, Stillman DJ, Svejstrup JQ. 2000. Overlapping roles for the histone acetyltransferase activities of SAGA and elongator in vivo. *EMBO J* 19:3060–3068.
69. Frohloff F, Fichtner L, Jablonowski D, Breunig KD, Schaffrath R. 2001. *Saccharomyces cerevisiae* Elongator mutations confer resistance to the *Kluyveromyces lactis* zymocin. *EMBO J* 20:1993–2003.
70. Fichtner L, Frohloff F, Jablonowski D, Stark MJR, Schaffrath R. 2002. Protein interactions within *Saccharomyces cerevisiae* Elongator, a complex essential for *Kluyveromyces lactis* zymocin. *Mol Microbiol* 45:817–826.
71. Butler AR, Porter M, Stark MJ. 1991. Intracellular expression of *Kluyveromyces lactis* toxin gamma subunit mimics treatment with exogenous toxin and distinguishes two classes of toxin-resistant mutant. *Yeast* 7:617–625.
72. Kitamoto HK, Jablonowski D, Nagase J, Schaffrath R. 2002. Defects in yeast RNA polymerase II transcription elicit hypersensitivity to G1 arrest induced by *Kluyveromyces lactis* zymocin. *Mol Genet Genomics* 268:49–55.
73. Jablonowski D, Frohloff F, Fichtner L, Stark MJ, Schaffrath R. 2001. *Kluyveromyces lactis* zymocin mode of action is linked to RNA polymerase II function via Elongator. *Mol Microbiol* 42:1095–1105.
74. Jablonowski D, Schaffrath R. 2002. *Saccharomyces cerevisiae* RNA polymerase II is affected by *Kluyveromyces lactis* zymocin. *J Biol Chem* 277:26276–26280.
75. Frohloff F, Jablonowski D, Fichtner L, Schaffrath R. 2003. Subunit communications crucial for the functional integrity of the yeast RNA polymerase II elongator (gamma-toxin target (TOT)) complex. *J Biol Chem* 278:956–961.
76. Hawkes NA, Otero G, Winkler GS, Marshall N, Dahmus ME, Krappmann D, Scheidereit C, Thomas CL, Schiavo G, Erdjument-Bromage H, Tempst P, Svejstrup JQ. 2002. Purification and characterization of the human elongator complex. *J Biol Chem* 277:3047–3052.

77. Nelissen H, Fleury D, Bruno L, Robles P, De Veylder L, Traas J, Micol JL, Van Montagu M, Inzé D, Van Lijsebettens M. 2005. The elongata mutants identify a functional Elongator complex in plants with a role in cell proliferation during organ growth. *Proc Natl Acad Sci USA* 102:7754–7759.
78. Wynshaw-Boris A. 2009. Elongator bridges tubulin acetylation and neuronal migration. *Cell* 136:393–394.
79. Singh N, Lorbeck MT, Zervos A, Zimmerman J, Elefant F. 2010. The histone acetyltransferase Elp3 plays an active role in the control of synaptic bouton expansion and sleep in *Drosophila*. *J Neurochem* 115:493–504.
80. Solinger JA, Paolinelli R, Klöss H, Scorza FB, Marchesi S, Sauder U, Mitsushima D, Capuani F, Stürzenbaum SR, Cassata G. 2010. The *Caenorhabditis elegans* Elongator complex regulates neuronal alpha-tubulin acetylation. *PLoS Genet* 6:e1000820.
81. Creppe C, Malinouskaya L, Volvert M-L, Gillard M, Close P, Malaise O, Laguesse S, Cornez I, Rahmouni S, Ormenese S, Belachew S, Malgrange B, Chapelle J-P, Siebenlist U, Moonen G, Chariot A, Nguyen L. 2009. Elongator controls the migration and differentiation of cortical neurons through acetylation of alpha-tubulin. *Cell* 136:551–564.
82. Okada Y, Yamagata K, Hong K, Wakayama T, Zhang Y. 2010. A role for the elongator complex in zygotic paternal genome demethylation. *Nature* 463:554–558.
83. Stilger KL, Sullivan WJ. 2013. Elongator protein 3 (Elp3) lysine acetyltransferase is a tail-anchored mitochondrial protein in *Toxoplasma gondii*. *J Biol Chem* 288:25318–25329.
84. Selvadurai K, Wang P, Seimetz J, Huang RH. 2014. Archaeal Elp3 catalyzes tRNA wobble uridine modification at C5 via a radical mechanism. *Nat Chem Biol* 10:810–812.
85. Esberg A, Huang B, Johansson MJO, Byström AS. 2006. Elevated levels of two tRNA species bypass the requirement for elongator complex in transcription and exocytosis. *Mol Cell* 24:139–148.
86. Huang B, Johansson MJO, Byström AS. 2005. An early step in wobble uridine tRNA modification requires the Elongator complex. *RNA* 11:424–436.
87. Johansson MJO, Esberg A, Huang B, Björk GR, Byström AS. 2008. Eukaryotic wobble uridine modifications promote a functionally redundant decoding system. *Mol Cell Biol* 28:3301–3312.

88. Nedialkova DD, Leidel SA. 2015. Optimization of Codon Translation Rates via tRNA Modifications Maintains Proteome Integrity. *Cell* 161:1606–1618.
89. Gardiner J, Barton D, Marc J, Overall R. 2007. Potential role of tubulin acetylation and microtubule-based protein trafficking in familial dysautonomia. *Traffic* 8:1145–1149.
90. Cheishvili D, Maayan C, Cohen-Kupiec R, Lefler S, Weil M, Ast G, Razin A. 2011. IKAP/Elp1 involvement in cytoskeleton regulation and implication for familial dysautonomia. *Hum Mol Genet* 20:1585–1594.
91. Close P, Hawkes N, Cornez I, Creppe C, Lambert CA, Rogister B, Siebenlist U, Merville M-P, Slaugenhaupt SA, Bours V, Svejstrup JQ, Chariot A. 2006. Transcription impairment and cell migration defects in elongator-depleted cells: implication for familial dysautonomia. *Mol Cell* 22:521–531.
92. Kwee LC, Liu Y, Haynes C, Gibson JR, Stone A, Schichman SA, Kamel F, Nelson LM, Topol B, Van den Eeden SK, Tanner CM, Cudkowicz ME, Grasso DL, Lawson R, Muralidhar S, Oddone EZ, Schmidt S, Hauser MA. 2012. A high-density genome-wide association screen of sporadic ALS in US veterans. *PLoS ONE* 7:e32768.
93. Simpson CL, Lemmens R, Miskiewicz K, Broom WJ, Hansen VK, van Vught PWJ, Landers JE, Sapp P, Van Den Bosch L, Knight J, Neale BM, Turner MR, Veldink JH, Ophoff RA, Tripathi VB, Beleza A, Shah MN, Proitsi P, Van Hoecke A, Carmeliet P, Horvitz HR, Leigh PN, Shaw CE, van den Berg LH, Sham PC, Powell JF, Verstreken P, Brown RH, Robberecht W, Al-Chalabi A. 2009. Variants of the elongator protein 3 (ELP3) gene are associated with motor neuron degeneration. *Hum Mol Genet* 18:472–481.
94. Ladang A, Rapino F, Heukamp LC, Tharun L, Shostak K, Hermand D, Delaunay S, Klevernic I, Jiang Z, Jacques N, Jamart D, Migeot V, Florin A, Göktuna S, Malgrange B, Sansom OJ, Nguyen L, Büttner R, Close P, Chariot A. 2015. Elp3 drives Wnt-dependent tumor initiation and regeneration in the intestine. *J Exp Med* 212:2057–2075.
95. Delaunay S, Rapino F, Tharun L, Zhou Z, Heukamp L, Termathe M, Shostak K, Klevernic I, Florin A, Desmecht H, Desmet CJ, Nguyen L, Leidel SA, Willis AE, Büttner R, Chariot A, Close P. 2016. Elp3 links tRNA modification to IRES-dependent translation of LEF1 to sustain metastasis in breast cancer. *J Exp Med* 213:2503–2523.
96. Svejstrup JQ. 2007. Elongator complex: how many roles does it play? *Curr Opin Cell Biol* 19:331–336.

97. Pokholok DK, Hannett NM, Young RA. 2002. Exchange of RNA polymerase II initiation and elongation factors during gene expression in vivo. *Mol Cell* 9:799–809.
98. Gilbert C, Kristjuhan A, Winkler GS, Svejstrup JQ. 2004. Elongator interactions with nascent mRNA revealed by RNA immunoprecipitation. *Mol Cell* 14:457–464.
99. Bhatti MM, Sullivan WJ. 2005. Histone acetylase GCN5 enters the nucleus via importin-alpha in protozoan parasite *Toxoplasma gondii*. *J Biol Chem* 280:5902–5908.
100. Donald RG, Roos DS. 1993. Stable molecular transformation of *Toxoplasma gondii*: a selectable dihydrofolate reductase-thymidylate synthase marker based on drug-resistance mutations in malaria. *Proc Natl Acad Sci USA* 90:11703–11707.
101. Donald RG, Roos DS. 1998. Gene knock-outs and allelic replacements in *Toxoplasma gondii*: HXGPRT as a selectable marker for hit-and-run mutagenesis. *Mol Biochem Parasitol* 91:295–305.
102. Fox BA, Ristuccia JG, Gigley JP, Bzik DJ. 2009. Efficient gene replacements in *Toxoplasma gondii* strains deficient for nonhomologous end joining. *Eukaryotic Cell* 8:520–529.
103. Huynh M-H, Carruthers VB. 2009. Tagging of endogenous genes in a *Toxoplasma gondii* strain lacking Ku80. *Eukaryotic Cell* 8:530–539.
104. Reikvam A, Lorentzen-Styr AM. 1976. Virulence of different strains of *Toxoplasma gondii* and host response in mice. *Nature* 261:508–509.
105. Black M, Seeber F, Soldati D, Kim K, Boothroyd JC. 1995. Restriction enzyme-mediated integration elevates transformation frequency and enables co-transfection of *Toxoplasma gondii*. *Mol Biochem Parasitol* 74:55–63.
106. van den Hoff MJ, Moorman AF, Lamers WH. 1992. Electroporation in “intracellular” buffer increases cell survival. *Nucleic Acids Res* 20:2902.
107. Soldati D, Boothroyd JC. 1993. Transient transfection and expression in the obligate intracellular parasite *Toxoplasma gondii*. *Science* 260:349–352.
108. Beck JR, Chen AL, Kim EW, Bradley PJ. 2014. RON5 is critical for organization and function of the *Toxoplasma* moving junction complex. *PLoS Pathog* 10:e1004025.



109. Lavine MD, Arrizabalaga G. 2012. Analysis of monensin sensitivity in *Toxoplasma gondii* reveals autophagy as a mechanism for drug induced death. *PLoS ONE* 7:e42107.
110. Ufermann C-M, Müller F, Frohnecke N, Laue M, Seeber F. 2016. *Toxoplasma gondii* plaque assays revisited: Improvements for ultrastructural and quantitative evaluation of lytic parasite growth. *Exp Parasitol*.
111. Chaparas SD, Schlesinger RW. 1959. Plaque assay of *Toxoplasma* on monolayers of chick embryo fibroblasts. *Proc Soc Exp Biol Med* 102:431–437.
112. Dvorak JA, Howe CL. 1979. *Toxoplasma gondii*-vertebrate cell interactions. II. The intracellular reproductive phase. *J Protozool* 26:114–117.
113. Roos DS, Donald RG, Morrisette NS, Moulton AL. 1994. Molecular tools for genetic dissection of the protozoan parasite *Toxoplasma gondii*. *Methods Cell Biol* 45:27–63.
114. Ramirez M, Wek RC, Hinnebusch AG. 1991. Ribosome association of GCN2 protein kinase, a translational activator of the GCN4 gene of *Saccharomyces cerevisiae*. *Mol Cell Biol* 11:3027–3036.
115. Narasimhan J, Joyce BR, Naguleswaran A, Smith AT, Livingston MR, Dixon SE, Coppens I, Wek RC, Sullivan WJ. 2008. Translation regulation by eukaryotic initiation factor-2 kinases in the development of latent cysts in *Toxoplasma gondii*. *J Biol Chem* 283:16591–16601.
116. Levine EM, Becker Y, Boone CW, Eagle H. 1965. CONTACT INHIBITION, MACROMOLECULAR SYNTHESIS, AND POLYRIBOSOMES IN CULTURED HUMAN DIPLOID FIBROBLASTS. *Proc Natl Acad Sci USA* 53:350–356.
117. Roux KJ, Kim DI, Raida M, Burke B. 2012. A promiscuous biotin ligase fusion protein identifies proximal and interacting proteins in mammalian cells. *J Cell Biol* 196:801–810.
118. Chen AL, Kim EW, Toh JY, Vashisht AA, Rashoff AQ, Van C, Huang AS, Moon AS, Bell HN, Bentolila LA, Wohlschlegel JA, Bradley PJ. 2015. Novel components of the *Toxoplasma* inner membrane complex revealed by BioID. *MBio* 6:e02357-02314.
119. Padgett LR, Arrizabalaga G, Sullivan WJ. 2017. Targeting of tail-anchored membrane proteins to subcellular organelles in *Toxoplasma gondii*. *Traffic* 18:149–158.

120. Defraia CT, Wang Y, Yao J, Mou Z. 2013. Elongator subunit 3 positively regulates plant immunity through its histone acetyltransferase and radical S-adenosylmethionine domains. *BMC Plant Biol* 13:102.
121. Herm-Götz A, Agop-Nersesian C, Münter S, Grimley JS, Wandless TJ, Frischknecht F, Meissner M. 2007. Rapid control of protein level in the apicomplexan *Toxoplasma gondii*. *Nat Methods* 4:1003–1005.
122. Banaszynski LA, Chen L-C, Maynard-Smith LA, Ooi AGL, Wandless TJ. 2006. A rapid, reversible, and tunable method to regulate protein function in living cells using synthetic small molecules. *Cell* 126:995–1004.
123. Glatt S, Zabel R, Kolaj-Robin O, Onuma OF, Baudin F, Graziadei A, Taverniti V, Lin T-Y, Baymann F, Séraphin B, Breunig KD, Müller CW. 2016. Structural basis for tRNA modification by Elp3 from *Dehalococcoides mccartyi*. *Nat Struct Mol Biol* 23:794–802.
124. Landgraf BJ, McCarthy EL, Booker SJ. 2016. Radical S-Adenosylmethionine Enzymes in Human Health and Disease. *Annu Rev Biochem* 85:485–514.
125. Fernández-Vázquez J, Vargas-Pérez I, Sansó M, Buhne K, Carmona M, Paulo E, Hermand D, Rodríguez-Gabriel M, Ayté J, Leidel S, Hidalgo E. 2013. Modification of tRNA(Lys) UUU by elongator is essential for efficient translation of stress mRNAs. *PLoS Genet* 9:e1003647.
126. Huang B, Lu J, Byström AS. 2008. A genome-wide screen identifies genes required for formation of the wobble nucleoside 5-methoxycarbonylmethyl-2-thiouridine in *Saccharomyces cerevisiae*. *RNA* 14:2183–2194.
127. Lu J, Huang B, Esberg A, Johansson MJO, Byström AS. 2005. The *Kluyveromyces lactis* gamma-toxin targets tRNA anticodons. *RNA* 11:1648–1654.
128. Björk GR, Huang B, Persson OP, Byström AS. 2007. A conserved modified wobble nucleoside (mcm5s2U) in lysyl-tRNA is required for viability in yeast. *RNA* 13:1245–1255.
129. Chen C, Huang B, Anderson JT, Byström AS. 2011. Unexpected accumulation of ncm(5)U and ncm(5)S(2) (U) in a *trm9* mutant suggests an additional step in the synthesis of mcm(5)U and mcm(5)S(2)U. *PLoS ONE* 6:e20783.
130. Dewez M, Bauer F, Dieu M, Raes M, Vandehaute J, Hermand D. 2008. The conserved Wobble uridine tRNA thiolase Ctu1-Ctu2 is required to maintain genome integrity. *Proc Natl Acad Sci USA* 105:5459–5464.

131. Paraskevopoulou C, Fairhurst SA, Lowe DJ, Brick P, Onesti S. 2006. The Elongator subunit Eip3 contains a Fe<sub>4</sub>S<sub>4</sub> cluster and binds S-adenosylmethionine. *Mol Microbiol* 59:795–806.
132. Walsby CJ, Ortillo D, Broderick WE, Broderick JB, Hoffman BM. 2002. An anchoring role for FeS clusters: chelation of the amino acid moiety of S-adenosylmethionine to the unique iron site of the [4Fe-4S] cluster of pyruvate formate-lyase activating enzyme. *J Am Chem Soc* 124:11270–11271.
133. Sofia HJ, Chen G, Hetzler BG, Reyes-Spindola JF, Miller NE. 2001. Radical SAM, a novel protein superfamily linking unresolved steps in familiar biosynthetic pathways with radical mechanisms: functional characterization using new analysis and information visualization methods. *Nucleic Acids Res* 29:1097–1106.
134. Outten FW. 2007. Iron-sulfur clusters as oxygen-responsive molecular switches. *Nat Chem Biol* 3:206–207.
135. Rousset M, Montet Y, Guigliarelli B, Forget N, Asso M, Bertrand P, Fontecilla-Camps JC, Hatchikian EC. 1998. [3Fe-4S] to [4Fe-4S] cluster conversion in *Desulfovibrio fructosovorans* [NiFe] hydrogenase by site-directed mutagenesis. *Proc Natl Acad Sci USA* 95:11625–11630.
136. Imlay JA. 2006. Iron-sulphur clusters and the problem with oxygen. *Mol Microbiol* 59:1073–1082.
137. Grove TL, Radle MI, Krebs C, Booker SJ. 2011. Cfr and RlmN contain a single [4Fe-4S] cluster, which directs two distinct reactivities for S-adenosylmethionine: methyl transfer by SN<sub>2</sub> displacement and radical generation. *J Am Chem Soc* 133:19586–19589.
138. Grove TL, Lee K-H, St Clair J, Krebs C, Booker SJ. 2008. In vitro characterization of AtsB, a radical SAM formylglycine-generating enzyme that contains three [4Fe-4S] clusters. *Biochemistry* 47:7523–7538.
139. Duschene KS, Broderick JB. 2010. The antiviral protein viperin is a radical SAM enzyme. *FEBS Lett* 584:1263–1267.
140. Agris PF, Vendeix FAP, Graham WD. 2007. tRNA's wobble decoding of the genome: 40 years of modification. *J Mol Biol* 366:1–13.
141. Klassen R, Grunewald P, Thüring KL, Eichler C, Helm M, Schaffrath R. 2015. Loss of anticodon wobble uridine modifications affects tRNA(Lys) function and protein levels in *Saccharomyces cerevisiae*. *PLoS ONE* 10:e0119261.

142. Bauer F, Matsuyama A, Candiracci J, Dieu M, Scheliga J, Wolf DA, Yoshida M, Hermand D. 2012. Translational control of cell division by Elongator. *Cell Rep* 1:424–433.
143. Ladang A, Rapino F, Heukamp LC, Tharun L, Shostak K, Hermand D, Delaunay S, Klevernic I, Jiang Z, Jacques N, Jamart D, Migeot V, Florin A, Göktuna S, Malgrange B, Sansom OJ, Nguyen L, Büttner R, Close P, Chariot A. 2017. Correction: Eip3 drives Wnt-dependent tumor initiation and regeneration in the intestine. *J Exp Med* 214:1199.
144. Goodman CA, Hornberger TA. 2013. Measuring protein synthesis with SUnSET: a valid alternative to traditional techniques? *Exerc Sport Sci Rev* 41:107–115.
145. Schmidt EK, Clavarino G, Ceppi M, Pierre P. 2009. SUnSET, a nonradioactive method to monitor protein synthesis. *Nat Methods* 6:275–277.
146. Lodish HF, Jacobsen M. 1972. Regulation of hemoglobin synthesis. Equal rates of translation and termination of  $\alpha$ - and  $\beta$ -globin chains. *J Biol Chem* 247:3622–3629.
147. Walden WE, Godefroy-Colburn T, Thach RE. 1981. The role of mRNA competition in regulating translation. I. Demonstration of competition in vivo. *J Biol Chem* 256:11739–11746.
148. Tyagi K, Pedrioli PGA. 2015. Protein degradation and dynamic tRNA thiolation fine-tune translation at elevated temperatures. *Nucleic Acids Res* 43:4701–4712.
149. Schaffrath R, Leidel SA. 2017. Wobble uridine modifications - a reason to live, a reason to die?! *RNA Biol* 0.
150. Kaneko T, Suzuki T, Kapushoc ST, Rubio MA, Ghazvini J, Watanabe K, Simpson L, Suzuki T. 2003. Wobble modification differences and subcellular localization of tRNAs in *Leishmania tarentolae*: implication for tRNA sorting mechanism. *EMBO J* 22:657–667.
151. Paris Z, Rubio MAT, Lukes J, Alfonzo JD. 2009. Mitochondrial tRNA import in *Trypanosoma brucei* is independent of thiolation and the Rieske protein. *RNA* 15:1398–1406.
152. Morrissette N. 2015. Targeting *Toxoplasma* tubules: tubulin, microtubules, and associated proteins in a human pathogen. *Eukaryotic Cell* 14:2–12.

153. Sheffield HG, Melton ML. 1968. The fine structure and reproduction of *Toxoplasma gondii*. *J Parasitol* 54:209–226.
154. Hu K, Mann T, Striepen B, Beckers CJM, Roos DS, Murray JM. 2002. Daughter cell assembly in the protozoan parasite *Toxoplasma gondii*. *Mol Biol Cell* 13:593–606.
155. Shaw MK, Compton HL, Roos DS, Tilney LG. 2000. Microtubules, but not actin filaments, drive daughter cell budding and cell division in *Toxoplasma gondii*. *J Cell Sci* 113 ( Pt 7):1241–1254.
156. Morrissette NS, Sibley LD. 2002. Disruption of microtubules uncouples budding and nuclear division in *Toxoplasma gondii*. *J Cell Sci* 115:1017–1025.
157. Gordon JL, Beatty WL, Sibley LD. 2008. A novel actin-related protein is associated with daughter cell formation in *Toxoplasma gondii*. *Eukaryotic Cell* 7:1500–1512.
158. Verhey KJ, Gaertig J. 2007. The tubulin code. *Cell Cycle* 6:2152–2160.
159. Janke C. 2014. The tubulin code: molecular components, readout mechanisms, and functions. *J Cell Biol* 206:461–472.
160. Song Y, Brady ST. 2015. Post-translational modifications of tubulin: pathways to functional diversity of microtubules. *Trends Cell Biol* 25:125–136.
161. Yu I, Garnham CP, Roll-Mecak A. 2015. Writing and Reading the Tubulin Code. *J Biol Chem* 290:17163–17172.
162. Hammond JW, Cai D, Verhey KJ. 2008. Tubulin modifications and their cellular functions. *Curr Opin Cell Biol* 20:71–76.
163. Janke C, Bulinski JC. 2011. Post-translational regulation of the microtubule cytoskeleton: mechanisms and functions. *Nat Rev Mol Cell Biol* 12:773–786.
164. Al-Bassam J, Corbett KD. 2012.  $\alpha$ -Tubulin acetylation from the inside out. *Proc Natl Acad Sci USA* 109:19515–19516.
165. Perdiz D, Mackeh R, Poüs C, Baillet A. 2011. The ins and outs of tubulin acetylation: more than just a post-translational modification? *Cell Signal* 23:763–771.

166. Chuong SDX, Good AG, Taylor GJ, Freeman MC, Moorhead GBG, Muench DG. 2004. Large-scale identification of tubulin-binding proteins provides insight on subcellular trafficking, metabolic channeling, and signaling in plant cells. *Mol Cell Proteomics* 3:970–983.
167. Shida T, Cueva JG, Xu Z, Goodman MB, Nachury MV. 2010. The major alpha-tubulin K40 acetyltransferase alphaTAT1 promotes rapid ciliogenesis and efficient mechanosensation. *Proc Natl Acad Sci USA* 107:21517–21522.
168. Akella JS, Wloga D, Kim J, Starostina NG, Lyons-Abbott S, Morrisette NS, Dougan ST, Kipreos ET, Gaertig J. 2010. MEC-17 is an alpha-tubulin acetyltransferase. *Nature* 467:218–222.
169. LeDizet M, Piperno G. 1987. Identification of an acetylation site of *Chlamydomonas* alpha-tubulin. *Proc Natl Acad Sci USA* 84:5720–5724.
170. L'Hernault SW, Rosenbaum JL. 1983. *Chlamydomonas* alpha-tubulin is posttranslationally modified in the flagella during flagellar assembly. *J Cell Biol* 97:258–263.
171. Cambray-Deakin MA, Burgoyne RD. 1987. Posttranslational modifications of alpha-tubulin: acetylated and detyrosinated forms in axons of rat cerebellum. *J Cell Biol* 104:1569–1574.
172. Witte H, Neukirchen D, Bradke F. 2008. Microtubule stabilization specifies initial neuronal polarization. *J Cell Biol* 180:619–632.
173. Cueva JG, Hsin J, Huang KC, Goodman MB. 2012. Posttranslational acetylation of  $\alpha$ -tubulin constrains protofilament number in native microtubules. *Curr Biol* 22:1066–1074.
174. Xiong X, Xu D, Yang Z, Huang H, Cui X. 2013. A single amino-acid substitution at lysine 40 of an *Arabidopsis thaliana*  $\alpha$ -tubulin causes extensive cell proliferation and expansion defects. *J Integr Plant Biol* 55:209–220.
175. Kozminski KG, Diener DR, Rosenbaum JL. 1993. High level expression of nonacetylatable alpha-tubulin in *Chlamydomonas reinhardtii*. *Cell Motil Cytoskeleton* 25:158–170.
176. Kim G-W, Li L, Gorbani M, You L, Yang X-J. 2013. Mice lacking  $\alpha$ -tubulin acetyltransferase 1 are viable but display  $\alpha$ -tubulin acetylation deficiency and dentate gyrus distortion. *J Biol Chem* 288:20334–20350.

177. Xiao H, El Bissati K, Verdier-Pinard P, Burd B, Zhang H, Kim K, Fiser A, Angeletti RH, Weiss LM. 2010. Post-translational modifications to *Toxoplasma gondii* alpha- and beta-tubulins include novel C-terminal methylation. *J Proteome Res* 9:359–372.
178. Plessmann U, Reiter-Owona I, Lechtreck K-F. 2004. Posttranslational modifications of alpha-tubulin of *Toxoplasma gondii*. *Parasitol Res* 94:386–389.
179. Chen C-T, Kelly M, Leon J de, Nwagbara B, Ebbert P, Ferguson DJP, Lowery LA, Morrissette N, Gubbels M-J. 2015. Compartmentalized *Toxoplasma* EB1 bundles spindle microtubules to secure accurate chromosome segregation. *Mol Biol Cell* 26:4562–4576.
180. Gubbels M-J, Wieffer M, Striepen B. 2004. Fluorescent protein tagging in *Toxoplasma gondii*: identification of a novel inner membrane complex component conserved among Apicomplexa. *Mol Biochem Parasitol* 137:99–110.
181. Beck JR, Rodriguez-Fernandez IA, de Leon JC, Huynh M-H, Carruthers VB, Morrissette NS, Bradley PJ. 2010. A novel family of *Toxoplasma* IMC proteins displays a hierarchical organization and functions in coordinating parasite division. *PLoS Pathog* 6:e1001094.
182. Sanders MA, Salisbury JL. 1994. Centrin plays an essential role in microtubule severing during flagellar excision in *Chlamydomonas reinhardtii*. *J Cell Biol* 124:795–805.
183. DeRocher AE, Coppens I, Karnataki A, Gilbert LA, Rome ME, Feagin JE, Bradley PJ, Parsons M. 2008. A thioredoxin family protein of the apicoplast periphery identifies abundant candidate transport vesicles in *Toxoplasma gondii*. *Eukaryotic Cell* 7:1518–1529.
184. Morrissette NS, Mitra A, Sept D, Sibley LD. 2004. Dinitroanilines bind alpha-tubulin to disrupt microtubules. *Mol Biol Cell* 15:1960–1968.
185. Wang X, Hayes JJ. 2008. Acetylation mimics within individual core histone tail domains indicate distinct roles in regulating the stability of higher-order chromatin structure. *Mol Cell Biol* 28:227–236.
186. Stokkermans TJ, Schwartzman JD, Keenan K, Morrissette NS, Tilney LG, Roos DS. 1996. Inhibition of *Toxoplasma gondii* replication by dinitroaniline herbicides. *Exp Parasitol* 84:355–370.

187. Lyons-Abbott S, Sackett DL, Wloga D, Gaertig J, Morgan RE, Werbovetz KA, Morrissette NS. 2010.  $\alpha$ -Tubulin mutations alter oryzalin affinity and microtubule assembly properties to confer dinitroaniline resistance. *Eukaryotic Cell* 9:1825–1834.
188. Varberg JM, Padgett LR, Arrizabalaga G, Sullivan WJ. 2016. TgATAT-Mediated  $\alpha$ -Tubulin Acetylation Is Required for Division of the Protozoan Parasite *Toxoplasma gondii*. *mSphere* 1.
189. Ma C, Li C, Ganesan L, Oak J, Tsai S, Sept D, Morrissette NS. 2007. Mutations in alpha-tubulin confer dinitroaniline resistance at a cost to microtubule function. *Mol Biol Cell* 18:4711–4720.
190. Gaertig J, Cruz MA, Bowen J, Gu L, Pennock DG, Gorovsky MA. 1995. Acetylation of lysine 40 in alpha-tubulin is not essential in *Tetrahymena thermophila*. *J Cell Biol* 129:1301–1310.
191. Davenport AM, Collins LN, Chiu H, Minor PJ, Sternberg PW, Hoelz A. 2014. Structural and functional characterization of the  $\alpha$ -tubulin acetyltransferase MEC-17. *J Mol Biol* 426:2605–2616.
192. Gajria B, Bahl A, Brestelli J, Dommer J, Fischer S, Gao X, Heiges M, Iodice J, Kissinger JC, Mackey AJ, Pinney DF, Roos DS, Stoeckert CJ, Wang H, Brunk BP. 2008. ToxoDB: an integrated *Toxoplasma gondii* database resource. *Nucleic Acids Res* 36:D553-556.
193. Sievers F, Wilm A, Dineen D, Gibson TJ, Karplus K, Li W, Lopez R, McWilliam H, Remmert M, Söding J, Thompson JD, Higgins DG. 2011. Fast, scalable generation of high-quality protein multiple sequence alignments using Clustal Omega. *Mol Syst Biol* 7:539.
194. Behnke MS, Wootton JC, Lehmann MM, Radke JB, Lucas O, Nawas J, Sibley LD, White MW. 2010. Coordinated progression through two subtranscriptomes underlies the tachyzoite cycle of *Toxoplasma gondii*. *PLoS ONE* 5:e12354.
195. Sidik SM, Hackett CG, Tran F, Westwood NJ, Lourido S. 2014. Efficient genome engineering of *Toxoplasma gondii* using CRISPR/Cas9. *PLoS ONE* 9:e100450.
196. Shen B, Brown KM, Lee TD, Sibley LD. 2014. Efficient gene disruption in diverse strains of *Toxoplasma gondii* using CRISPR/CAS9. *MBio* 5:e01114-01114.



197. Anderson-White B, Beck JR, Chen C-T, Meissner M, Bradley PJ, Gubbels M-J. 2012. Cytoskeleton assembly in *Toxoplasma gondii* cell division. *Int Rev Cell Mol Biol* 298:1–31.
198. Nishi M, Hu K, Murray JM, Roos DS. 2008. Organellar dynamics during the cell cycle of *Toxoplasma gondii*. *J Cell Sci* 121:1559–1568.
199. Gubbels M-J, Vaishnava S, Boot N, Dubremetz J-F, Striepen B. 2006. A MORN-repeat protein is a dynamic component of the *Toxoplasma gondii* cell division apparatus. *J Cell Sci* 119:2236–2245.
200. Striepen B, Crawford MJ, Shaw MK, Tilney LG, Seeber F, Roos DS. 2000. The plastid of *Toxoplasma gondii* is divided by association with the centrosomes. *J Cell Biol* 151:1423–1434.
201. Li L, Wei D, Wang Q, Pan J, Liu R, Zhang X, Bao L. 2012. MEC-17 deficiency leads to reduced  $\alpha$ -tubulin acetylation and impaired migration of cortical neurons. *J Neurosci* 32:12673–12683.
202. Mitra A, Sept D. 2006. Binding and interaction of dinitroanilines with apicomplexan and kinetoplastid  $\alpha$ -tubulin. *J Med Chem* 49:5226–5231.
203. Szyk A, Deaconescu AM, Spector J, Goodman B, Valenstein ML, Ziolkowska NE, Kormendi V, Grigorieff N, Roll-Mecak A. 2014. Molecular basis for age-dependent microtubule acetylation by tubulin acetyltransferase. *Cell* 157:1405–1415.
204. Howes SC, Alushin GM, Shida T, Nachury MV, Nogales E. 2014. Effects of tubulin acetylation and tubulin acetyltransferase binding on microtubule structure. *Mol Biol Cell* 25:257–266.
205. Soppina V, Herbstman JF, Skiniotis G, Verhey KJ. 2012. Luminal localization of  $\alpha$ -tubulin K40 acetylation by cryo-EM analysis of fab-labeled microtubules. *PLoS ONE* 7:e48204.
206. Kalebic N, Martinez C, Perlas E, Hublitz P, Bilbao-Cortes D, Fiedorczuk K, Andolfo A, Heppenstall PA. 2013. Tubulin acetyltransferase  $\alpha$ TAT1 destabilizes microtubules independently of its acetylation activity. *Mol Cell Biol* 33:1114–1123.
207. Borgese N, Colombo S, Pedrazzini E. 2003. The tale of tail-anchored proteins: coming from the cytosol and looking for a membrane. *J Cell Biol* 161:1013–1019.
208. Kutay U, Hartmann E, Rapoport TA. 1993. A class of membrane proteins with a C-terminal anchor. *Trends Cell Biol* 3:72–75.

209. Yao Y, Nisan D, Fujimoto LM, Antignani A, Barnes A, Tjandra N, Youle RJ, Marassi FM. 2016. Characterization of the membrane-inserted C-terminus of cytoprotective BCL-XL. *Protein Expr Purif* 122:56–63.
210. Kutay U, Ahnert-Hilger G, Hartmann E, Wiedenmann B, Rapoport TA. 1995. Transport route for synaptobrevin via a novel pathway of insertion into the endoplasmic reticulum membrane. *EMBO J* 14:217–223.
211. Horie C, Suzuki H, Sakaguchi M, Mihara K. 2002. Characterization of signal that directs C-tail-anchored proteins to mammalian mitochondrial outer membrane. *Mol Biol Cell* 13:1615–1625.
212. Abell BM, Pool MR, Schlenker O, Sinning I, High S. 2004. Signal recognition particle mediates post-translational targeting in eukaryotes. *EMBO J* 23:2755–2764.
213. Borgese N, Fasana E. 2011. Targeting pathways of C-tail-anchored proteins. *Biochim Biophys Acta* 1808:937–946.
214. Abell BM, Rabu C, Leznicki P, Young JC, High S. 2007. Post-translational integration of tail-anchored proteins is facilitated by defined molecular chaperones. *J Cell Sci* 120:1743–1751.
215. Brkljacic J, Zhao Q, Meier I. 2009. WPP-domain proteins mimic the activity of the HSC70-1 chaperone in preventing mistargeting of RanGAP1-anchoring protein WIT1. *Plant Physiol* 151:142–154.
216. Rabu C, Wipf P, Brodsky JL, High S. 2008. A precursor-specific role for Hsp40/Hsc70 during tail-anchored protein integration at the endoplasmic reticulum. *J Biol Chem* 283:27504–27513.
217. Colombo SF, Cardani S, Maroli A, Vitiello A, Soffientini P, Crespi A, Bram RF, Benfante R, Borgese N. 2016. Tail-anchored Protein Insertion in Mammals: FUNCTION AND RECIPROCAL INTERACTIONS OF THE TWO SUBUNITS OF THE TRC40 RECEPTOR. *J Biol Chem* 291:15292–15306.
218. Schuldiner M, Metz J, Schmid V, Denic V, Rakwalska M, Schmitt HD, Schwappach B, Weissman JS. 2008. The GET complex mediates insertion of tail-anchored proteins into the ER membrane. *Cell* 134:634–645.
219. Favalaro V, Vilardi F, Schlecht R, Mayer MP, Dobberstein B. 2010. Asna1/TRC40-mediated membrane insertion of tail-anchored proteins. *J Cell Sci* 123:1522–1530.

220. Colombo SF, Fasana E. 2011. Mechanisms of insertion of tail-anchored proteins into the membrane of the endoplasmic reticulum. *Curr Protein Pept Sci* 12:736–742.
221. Enoch HG, Fleming PJ, Strittmatter P. 1979. The binding of cytochrome b5 to phospholipid vesicles and biological membranes. Effect of orientation on intermembrane transfer and digestion by carboxypeptidase Y. *J Biol Chem* 254:6483–6488.
222. Colombo SF, Longhi R, Borgese N. 2009. The role of cytosolic proteins in the insertion of tail-anchored proteins into phospholipid bilayers. *J Cell Sci* 122:2383–2392.
223. Brambillasca S, Yabal M, Soffientini P, Stefanovic S, Makarow M, Hegde RS, Borgese N. 2005. Transmembrane topogenesis of a tail-anchored protein is modulated by membrane lipid composition. *EMBO J* 24:2533–2542.
224. Krumpke K, Frumkin I, Herzig Y, Rimon N, Özbalci C, Brügger B, Rapaport D, Schuldiner M. 2012. Ergosterol content specifies targeting of tail-anchored proteins to mitochondrial outer membranes. *Mol Biol Cell* 23:3927–3935.
225. Marty NJ, Teresinski HJ, Hwang YT, Clendening EA, Gidda SK, Sliwinska E, Zhang D, Miernyk JA, Brito GC, Andrews DW, Dyer JM, Mullen RT. 2014. New insights into the targeting of a subset of tail-anchored proteins to the outer mitochondrial membrane. *Front Plant Sci* 5:426.
226. Beilharz T, Egan B, Silver PA, Hofmann K, Lithgow T. 2003. Bipartite signals mediate subcellular targeting of tail-anchored membrane proteins in *Saccharomyces cerevisiae*. *J Biol Chem* 278:8219–8223.
227. Kriechbaumer V, Shaw R, Mukherjee J, Bowsher CG, Harrison A-M, Abell BM. 2009. Subcellular distribution of tail-anchored proteins in *Arabidopsis*. *Traffic* 10:1753–1764.
228. Kalbfleisch T, Cambon A, Wattenberg BW. 2007. A bioinformatics approach to identifying tail-anchored proteins in the human genome. *Traffic* 8:1687–1694.
229. Krogh A, Larsson B, von Heijne G, Sonnhammer EL. 2001. Predicting transmembrane protein topology with a hidden Markov model: application to complete genomes. *J Mol Biol* 305:567–580.

230. Cserzö M, Eisenhaber F, Eisenhaber B, Simon I. 2002. On filtering false positive transmembrane protein predictions. *Protein Eng* 15:745–752.
231. Kyte J, Doolittle RF. 1982. A simple method for displaying the hydropathic character of a protein. *J Mol Biol* 157:105–132.
232. Sloves P-J, Delhaye S, Mouveaux T, Werkmeister E, Slomianny C, Hovasse A, Dilezitoko Alayi T, Callebaut I, Gaji RY, Schaeffer-Reiss C, Van Dorsselear A, Carruthers VB, Tomavo S. 2012. Toxoplasma sortilin-like receptor regulates protein transport and is essential for apical secretory organelle biogenesis and host infection. *Cell Host Microbe* 11:515–527.
233. Nagamune K, Beatty WL, Sibley LD. 2007. Artemisinin induces calcium-dependent protein secretion in the protozoan parasite *Toxoplasma gondii*. *Eukaryotic Cell* 6:2147–2156.
234. Cserzö M, Wallin E, Simon I, von Heijne G, Elofsson A. 1997. Prediction of transmembrane alpha-helices in prokaryotic membrane proteins: the dense alignment surface method. *Protein Eng* 10:673–676.
235. Mall S, Broadbridge R, Sharma RP, Lee AG, East JM. 2000. Effects of aromatic residues at the ends of transmembrane alpha-helices on helix interactions with lipid bilayers. *Biochemistry* 39:2071–2078.
236. Webb RJ, East JM, Sharma RP, Lee AG. 1998. Hydrophobic mismatch and the incorporation of peptides into lipid bilayers: a possible mechanism for retention in the Golgi. *Biochemistry* 37:673–679.
237. Sharpe HJ, Stevens TJ, Munro S. 2010. A comprehensive comparison of transmembrane domains reveals organelle-specific properties. *Cell* 142:158–169.
238. Cosson P, Perrin J, Bonifacino JS. 2013. Anchors aweigh: protein localization and transport mediated by transmembrane domains. *Trends Cell Biol* 23:511–517.
239. Roth KA, Cohn SM, Rubin DC, Trahair JF, Neutra MR, Gordon JI. 1992. Regulation of gene expression in gastric epithelial cell populations of fetal, neonatal, and adult transgenic mice. *Am J Physiol* 263:G186-197.
240. Wilkins MR, Gasteiger E, Bairoch A, Sanchez JC, Williams KL, Appel RD, Hochstrasser DF. 1999. Protein identification and analysis tools in the ExPASy server. *Methods Mol Biol* 112:531–552.

241. Lee J, Lee H, Kim J, Lee S, Kim DH, Kim S, Hwang I. 2011. Both the hydrophobicity and a positively charged region flanking the C-terminal region of the transmembrane domain of signal-anchored proteins play critical roles in determining their targeting specificity to the endoplasmic reticulum or endosymbiotic organelles in Arabidopsis cells. *Plant Cell* 23:1588–1607.
242. Hegde RS, Keenan RJ. 2011. Tail-anchored membrane protein insertion into the endoplasmic reticulum. *Nat Rev Mol Cell Biol* 12:787–798.
243. Byers JT, Guzzo RM, Salih M, Tuana BS. 2009. Hydrophobic profiles of the tail anchors in SLMAP dictate subcellular targeting. *BMC Cell Biol* 10:48.
244. Malsam J, Söllner TH. 2011. Organization of SNAREs within the Golgi stack. *Cold Spring Harb Perspect Biol* 3:a005249.
245. Walter J, Urban J, Volkwein C, Sommer T. 2001. Sec61p-independent degradation of the tail-anchored ER membrane protein Ubc6p. *EMBO J* 20:3124–3131.
246. Yang M, Ellenberg J, Bonifacino JS, Weissman AM. 1997. The transmembrane domain of a carboxyl-terminal anchored protein determines localization to the endoplasmic reticulum. *J Biol Chem* 272:1970–1975.
247. Maggio C, Barbante A, Ferro F, Frigerio L, Pedrazzini E. 2007. Intracellular sorting of the tail-anchored protein cytochrome b5 in plants: a comparative study using different isoforms from rabbit and Arabidopsis. *J Exp Bot* 58:1365–1379.
248. Henderson MPA, Hwang YT, Dyer JM, Mullen RT, Andrews DW. 2007. The C-terminus of cytochrome b5 confers endoplasmic reticulum specificity by preventing spontaneous insertion into membranes. *Biochem J* 401:701–709.
249. Mitoma J, Ito A. 1992. The carboxy-terminal 10 amino acid residues of cytochrome b5 are necessary for its targeting to the endoplasmic reticulum. *EMBO J* 11:4197–4203.
250. Hwang YT, Pelitire SM, Henderson MPA, Andrews DW, Dyer JM, Mullen RT. 2004. Novel targeting signals mediate the sorting of different isoforms of the tail-anchored membrane protein cytochrome b5 to either endoplasmic reticulum or mitochondria. *Plant Cell* 16:3002–3019.

251. Joglekar AP, Xu D, Rigotti DJ, Fairman R, Hay JC. 2003. The SNARE motif contributes to rbet1 intracellular targeting and dynamics independently of SNARE interactions. *J Biol Chem* 278:14121–14133.
252. Egan B, Beilharz T, George R, Isenmann S, Gratzer S, Wattenberg B, Lithgow T. 1999. Targeting of tail-anchored proteins to yeast mitochondria in vivo. *FEBS Lett* 451:243–248.
253. Horie C, Suzuki H, Sakaguchi M, Mihara K. 2003. Targeting and assembly of mitochondrial tail-anchored protein Tom5 to the TOM complex depend on a signal distinct from that of tail-anchored proteins dispersed in the membrane. *J Biol Chem* 278:41462–41471.
254. Schwalm EL, Grove TL, Booker SJ, Boal AK. 2016. Crystallographic capture of a radical S-adenosylmethionine enzyme in the act of modifying tRNA. *Science* 352:309–312.
255. Rezgui VAN, Tyagi K, Ranjan N, Konevega AL, Mittelstaet J, Rodnina MV, Peter M, Pedrioli PGA. 2013. tRNA tKUUU, tQUUG, and tEUUC wobble position modifications fine-tune protein translation by promoting ribosome A-site binding. *Proc Natl Acad Sci USA* 110:12289–12294.
256. Benítez-Páez A, Villarroja M, Armengod M-E. 2012. The Escherichia coli RlmN methyltransferase is a dual-specificity enzyme that modifies both rRNA and tRNA and controls translational accuracy. *RNA* 18:1783–1795.
257. Borgese N, Gazzoni I, Barberi M, Colombo S, Pedrazzini E. 2001. Targeting of a tail-anchored protein to endoplasmic reticulum and mitochondrial outer membrane by independent but competing pathways. *Mol Biol Cell* 12:2482–2496.
258. Stojanovski D, Koutsopoulos OS, Okamoto K, Ryan MT. 2004. Levels of human Fis1 at the mitochondrial outer membrane regulate mitochondrial morphology. *J Cell Sci* 117:1201–1210.
259. Habib SJ, Vasiljev A, Neupert W, Rapaport D. 2003. Multiple functions of tail-anchor domains of mitochondrial outer membrane proteins. *FEBS Lett* 555:511–515.
260. Kemper C, Habib SJ, Engl G, Heckmeyer P, Dimmer KS, Rapaport D. 2008. Integration of tail-anchored proteins into the mitochondrial outer membrane does not require any known import components. *J Cell Sci* 121:1990–1998.

261. Yoon Y, Krueger EW, Oswald BJ, McNiven MA. 2003. The mitochondrial protein hFis1 regulates mitochondrial fission in mammalian cells through an interaction with the dynamin-like protein DLP1. *Mol Cell Biol* 23:5409–5420.
262. Koch A, Yoon Y, Bonekamp NA, McNiven MA, Schrader M. 2005. A role for Fis1 in both mitochondrial and peroxisomal fission in mammalian cells. *Mol Biol Cell* 16:5077–5086.
263. Ding M, Clayton C, Soldati D. 2000. *Toxoplasma gondii* catalase: are there peroxisomes in toxoplasma? *J Cell Sci* 113 ( Pt 13):2409–2419.
264. Kaasch AJ, Joiner KA. 2000. Targeting and subcellular localization of *Toxoplasma gondii* catalase. Identification of peroxisomes in an apicomplexan parasite. *J Biol Chem* 275:1112–1118.
265. Linstedt AD, Foguet M, Renz M, Seelig HP, Glick BS, Hauri HP. 1995. A C-terminally-anchored Golgi protein is inserted into the endoplasmic reticulum and then transported to the Golgi apparatus. *Proc Natl Acad Sci USA* 92:5102–5105.
266. D'Arrigo A, Manera E, Longhi R, Borgese N. 1993. The specific subcellular localization of two isoforms of cytochrome b5 suggests novel targeting pathways. *J Biol Chem* 268:2802–2808.
267. Kuroda R, Ikenoue T, Honsho M, Tsujimoto S, Mitoma JY, Ito A. 1998. Charged amino acids at the carboxyl-terminal portions determine the intracellular locations of two isoforms of cytochrome b5. *J Biol Chem* 273:31097–31102.
268. Isenmann S, Khew-Goodall Y, Gamble J, Vadas M, Wattenberg BW. 1998. A splice-isoform of vesicle-associated membrane protein-1 (VAMP-1) contains a mitochondrial targeting signal. *Mol Biol Cell* 9:1649–1660.
269. Bauer F, Hermand D. 2012. A coordinated codon-dependent regulation of translation by Elongator. *Cell Cycle* 11:4524–4529.
270. Tigano M, Ruotolo R, Dallabona C, Fontanesi F, Barrientos A, Donnini C, Ottonello S. 2015. Elongator-dependent modification of cytoplasmic tRNA<sup>Lys</sup>UUU is required for mitochondrial function under stress conditions. *Nucleic Acids Res* 43:8368–8380.

## CURRICULUM VITAE

Leah R. Padgett

### EDUCATION

- 2012-2017      Doctor of Philosophy in Pharmacology  
Indiana University  
Indianapolis, IN  
Mentor: William J. Sullivan, Jr., Ph.D.
- 2006-2008      Certificate in Biotechnology  
Indiana University  
Indianapolis, IN
- 2001-2005      Ball State University  
Muncie, IN  
B.S. Genetic Biology  
Minors: Chemistry and Anthropology

### FUNDING

- 2015-2017      **American Heart Association**  
**MWA Winter Predoctoral Fellowship**  
TgElp3: a novel mitochondrial acetyltransferase and drug  
target in the heart pathogen *Toxoplasma gondii*  
(15PRE25550023)

### WORK EXPERIENCE

- 2009-2012      **Research Analyst I**  
Indiana University School of Medicine, Endocrinology  
Indianapolis, IN  
Principal Investigator: Michael Econs, M.D.
- 2008              **Math and Biology Tutor**  
Ivy Tech Community College, Indianapolis, IN
- 2005-2009      **Research Technician**  
Indiana University School of Medicine, Endocrinology  
Indianapolis, IN  
Principal Investigator: Michael Econs, M.D.



## **PUBLICATIONS (Also published under Leah R. Curry)**

### **\*co-first author**

1. **Padgett LR**, Arrizabalaga G, Sullivan WJ Jr. Targeting of tail-anchored membrane proteins to subcellular organelles in *Toxoplasma gondii*. *Traffic*. 2017 Mar; 418(3):149-158.
2. Imel EA, Liu Z, McQueen AK, Acton D, Acton A, **Padgett LR**, Peacock M, Econs MJ. Serum fibroblast growth factor 23, serum iron and bone mineral density in premenopausal women. *Bone*. 2016 May; 86:98-105. 2016 Mar 8.
3. **Padgett LR\***, Varberg JM\*, Arrizabalaga G, Sullivan WJ. TgATAT-mediated alpha-tubulin acetylation is required for division of the protozoan parasite *Toxoplasma gondii*. *mSphere*. 2016 Jan; (1) 1.
  - *Article chosen for cover image*
4. Koller DL, Imel EA, Lai D, **Padgett LR**, Acton D, Gray A, Peacock M, Econs MJ, Foroud T. Genome-wide association study of serum iron phenotypes in premenopausal women of European descent. *Blood Cells, Molecules and Diseases*. 2016 Mar; 16 (57) 50-53.
5. Ichikawa S, Gray AK, **Padgett LR**, Allen MR, Clinkenbeard EL, Sarpa NM, White KE, Econs MJ. Genetic rescue of glycosylation-deficient Fgf23 in the Galnt3 knockout mouse. *Endocrinology*. 2014 Oct; 155(10):3891-8.
6. Ichikawa S, Gray AK, **Padgett LR**, Reilly AM, Unsicker TR. High dietary phosphate intake induces development of ectopic calcifications in a murine model of familial tumoral calcinosis. *J Bone Miner Res*. 2014 Sep; 29(9):2017-23.
7. **Padgett LR\***, Alam I\*, Ichikawa S, Alkhouli M, Koller DL, Lai D, Peacock M, Xuei X, Foroud T, Edenberg HJ, Econs MJ. SIBLING family genes and bone mineral density: association and allele-specific expression in humans. *Bone*. 2014 Jul; 64:166-72.
8. Imel EA, Gray AK, **Padgett LR**, Econs MJ. Iron and fibroblast growth factor 23 in X-linked hypophosphatemia. *Bone*. 2014 Mar; 60:87-92.
9. Ichikawa S, Tuchman S, **Padgett LR**, Gray AK, Baluarte HJ, Econs MJ. Intronic deletions in the SLC34A3 gene: a cautionary tale for mutation analysis of hereditary hypophosphatemic rickets with hypercalciuria. *Bone*. 2014 Feb; 59:53-6.

10. Teng M, Ichikawa S, **Padgett LR**, Wang Y, Mort M, Cooper DN, Koller DL, Foroud T, Edenberg HJ, Econs MJ, Liu Y. regSNPs: a strategy for prioritizing regulatory single nucleotide substitutions. *Bioinformatics*. 2012 Jul 15; 28(14):1879-86.
11. EA Imel, M Peacock, AK Gray, **LR Padgett**, SL Hui, MJ Econs. Iron Modifies Plasma FGF23 Differently in Autosomal Dominant Hypophosphatemic Rickets and Healthy Humans. *Journal of Clinical Endocrinology & Metabolism* 2011 Nov 1; 96 (11), 3541-3549.
  - *2012 International Award for Publishing Excellence in the Journal of Clinical Endocrinology and Metabolism*
12. Ichikawa S, Baujat G, Seyahi A, Garoufali AG, Imel EA, **Padgett LR**, Austin AM, Sorenson AH, Pejin Z, Topouchian V, Quartier P, Cormier-Daire V, Dechaux M, Malandrino FCh, Singhellakis PN, Le Merrer M, Econs MJ. Clinical variability of familial tumoral calcinosis caused by novel GALNT3 mutations. *Am J Med Genet A*. 2010 Apr; 152A(4): 896-903.
13. Koller DL, Ichikawa S, Lai D, **Padgett LR**, Doheny KF, Pugh E, Paschall J, Hui SL, Edenberg HJ, Xuei X, Peacock M, Econs MJ, Foroud T. Genome-wide association study of bone mineral density in premenopausal European-American women and replication in African-American women. *J Clin Endocrinol Metab*. 2010 Apr; 95(4):1802-9.
14. Ichikawa S, Koller DL, **Padgett LR**, Lai D, Hui SL, Peacock M, Foroud T, Econs MJ. Replication of previous genome-wide association studies of bone mineral density in premenopausal American women. *J Bone Miner Res*. 2010 Feb 8.
15. Ichikawa S, Koller DL, **Curry LR**, Lai D, Xuei X, Edenberg HJ, Hui SL, Peacock M, Foroud T, Econs MJ. Association of adenylate cyclase 10 (ADCY10) polymorphisms and bone mineral density in healthy adults. *Calcif Tissue Int*. 2009 Feb; 84(2):97-102.
16. Ichikawa S, Traxler EA, Estwick SA, **Curry LR**, Johnson ML, Sorenson AH, Imel EA, Econs MJ. Mutational survey of the PHEX gene in patients with X-linked hypophosphatemic rickets. *Bone*. 2008 Oct; 43(4):663-6.
17. Ichikawa S, Koller DL, **Curry LR**, Lai D, Xuei X, Pugh EW, Tsai YY, Doheny KF, Edenberg HJ, Hui SL, Foroud T, Peacock M, Econs MJ. Identification of a linkage disequilibrium block in chromosome 1q associated with BMD in premenopausal white women. *J Bone Miner Res*. 2008 Oct; 23(10):1680-8.

18. Chu K, Koller DL, Ichikawa S, Snyder R, **Curry L**, Lai D, Austin A, Xuei X, Edenberg HJ, Hui SL, Foroud TM, Peacock M, Econs MJ. CLCN7 polymorphisms and bone mineral density in healthy premenopausal white women and in white men. *Bone*. 2008 Dec; 43(6):995-8.
19. T. Foroud, S. Ichikawa, D. Koller, D. Lai, **L. Curry**, X. Xuei, H. J. Edenberg, S. Hui, M. Peacock, and M. J. Econs. Association studies of *ALOX5* and bone mineral density in healthy adults. *Osteoporos Int*. 2008 May; 19(5): 637–643.

## **PRESENTATIONS**

### ***Oral Presentations***

**Padgett LR**, Stilger K, Sullivan WJ. April 2015. Elp3 is an essential tail-anchored mitochondrial protein in *Toxoplasma gondii*. Indiana University-University of Kentucky Parasitology Conference, Indianapolis, IN.

**Padgett LR**, Stilger K, Sullivan WJ. August 2014. Elp3 lysine acetyltransferase is a tail-anchored mitochondrial protein in *Toxoplasma gondii*. Abstract selected for oral presentation, The 3rd Annual Midwest Neglected Infectious Disease Meeting, Notre Dame, IN.

### ***Poster Presentations***

**Padgett LR**, Sullivan WJ. September, 2016. Investigation into the molecular role of Elp3 as a putative tRNA modification enzyme in *Toxoplasma gondii*. RNA Modifications and Epitranscriptomics Conference, Chicago, IL.

**Padgett LR**, Sullivan WJ. March 2016. Investigation into the molecular role of Elp3 as a putative tRNA modification enzyme in *Toxoplasma gondii*. 3<sup>RD</sup> Annual Symposium on RNA Science: Epitranscriptomics, Albany, NY.

**Padgett LR**, Stilger K, Sullivan WJ. August 2015. Elp3 is an essential tail-anchored mitochondrial protein in *Toxoplasma gondii*. The 4<sup>th</sup> Annual Midwest Neglected Infectious Disease Meeting, Notre Dame, IN.

**Padgett LR**, Stilger K, Sullivan WJ. June 2015. Elp3 is an essential tail-anchored mitochondrial protein in *Toxoplasma gondii*. 13<sup>th</sup> International Congress on Toxoplasmosis, Gettysburg, PA.

**Padgett LR**, Stilger K, Jeffers V, Sullivan WJ. September 2013. The *Toxoplasma* mitochondrion wears a HAT. Abstract for poster presentation, Molecular Parasitology Meeting, Woods Hole, MA.

**Padgett LR**, Stilger K, Sullivan WJ. September 2014. Eip3 lysine acetyltransferase is a tail-anchored mitochondrial protein in *Toxoplasma gondii*. Abstract for poster presentation, Molecular Parasitology Meeting, Woods Hole, MA.

### **HONORS/AWARDS**

December 2016	Advanced Communicator Bronze Award Scientific Toasters at IUSM-Toastmasters International
November 2016	Competent Leader Award Scientific Toasters at IUSM -Toastmasters International
Spring 2016	Paradise Travel Award (\$400)
Fall 2015	Student Volunteer of the Year Award Indiana University School of Medicine
June 2015	Competent Communicator Award Scientific Toasters at IUSM -Toastmasters International
Summer 2015	President's Distinguished Club Scientific Toasters-Toastmasters International
Spring 2015	Graduate-Professional Education Travel Grant (\$500)
Fall 2014	Paradise Travel Award (\$400)

### **SERVICE**

2016-current	Toastmaster's International Scientific Toaster's at IUSM Treasurer
January 2017	Volunteer at the Susan G. Komen Tissue Bank Indiana University Simon Cancer Center
2014-2016	Toastmaster's International Vice President of Membership Founding Member of Scientific Toasters at IUSM
January 2016	Organized and Hosted Toaster Talks Ted talks for prospective graduate students Indiana University School of Medicine Biomedical Gateway program Indiana University School of Medicine, Indianapolis

2012-2017	Volunteer for Graduate Student Recruitment Campus Visits Indiana University School of Medicine Biomedical Gateway program Indiana University School of Medicine, Indianapolis
2015	Elite 50 Application Review Committee Graduate and Professional Student Government Indiana University-Purdue University Indianapolis (IUPUI)
2014-2015	Admissions Committee Student Representative Indiana University School of Medicine Biomedical Gateway program Indiana University School of Medicine, Indianapolis
2014-2015	Indiana University School of Medicine Representative Graduate and Professional Student Government Indiana University-Purdue University Indianapolis (IUPUI)
2014-2015	Graduate Student President Department of Pharmacology and Toxicology Indiana University School of Medicine, Indianapolis
2014-2015	Education Grant Review Committee Graduate and Professional Student Government Indiana University-Purdue University Indianapolis (IUPUI)
November 2014	Volunteer at the Susan G. Komen Tissue Bank Indiana University Simon Cancer Center
August 2014	Participant in the Panel for Women in Science (WIS) - Indiana BioMedical Gateway (IBMG) Program Summer Research Internship program